Doped Polyaniline for Gas Sensors for the Detection of Formaldehyde

by

Katherine Mariann Elizabeth Stewart

A thesis
presented to the University of Waterloo
in fulfillment of the
thesis requirement for the degree of
Master of Applied Science
in
Chemical Engineering

Waterloo, Ontario, Canada, 2011

Author's Declaration

I hereby declare that I am the sole author of this thesis. This is a true copy of the thesis, including any required final revisions, as accepted by my examiners.

I understand that my thesis may be made electronically available to the public.

Abstract

Formaldehyde is one of the main gases that contribute to poor indoor air quality since it is so widely used in the manufacturing of goods. Over time, formaldehyde leaches out of various materials and reduces the quality of air. Formaldehyde, even at very low concentrations, can cause respiratory problems and a general feeling of unwellness. The World Health Organization (WHO) states that formaldehyde exposure should not exceed 0.08 ppm over a 30 minute period. Therefore, formaldehyde sensors are needed to ensure optimal indoor air quality.

Polyaniline (PANI), as well as PANI doped with NiO or NiO and Al_2O_3, were tested to determine their suitability as sensing materials for formaldehyde. It was found that at higher concentrations of formaldehyde (above 1 ppm), PANI doped with 5% NiO and 15% Al_2O_3 was the most suitable sensing material with respect to both sensitivity and selectivity. At lower concentrations (below 1 ppm), however, PANI doped with 5% NiO and 15% Al_2O_3 did not detect formaldehyde. PANI doped with 15% NiO only was a much better option since it was able to detect the highest concentration of formaldehyde at very low concentrations (0.09 ppm) and still have moderate selectivity.

A special test system was designed that could test single or multiple gases at various concentrations. Ethanol, acetaldehyde and benzene were chosen as interferents for formaldehyde and nitrogen was used to dilute the gases to achieve lower concentrations. A specialized gas chromatograph (GC) was used to determine the amount of gas or analyte that interacted with the sensing material being tested.

Replicate polymer samples of varying dopant concentrations were tested with different gases at different concentrations and statistically analyzed. Both sensitivity and selectivity towards formaldehyde was taken into consideration. Among all tests conducted with single and multiple gases, it was concluded that PANI doped with 5% NiO and 15% Al_2O_3 was the best sensing material at high concentrations of formaldehyde (above 1 ppm), whereas PANI doped with 15% NiO was the best sensing material at low concentrations (below 1 ppm).

Acknowledgements

I was honoured to have the opportunity to work with both Prof. A. Penlidis, Canada Research Chair, Polymer Engineering, and Prof. N. McManus of the University of Waterloo's Chemical Engineering Department and would like to acknowledge their guidance, direction, advice, and support through this entire project. I looked forward to my biweekly meetings with both Prof. Penlidis and Prof. McManus and always appreciated their help, humour, and focus. Special thanks also go to Prof. Abdel-Rahman, Mahmoud Khater as well as John Carroll and all the people at Seacoast Science Inc.

My thanks also go to my colleagues and friends Dave Dorschner, Ivan Kantor, Alex Proracki, James Rigsby, and Matt Wurtele, who came to my rescue time and time again to do much of the heavy lifting and with my friends Matt Callaghan, Nicole Cathcart, Bonnie De Baets, Nicholas Flinn, Angela Leung, and Sahar Rahmani who kept me grounded and sane.

My parents have always been my staunchest supporters and I would like to thank my dad, Ken Stewart, for helping me clean out the area in the lab where I assembled my apparatus and who built the wooden shelves I designed to support the mass flow controllers. I would also like to thank my mom, Marilyn Stone, for taking the time to proofread my thesis. Finally, I would like to thank my boyfriend, Brian Abernethy, for always being there.

Table of Contents

List of Figures

List of Tables

Chapter 1: Thesis Objectives and Outline

1.1 Objectives

The objective of this thesis is to find a sensing material that would be best for the detection of formaldehyde. The final goal would be to use this sensing material on a sensor designed for indoor air quality. Therefore, the sensing material must be able to detect formaldehyde at levels below 0.08 ppm, since that is the maximum exposure level over 30 minutes defined by the World Health Organization (WHO) (WHO, 2001), at room temperature.

The sensing material must also be able to be stored at room temperature, without degrading. The sensor should not react with formaldehyde or any other vapour in the air during storage. Therefore, an activator is needed to overcome this problem or the sensor must be regenerated before the measurement is taken.

A common issue is the selectivity of the polymer sensors available. Another concern is the adsorption of water vapour (i.e. humidity). Also, many of the sensors available detect acetylaldehyde as well, since it is chemically very similar to formaldehyde. Therefore, a sensing material must be found that is selective to formaldehyde only.

1.2 Outline

In the second chapter, there is an extensive literature review of sensors. It begins with an overview of why formaldehyde has been chosen to sense and moves into different types of sensors. Sensors that have previously been developed for formaldehyde are compared, followed by a more in depth look into sensing materials. The chapter is completed by a summary of sensors for both organic and inorganic analytes.

In the third chapter, the experimental design is discussed. It begins by laying out the sensor constraints required for this specific application, followed by an evaluation of sensing materials for the detection of formaldehyde. Finally, the experimental set-up and apparatus are discussed and the experimental data presented.

In the fourth chapter, a specialized gas chromatograph is evaluated based on the reproducibility of results, the signal-to-noise ratio, and the limit of detection of the sensing materials towards formaldehyde. The experimental data are also statistically analyzed. The more promising polymers for formaldehyde sensing are analyzed further, and practical tips are considered.

In the fifth chapter, overall conclusions are drawn as well as recommendations made for future work. This includes both short term and long term recommendations. The references used throughout the thesis follow this chapter.

There is one appendix attached at the end of this thesis, Appendix A. It includes a selection of collected gas chromatographs (raw data). There is also a disk available from professor A. Penlidis which contains all of the collected gas chromatographs.

Chapter 2: Literature Background

2.1 Formaldehyde as a Volatile Organic Compound (VOC)

Formaldehyde is one of the more toxic volatile organic compounds (VOCs) that pollute indoor air. Formaldehyde is used in a variety of manufactured products including glues, resins, plywood, insulating materials, fabrics, and pulp and paper products (WHO, 2001 and Wang et al., 2008b). Formaldehyde is also used in dry cleaning solutions, cosmetics, fabrics, and cleaning products (Zhang et al., 2005). Formaldehyde can be absorbed through the skin and eyes or inhaled, which may cause eye, nose and throat irritation, breathing difficulties, coughing, sneezing, nausea, and potentially death. The World Health Organization (WHO) states that the concentration of formaldehyde over a 30 minute period should be less than 0.08 ppm (WHO, 2001).

Gillett et al. (2000) compared formaldehyde concentrations of different rooms in six homes. Figure 2.1 summarizes the results. Overall, the highest concentrations were recorded in the kitchen. This is most likely due to the amount of cabinetry in the kitchen, in which formaldehyde is used in manufacturing, since glued wood products, such as cabinets, emit the most formaldehyde vapours; however, gas stoves would also contribute to the formaldehyde levels.

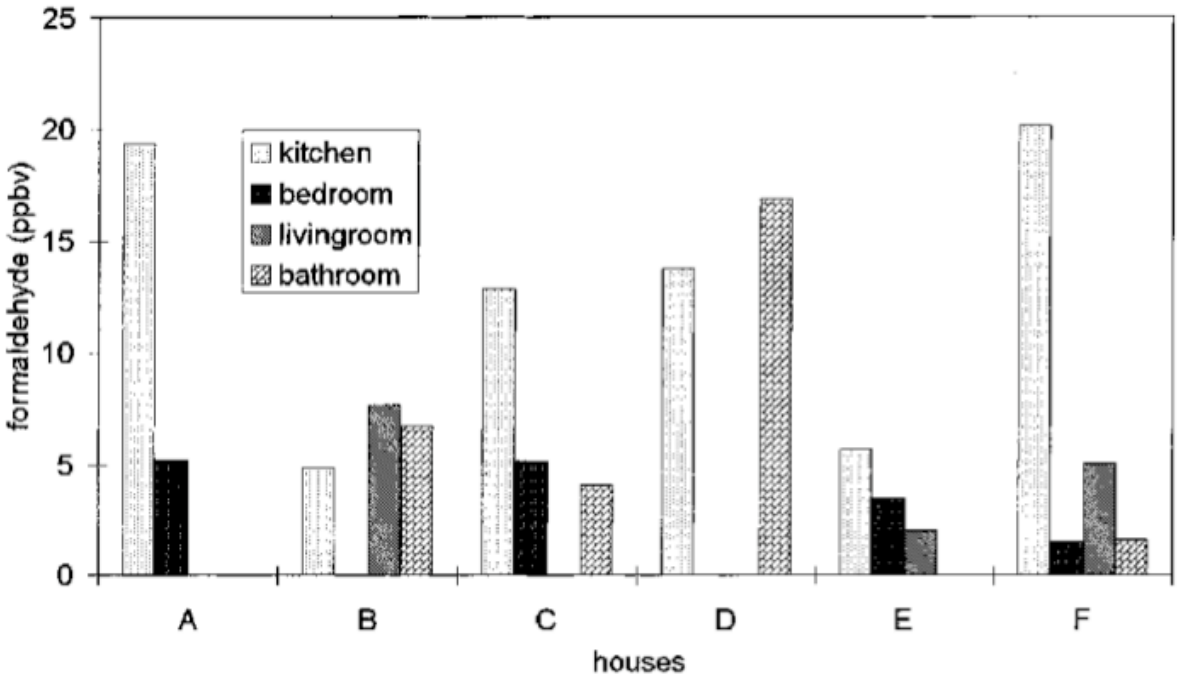

Figure 2.1: Indoor formaldehyde concentrations in six homes (Gillett et al., 2000).

House D, in Figure 2.1, has the highest concentration of formaldehyde in the bathroom. This may be due to recent bathroom cleaning and/or renovation, since both cleaning products and especially new materials emit more formaldehyde (Brown, 2002). Brown (2002) measured the levels of various VOCs over an extended period of time. The formaldehyde results for a new building are summarized in Table 2.1.

Table 2.1: Living Room, Bedroom, and Outdoor Concentrations of Formaldehyde of a New House

Concentration (µg/m^3) on Day Number										
Living Room				**Bedroom**				**Outdoor**		
2	**19**	**72**	**246**	**2**	**19**	**72**	**246**	**2**	**19**	**246**
120	87	60	46	120	93	56	64	<10	10	<10

(Brown, 2002)

To reduce the amount of VOCs in a room, construction materials that adsorb VOCs may be used. The use of these construction materials is beneficial since no special equipment is required (Ataka et al., 2004).

Ataka et al. (2004) examined the formaldehyde absorption properties of gypsum board (GB) and formaldehyde-decomposing gypsum board (FDGB), which is used for walls and ceilings. FDGB contains a chemical additive which reacts with formaldehyde causing the formaldehyde to adsorb onto the FDGB, and thus removes formaldehyde from the air (see Figure 2.2).

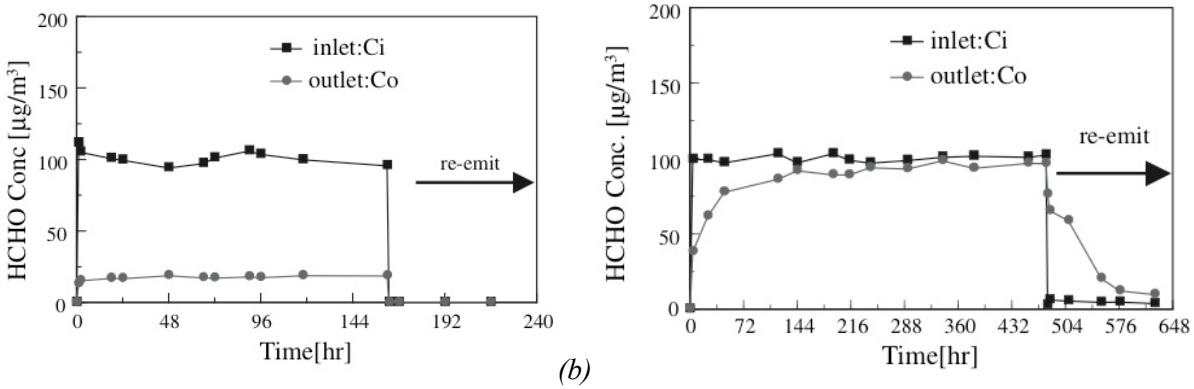

(a) *(b)*

Figure 2.2: Formaldehyde concentration absorbed and re-emitted from (a) FDGB and (b) GB (Ataka et al., 2004).

Absorptive construction materials work best when fully exposed to air. Ataka et al. (2004) compared FDGB covered with poly (vinyl chloride) (PVC) wallpaper and non-woven

wallpaper to uncovered FDGB and found that the PVC wallpaper did not allow formaldehyde to reach the FDGB, resulting in no change in the formaldehyde concentration, whereas the non-woven wallpaper only partially allowed formaldehyde to pass through to the FDGB; see Figure 2.3.

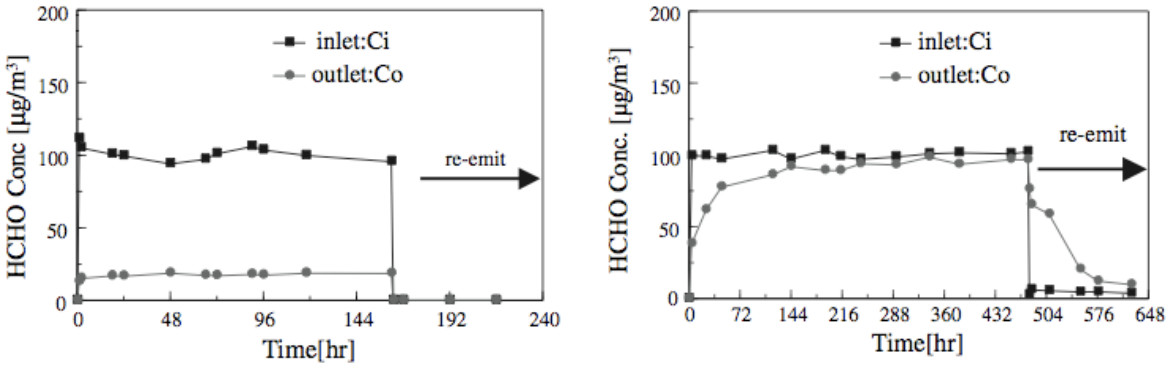

(a) *(b)*

Figure 2.3: Formaldehyde concentration absorbed and re-emitted from (a) PVC wallpaper and (b) non-woven wallpaper (Ataka et al., 2004).

2.2 Types of Sensors for Detection of VOCs

2.2.1 Inorganic Solid-state Sensors

Solid-state sensors are primarily based on catalytic reactions and can be made from semiconductors, insulators, metals, and catalytic material. Many of these sensors use conducting oxides as the sensing material. These are either catalytically active or used with a another component that is a catalyst (Adhikari and Majumdar, 2004).

Metal oxide semiconductor sensors are inexpensive to make, simple to use and provide real time detection since the gas concentration is converted directly into an electrical signal (Han et al., 2009 and Wang et al., 2008a). These sensors are also compact in size and provide reproducible results (Wang et al., 2009a).

Semiconductor sensors use a change in electrical properties caused by a reaction between the semiconductor and the analyte producing a new compound or a change in stoichiometry (Adhikari and Majumdar, 2004). Due to the solid state nature, semiconductor sensors have a long shelf life and do not deteriorate with use. On the other hand, they often function at high temperatures, which requires high power consumption and the sensors have low sensitivity and selectivity (Knake et al., 2005).

To improve the sensitivity and selectivity of semiconductor sensors, small amounts of another metal or metal oxide may be added. This is known as a dopant (Wang et al., 2009a). Dopants are discussed in Section 2.6. For example, Wang et al. (2009b) designed a Pd doped-

SnO_2 sensor that had high sensitivity for ethanol; however, it also had moderate sensitivity for formaldehyde, acetone, and methanol.

The addition of Pd increased the amount of adsorbed oxygen, which improved the sensing properties since the sensor operated based on the mechanism listed in Equations 2.1 to 2.6. Formaldehyde (HCHO) is shown, although the mechanism is the same for all small organic molecules (Wang et al., 2009b).

$$O_{2(gas)} \leftrightarrow O_{2(adsorbed)} \quad \text{(Equation 2.1)}$$

$$O_{2(adsorbed)} + e^- \leftrightarrow O_2^-{}_{(adsorbed)} \quad \text{(Equation 2.2)}$$

$$O_2^-{}_{(adsorbed)} + e^- \leftrightarrow 2O^-{}_{(adsorbed)} \quad \text{(Equation 2.3)}$$

$$O^-{}_{(adsorbed)} + e^- \leftrightarrow O^{2-}{}_{(adsorbed)} \quad \text{(Equation 2.4)}$$

$$HCHO_{(gas)} \leftrightarrow HCHO_{(adsorbed)} \quad \text{(Equation 2.5)}$$

$$O^{2-}{}_{(adsorbed)} + HCHO_{(adsorbed)} \leftrightarrow H_2O_{(adsorbed)} + CO_{2(adsorbed)} + 4e^- \quad \text{(Equation 2.6)}$$

As the oxidation proceeded, the amount of adsorbed oxygen decreased, which lowered the potential barrier of the semiconductor and thus increased the electron concentration, which resulted in the resistance of the sensor to decrease (Wang et al., 2009b).

The reaction described in Equations 2.1 through 2.6 is the general formaldehyde oxidation reaction over a catalyst. The sensors based on the oxidation of formaldehyde exploit the partial pressure of oxygen in the atmosphere by using the partial pressure of oxygen to determine the presence of formaldehyde. The catalytic oxidation of formaldehyde results in a decrease in the partial pressure of oxygen at the surface of the sensing film, which increases the electrical conductivity and thus decreases the resistance. The change in resistance is what is measured (Lee et al., 2006).

Wang et al. (2009a) doped In_2O_3 with Ag to improve the sensing properties of In_2O_3 for formaldehyde. The sensor detected a change in resistance caused by the oxidation of small molecules such as formaldehyde. Equations 2.1 through 2.6 describe the mechanism of oxidation. Doping with Ag increased the amount of adsorbed oxygen on the surface of the sensor which activated the adsorbed formaldehyde and thus catalyzed the oxidation of formaldehyde. The addition of Ag also lowered the operating temperature by 20°C and improved selectivity (Wang et al., 2009a); see Figure 2.4. Selectivity is the ability of a sensor to only give a signal when the target analyte (formaldehyde in this case) interacts with the sensor. It should be noted that the "response" on the y-axis represents the change in resistance caused by the oxidation of the analyte divided by the resistance of air, and thus is a unitless value.

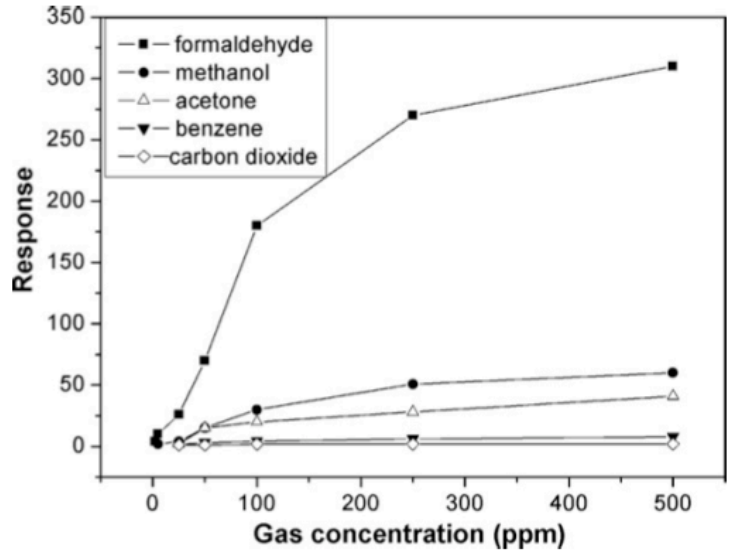

Figure 2.4: Selectivity of Ag doped In_2O_3 gas sensor (Wang et al., 2009a).

Chen et al. (2008) also created an In_2O_3-based sensor, but instead of doping it with Ag, a CdO-In_2O_3 mixture was used as the sensing material. This sensor worked based on the same mechanism as the previous sensor discussed (see Equations 2.1 to 2.6), where the adsorbed oxygen oxidized the adsorbed formaldehyde and this oxidation caused a change in resistance, which was measured. For the selectivity of the CdO-In_2O_3 sensor see Figure 2.5. Since the response in both Figure 2.4 and 2.5 was measured in the same way for both the Ag doped In_2O_3 and CdO-In_2O_3 sensors, they can be directly compared for formaldehyde. It can be seen that the CdO-In_2O_3 sensor was a better sensor for the detection of formaldehyde since the response is both much higher and selective, even at lower concentrations of formaldehyde.

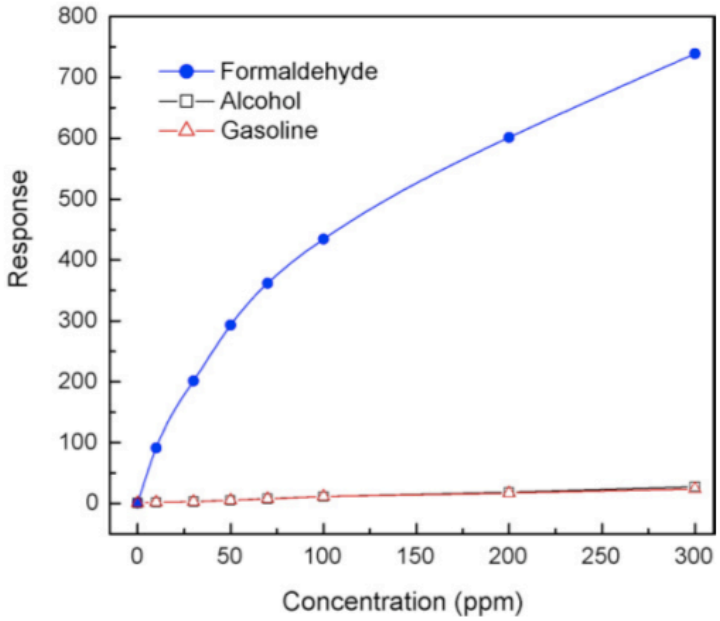

Figure 2.5: Selectivity for formaldehyde of CdO-In_2O_3 gas sensor (Chen et al., 2008).

An inorganic semiconductor sensor array, which contained eight tin oxide sensors with gold, copper, platinum, and/or palladium catalysts (Au/Cu/Pt/Pd SnO_2) as sensing materials, was developed by Lv et al. (2007). The Au/Cu/Pt/Pd SnO_2 was composed of eight sensors, two of each of the following: SnO_2/Pt, SnO_2-Cu/Pt, SnO_2/Au, and SnO_2/Pd. The data from the sensors were normalized and analyzed via principal component analysis (PCA), and the first two PC components (1 and 2) were plotted against one another (see Figure 2.6). It can be seen in Figure 2.6 that the sensor worked well for single gases (e.g. formaldehyde), but not for binary gas mixtures (e.g. formaldehyde and ethanol). This was because although the single gases were separated well on the plot, the binary gas mixture did not give two separate points corresponding to each gas component, but rather one point from which the gases could not be differentiated (Lv et al., 2007).

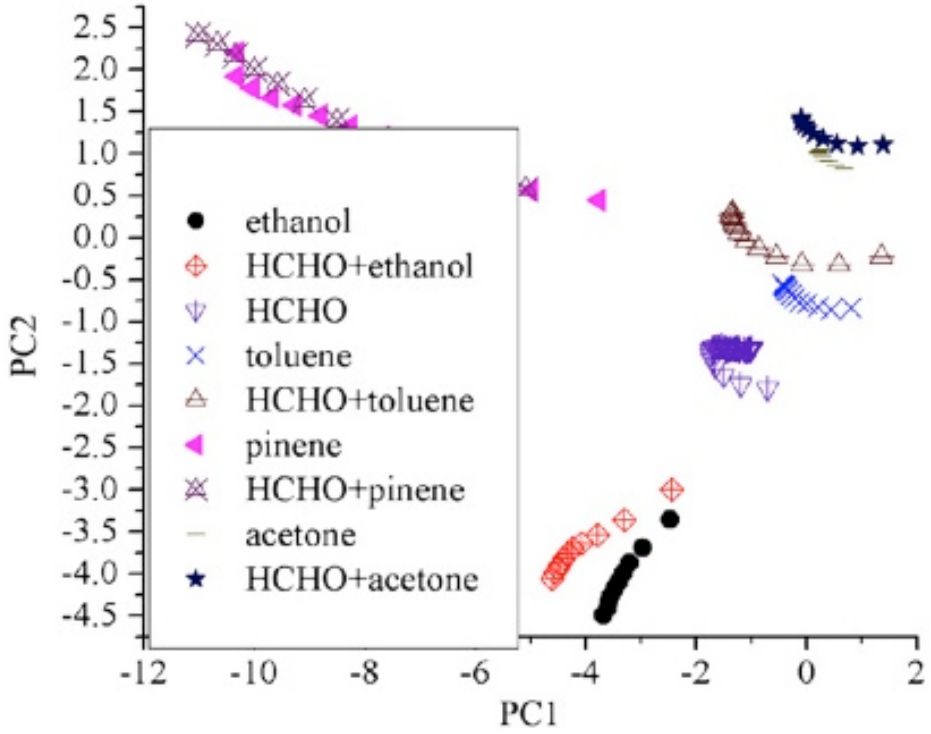

Figure 2.6: The compiled Au/Cu/Pt/Pd SnO_2 sensor graph for multiple VOCs (Lv et al., 2007).

2.2.2 Conductive Polymer-based Sensors

The conductive properties of conductive polymers, such as polyaniline (PANI) and its derivative poly (*o*-anisidine) (PoANI), are exploited by attaching electrodes to the polymer chains. The polymer chains then become a chemiresistor in the circuit and the resistivity of the polymer chains is measured (Agbor et al., 1995). The sensors detect the change in resistivity caused by the adsorption or absorption of a VOC onto the polymer chains. Conductive polymers are more easily prepared and processed, are available in a wide variety, and potentially have

greater sensitivity and selectivity to some gases at room temperature than inorganic semiconductor sensors (Wang et al., 2006; Dündar and Köleli, 2008). Conductive polymers also have high electrical stability and are capable of sensing over a wide range of analyte concentrations (Kukla et al., 1996).

Polymer-based sensors may consist of an organic/inorganic thin film made up of intercalated layers of PANI, PoANI, poly (2,5-dimethyl aniline) (P2,5-DMA), Poly (*N*-methyl aniline) (PNMA), or Polypyrrole (PPy) with molybdenum trioxide (MoO_3) (Hosono et al., 2005); see Figure 2.7. The semiconductive nature of MoO_3 increased the conductivity of the polymer. The highly ordered thin films increased the sensitivity (Chen et al., 1997) and the composition of the polymer determined the selectivity (Itoh et al., 2007a).

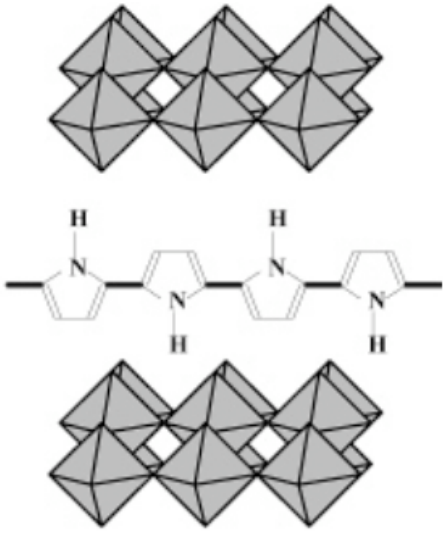

Figure 2.7: Layered MoO_3 and polypyrrole (PPy) (Hosono et al., 2005).

The organic/inorganic thin film was placed in a circuit by attaching electrodes to the thin film, which created a chemiresistor. The change in resistivity, caused by the absorption and adsorption of formaldehyde, was measured (Agbor et al., 1995). By purging the system with air or nitrogen, the formaldehyde detached from the thin film and the sensor could be reused (Wang et al., 2006).

2.2.3 Quartz Crystal Microbalance (QCM)-based Sensors

Chen et al. (1997) designed a QCM sensor using PoANI as the sensing material. The sensor was based on the change in frequency (or frequency shift) of the QCM which the result of the piezoelectric nature of the quartz. The change in weight, which resulted from the absorbed VOCs, caused the QCM to vibrate at a different frequency. The more mass absorbed onto the polymer surface, the larger the frequency shift. Therefore, if the same number of formic, acetic,

propionic and butyric acid molecules absorbed onto separate polymer surfaces, then butyric acid would cause the largest shift in frequency because of its higher molecular weight.

PoANI was mixed in a 3:1 ratio with stearic acid to produce a Langmuir-Blodgett (LB) film which could easily be transferred onto the gold-coated quartz crystal substrate, since PoANI alone was too rigid to be transferred (Chen et al., 1997); see Figure 2.8.

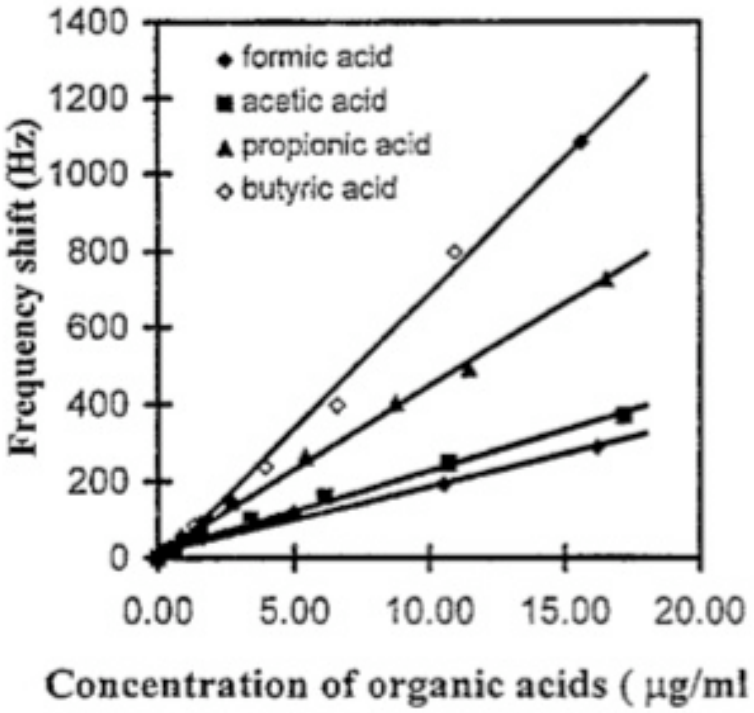

Figure 2.8: Concentration of organic acids versus frequency shift (Chen et al., 1997).

2.2.4 Microcantilever Sensors

Microcantilever sensors are similar to QCM in that they also measure a change in mass resulting from the adsorption of the gas; however, they do not use piezoelectric materials as the basis for the sensor. A microcantilever is coated with a sensing material and the adsorption of the target gas onto this sensing film is what causes the microcantilever to bend, which in turn records a signal (Ho and Webb, 2006).

Microcantilever sensors measure a frequency shift caused by change in mass resulting from the adsorption of the gas. The frequency shift is the result of a mechanical vibration due to the cantilever's displacement caused by the mass of the adsorbed gas. Zhou et al. (2002) used a resonating mode to improve the sensitivity of their sensor by amplifying the frequency measured (see Figure 2.9).

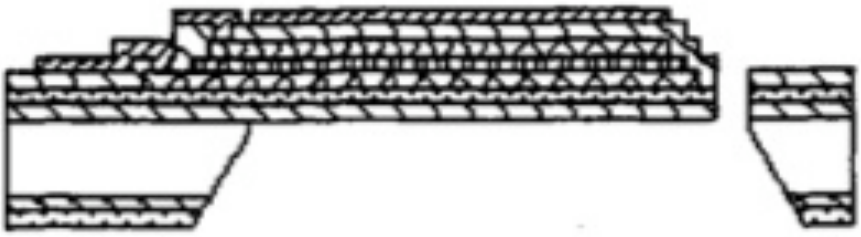

Figure 2.9: Schematic of a microcantilever (Zhou et al., 2002).

Zhou et al. (2002) used zeolite as the sensing layer to detect Freon-12. The zeolite was used as a molecular sieve that had a range of pore sizes and shapes, such that high selectivity could be achieved. Due to the small mass of the sensor, on the nanogram scale, very short response times of milliseconds, were achieved. To remove the freon-12, the films were placed under vacuum and the clean film was fully recovered within 20 seconds. These films were therefore reusable and showed good reproducibility for about three months.

2.2.5 Spectroscopic Techniques

Spectroscopic techniques are selective due to the unique spectrum a compound produces when electromagnetic radiation (or light) is shone on it. Each compound absorbs specific wavelengths and this can therefore be used in the identification of a compound in a mixture. These wavelengths may be chosen anywhere in the electromagnetic spectrum.

Cavity leak-out spectroscopy (CALOS) uses mid-infrared wavelengths to rapidly detect low concentrations of formaldehyde in ambient air. The wavelengths enter a cavity where they are looped to increase the amplitude of the wavelengths. Once the wavelengths have reached the threshold amplitude, they leak out and are detected. By looking at specific wavelengths, the analyte can be determined since each compound absorbs at specific wavelengths (see Figure 2.10). Several wavelengths may have to be compared to achieve high selectivity. CALOS had very high sensitivity since it could detect down to 2 ppb for formaldehyde (Dahnke et al., 2002).

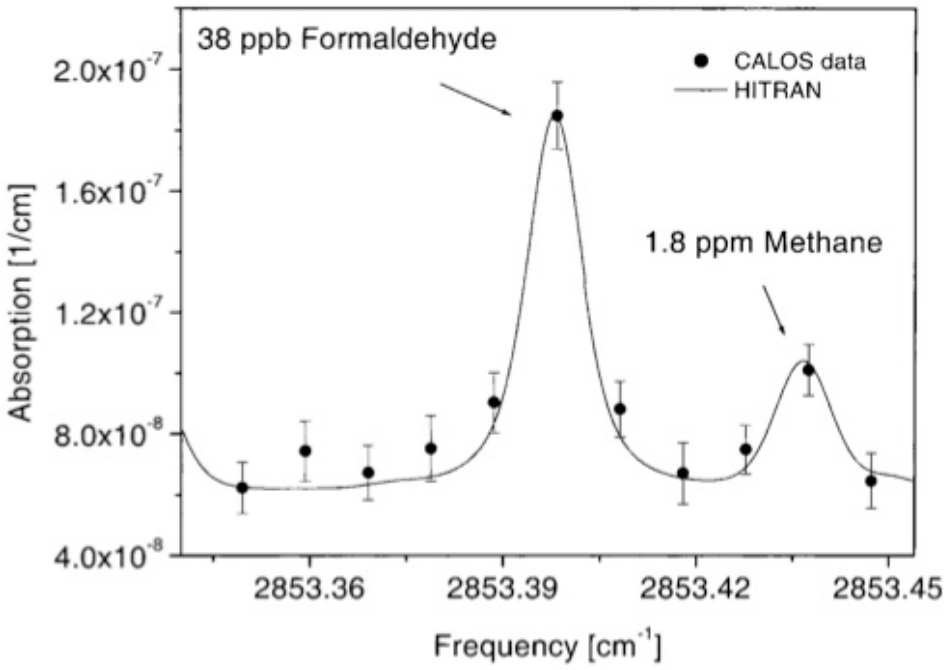

Figure 2.10: Spectrum of formaldehyde in ambient air. The spectrum is compared to HITRAN, which is a spectral database used to compare experimental data (Dahnke et al., 2002).

Horstjann et al. (2004) used a feedback loop to amplify the signal. The feedback loop was also used to achieve wavelengths between 2222 cm^{-1} and 3333 cm^{-1}, since 2853.4 cm^{-1} corresponds to the C-H stretching in aldehydes. Interband cascade lasers (ICLs) were used since they operate more efficiently at low threshold current densities. Formaldehyde was detected down to 1.2 ppmv; however, if 100mW power is reached, the detection limit may be as low as 25 ppbv.

2.2.6 Biosensors

Biosensors use biological materials, such as enzymes, microorganisms, antigens, antibodies, and organelles, as sensing materials due to their specificity towards certain chemicals (selectivity) (Mitsubayashi et al., 1994). The main problem with the use of these biological materials is their denaturation in gaseous environments (Mitsubayashi and Hashimoto, 2002a). Mitsubayashi et al. (2003) overcame this problem by using a flow cell that had separate liquid and gas compartments. The compartments were separated by a porous diaphragm membrane onto which the enzyme was attached, fully submerged in a phosphate buffer. The buffer kept the liquid at a neutral pH. A schematic diagram of the biosensor can be seen in Figure 2.11.

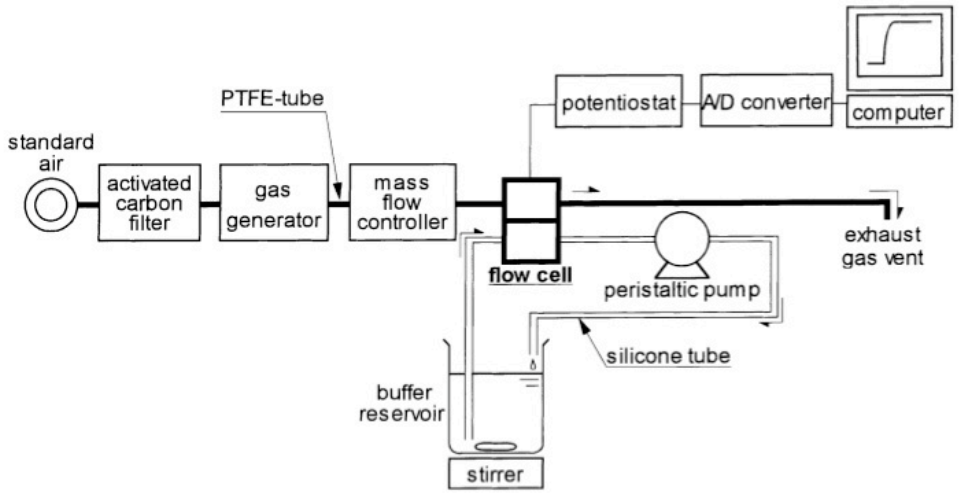

Figure 2.11: A schematic diagram of the biosensor (Mitsubayashi and Hashimoto, 2002b).

The gas diffused into the liquid compartment, where it interacted with the enzymes causing a reaction (see Figure 2.12). The oxygen produced was detected. From the amount of oxygen produced, the concentration of the analyte could be deduced (Mitsubayashi and Hashimoto, 2002a).

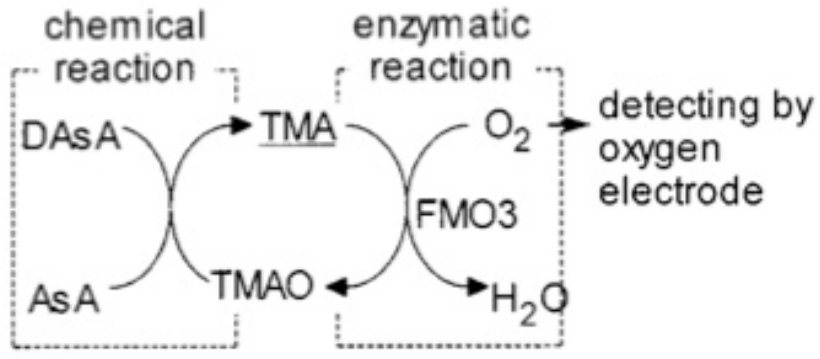

Figure 2.12: Principle of reaction for the biosensor for trimethylamine (TMA) using flavin-containing monooxygenase 3 (FeO3) enzyme and ascorbic acid (AsA) as a reducing agent. (TMAO: trimethylamine N-oxide, DAsA: dehydroascorbic acid); Mitsubayashi and Hashimoto (2002a).

The liquid buffer solution was constantly pumped through the cell to avoid a concentration build-up of the gas being detected (Mitsubayashi et al., 2003). This biosensor was modified to detect various gases, including acetylaldehyde (Mitsubayashi et al., 2003); trimethylamine (Mitsubayashi and Hashimoto, 2002a); methyl mercaptan (Mitsubayashi and Hashimoto, 2002b); and ethanol (Mitsubayashi et al., 1994). The specific enzyme and porous diaphragm were selected based on the target molecule and sensitivity required, respectively. The specificity of the enzyme detector can be seen in Figure 2.13, where it is compared to a semiconductor sensor.

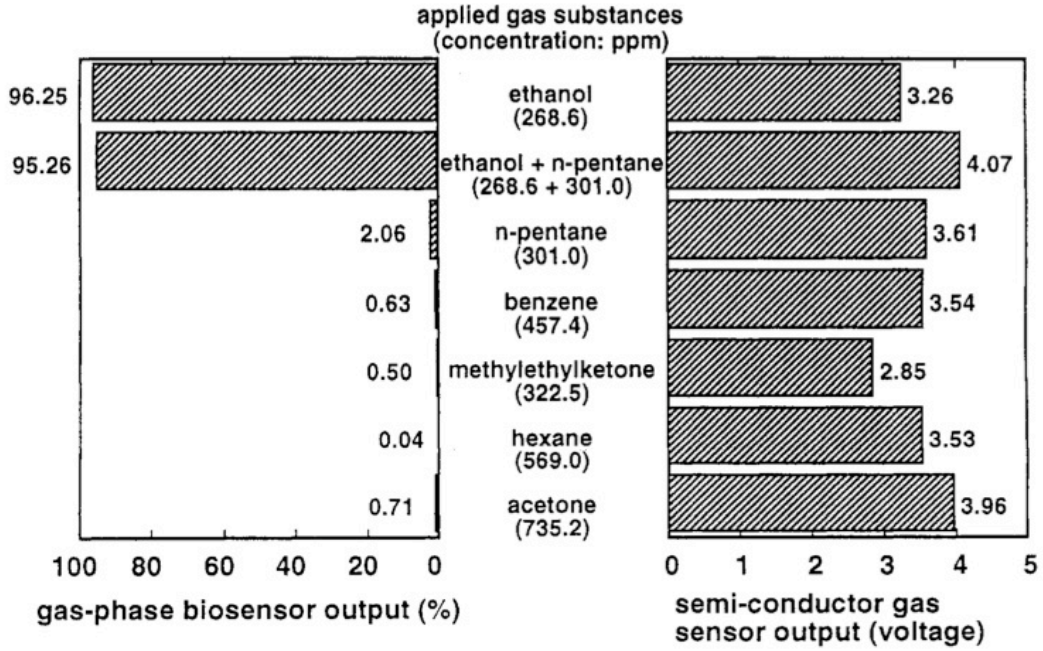

Figure 2.13: A comparison of the biosensor to a semiconductor gas sensor. A high selectivity for ethanol can be seen for the gas-phase biosensor (Mitsubayashi et al., 1994).

Vianello et al. (1996) designed a biosensor for formaldehyde which used the change in pH to determine the concentration of formaldehyde. The biosensor design was similar to that described above in which the enzyme was immobilized on a gold coated Nafion membrane (Au coated Nafion). Nafion is a perfluorinated polymer membrane that allows for cationic exchange. Due to the change in pH, the solution was buffered to avoid the denaturation of the enzyme.

Formaldehyde dehydrogenase (FDH) was the enzyme used to selectively target formaldehyde (HCHO) and nicotinamide adenine dinucleotide (NAD^+) was used to regenerate the enzyme after it had reacted with formaldehyde. FDH oxidized the formaldehyde into carboxylic acid, which produced one hydronium ion. A second hydronium ion was produced via the reaction of the reduced FDH from the first reaction per molecule HCHO of and oxidized NAD^+ (see Equations 2.7 and 2.8). The production of two hydronium ions (H^+) per formaldehyde molecule increased the sensitivity of the biosensor.

$$HCHO + FDH + H_2O \rightarrow HCOO^- + H_2FDH + H^+ \quad \text{(Equation 2.7)}$$

$$H_2FDH + NAD^+ \rightarrow NADH + FDH + H^+ \quad \text{(Equation 2.8)}$$

These biosensors had high selectivity, sensitivity in the ppm range, were capable of being miniaturized, and were easy to use. The time of detection varied with concentration of both the enzyme and the analyte. The main drawback of the membrane immobilized enzyme was that the membrane was expensive and time consuming to change (Vianello et al., 1996).

2.2.7 Electronic Noses

Electronic noses are designed to mimic the human or mammalian nose, although they are not as sophisticated. They consist of sensor materials that have partial selectivity for a variety of vapours and thus are capable of detecting multiple analytes at a time. This is combined with a pattern recognition program which identifies these analytes (De Wit et al., 1998).

De Wit et al. (1998) developed an iodine doped poly (2,5-thienylene vinylene) (PTV) sensor for multiple VOCs. The relative responses (R_a) and relative recoveries (R_b) were measured and are defined in Equations 2.9 and 2.10, respectively. The responses were measured while passing the vapour over the sensor for a period of one minute, while the recoveries were measured while passing dry air over the sensor for a period of four minutes. The relative responses and recoveries are summarized in Table 2.2.

$$Ra = \frac{R(2)-R(1)}{R(1)} \times 100\% \qquad \text{(Equation 2.9)}$$

$$Rb = \frac{R(2)-R(3)}{R(1)} \times 100\% \qquad \text{(Equation 2.10)}$$

In Equations 2.9 and 2.10, R(1) to R(3) represent, respectively, the absolute resistance of the reference signal measured immediately before exposure, the absolute resistance of the response signal measured immediately after one minute of exposure, and the absolute resistance of the recovery signal measured after four minutes of recovery time (De Wit et al., 1998).

Table 2.2: Mean Responses $<R_a>$ and Mean Recoveries $<R_b>$ of Nine Saturated Vapours

Saturated Vapour	**Experimental $<R_a>$ (%)**	**Experimental $<R_b>$ (%)**
Toluene	1.4	1.1
Water	1.7	2.6
N-propanol	5.5	4.8
Acetone	16.1	14.0
Acetic acid	29.0	4.4
Diethyl ether	9.5	6.8
Ethyl acetate	4.9	3.6
Methanol	16.1	10.5
Ethanol	9.8	7.3

$<R_a>$ and $<R_b>$ were averaged over five runs taken at 35°C (De Wit et al., 1998).

There was a large enough difference in the relative responses and recoveries for six out of the nine analytes, so that they could be distinguished in a R_b versus R_a plot (see Figure 2.14). Interference would come from the other three analytes that had similar values. For example, diethyl ether would interfere with ethanol since they have similar R_a and R_b values causing a greater signal response for ethanol. This sensor would be good as part of a sensor array that had multiple sensing materials which could be cross referenced to distinguish analytes such as diethyl ether and ethanol, which interfere with one another (De Wit et al., 1998).

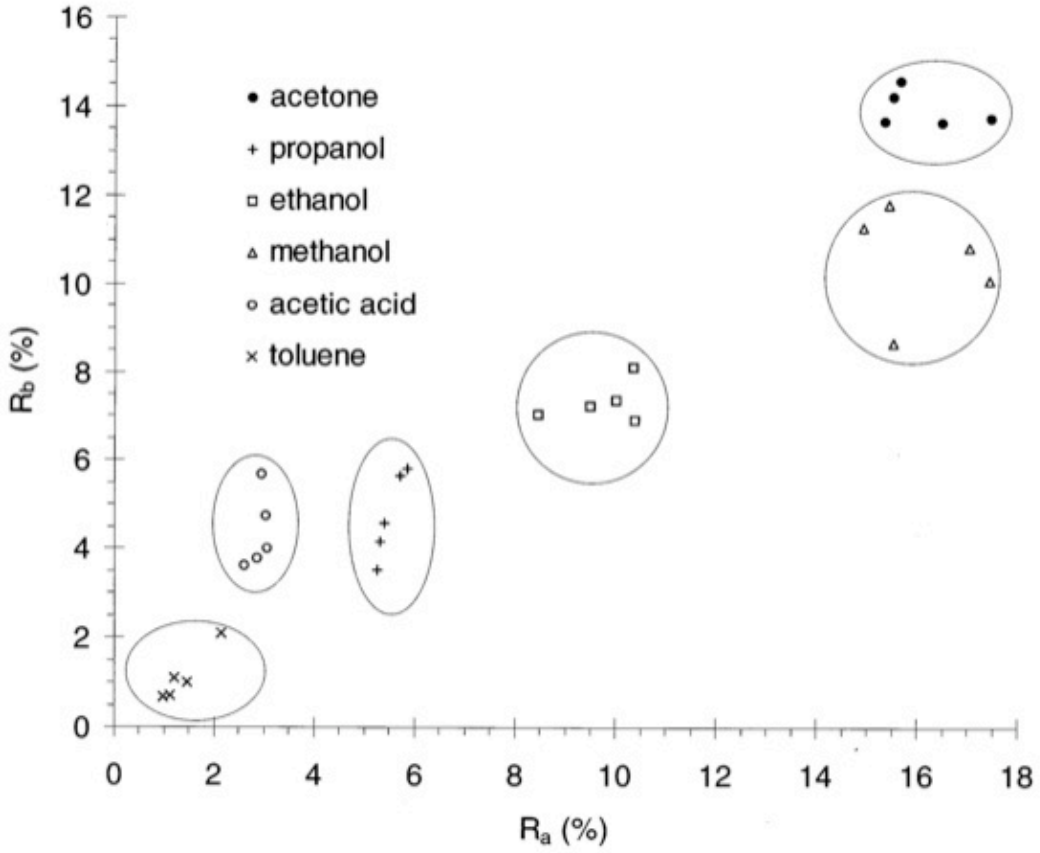

Figure 2.14: Two-dimensional plot of R_a and R_b values of saturated vapours resulting in distinguishable analytes (De Wit et al., 1998).

2.2.8 Chemical Reaction-based Sensors

A chemical reaction-based sensor uses a known chemical reaction with a specific analyte. A filter is saturated with reagents that selectively react with the target analyte creating a product that sticks to the filter. The filter is then tested for the product. The concentration of the analyte is determined from the amount of product on the filter.

Kawamura et al. (2005) developed a hand-held device that used glass filters saturated with 4-amino hydrazine-5-mercapto-1,2,4-triazole (AHMT) and potassium hydroxide (KOH) to

detect formaldehyde. AHMT was used since it has high sensitivity and selectivity toward formaldehyde. The sensor detected a change in colour that occurred when formaldehyde reacted with the reagents AHMT and KOH on the filter. The sensor was able to detect formaldehyde concentrations as low as 0.04 ppm with a sampling time of three minutes.

2.2.9 Passive Samplers

The previously discussed sensors are all active sensors. A passive sensor is a sensor that does not contain a pump mechanism; air is allowed to flow freely over the sensing material. Gillett et al. (2000) designed a passive sensor that used a filter impregnated with 2,4-dinitrophenylhydrazine (2,4-DNPH). The 2,4-DNPH reacted with formaldehyde to form formaldehyde-2,4-DNPH, which stuck to the filter. The sample was collected over a period of days, then removed from the filter into acetonitrile by ultrasonification and measured using high-performance liquid chromatogramy (HPLC).

Passive samplers can be more advantageous from a cost view point since they require no electricity, and they are small, light, silent, and inexpensive; however, they are less sensitive and they only measure average concentrations over a period of time (Gillett et al., 2000).

2.3 A Comparison of Sensors for Formaldehyde Detection

The detection characteristics for the previously discussed sensor materials are summarized in Table 2.3. AHMT is the best sensor overall since it has a detection limit below 0.08 ppm, operates at room temperature, has a long shelf life, and has a time of detection (response time) of three minutes.

Table 2.3: Summary of Detection Limit, Temperature of Detection and Time of Detection for Each Sensor Material

	Sensor Material	Detection Limit	Temperature of Detection	Time for Detection	Reference
1	PANI/MoO_3	25 ppb	100°C	20 minutes	Itoh et al., 2007a
2	PoANI/MoO_3	25 ppb	100°C	20 minutes	Itoh et al., 2007c
3	P2,5-DMA/MoO_3	9.1 ppm	40°C	20 minutes	Itoh et al., 2007a
4	PNMA/MoO_3	6.3 ppm	40°C	10 minutes	Itoh et al., 2007b
5	PPy/MoO_3	100 ppm	25°C	2.5 minutes	Hosono et al., 2005
6	PANI/NiO	39 ppm	600°C	1-3 minutes	Dirksen et al., 2001
7	PANI	500 ppm	20°C	60 minutes	Hosseini et al., 2005
8	Au coated Nafion	13 ppb	25°C	2 minutes	Knake et al., 2001
9	AHMT	0.04 ppm	25°C	3 minutes	Kawamura et al., 2005
10	8 SnO2 (Au, Cu, Pt, Pd)	0.06 ppm	200°C	15 minutes	Lv et al., 2007
11	CALOS	2 ppb	25°C	5 seconds	Dahnke et al., 2002
12	FDH/NAD^+ Biosensor	0.1 ppm	25°C	5 minutes	Vianello et al., 1996
13	Passive Sensor	7.6 ppbv	25°C	3 days	Gillett et al., 2000

The detection limit must be at or below 0.08 ppm; thus, sensors 3 through 7 are not able to be used to detect formaldehyde concentration in indoor air. The time of detection for the sensor should be less than five minutes (ideally in seconds). Therefore, sensors 1, 2, 10 and 13 are a poor choice since they all require long detection times. Sensors 8 and 12 use a buffer solution which drastically reduces the lifetime of the sensor device. The sensor should be reusable for months. The spectroscopic technique listed, sensor 11, requires costly and a large amount of equipment, and thus could not be transported easily.

Ideally, a sensor should be able to detect below 0.08 ppm, at a temperature between 15°C and 35°C, and over a short period of time (ideally in seconds). Since buildings and rooms have different temperatures, the range stated above should cover all cases. The detection limit of 0.08 ppm is based on a 30 minute measuring period according to the WHO; however, a detection time of less than five minutes would be more beneficial to a consumer.

Table 2.4: The Effect of Temperature on the AHMT Sensor

Temperature (°C)	**Reading (ppm)**
15	0.07
20	0.10
24	0.11
30	0.11
35	0.16

Concentration of formaldehyde: 0.11 ppm; sampling time: 3 minutes (Kawamura et al., 2005).

The AHMT sensor was tested over a range of temperatures (see Table 2.4). The concentration of formaldehyde tested was 0.11 ppm and the sampling time was three minutes. It can be seen that the temperature had an effect on the reading. Both 24°C and 30°C were in agreement with the set concentration and 20°C was in close agreement; thus the sensor worked well in that range (20-30°C). Both 15°C and 35°C were not in agreement with the actual concentration. Therefore, for the sensor to work over the full range, a correction factor or calibration was needed (Kawamura et al., 2005).

Several sensing materials were compared, including polymer- and non-polymer-based sensors. After comparing the sensing materials based on limit of detection, temperature of detection and time for detection, it was concluded that the AHMT sensor was the best for the detection of formaldehyde. The AHMT sensor was able to detect formaldehyde down to 0.04 ppm at room temperature after only three minutes.

2.4 Polyaniline (PANI) and Its Derivatives

PANI is made from the oxidation of aniline. Aniline is inexpensive, easily processed and produces a stable, conductive polymer (Feast et al., 1996). PANI exists in five oxidation states (see Figure 2.15). Emeraldine (see Figure 2.15) is the most stable form of PANI due to its high conjugation (Hosseini et al., 2005). Although none of the states are conductive, protonated forms of the moderately oxidized states, especially emeraldine, are conductive. This is referred to as “protonic acid doping”. The protonation creates charge carriers and this allows the charge to flow along the polymer chain. PANI is unique in that no electrons need to be added or removed from the insulating material to make it conductive (Feast et al., 1996).

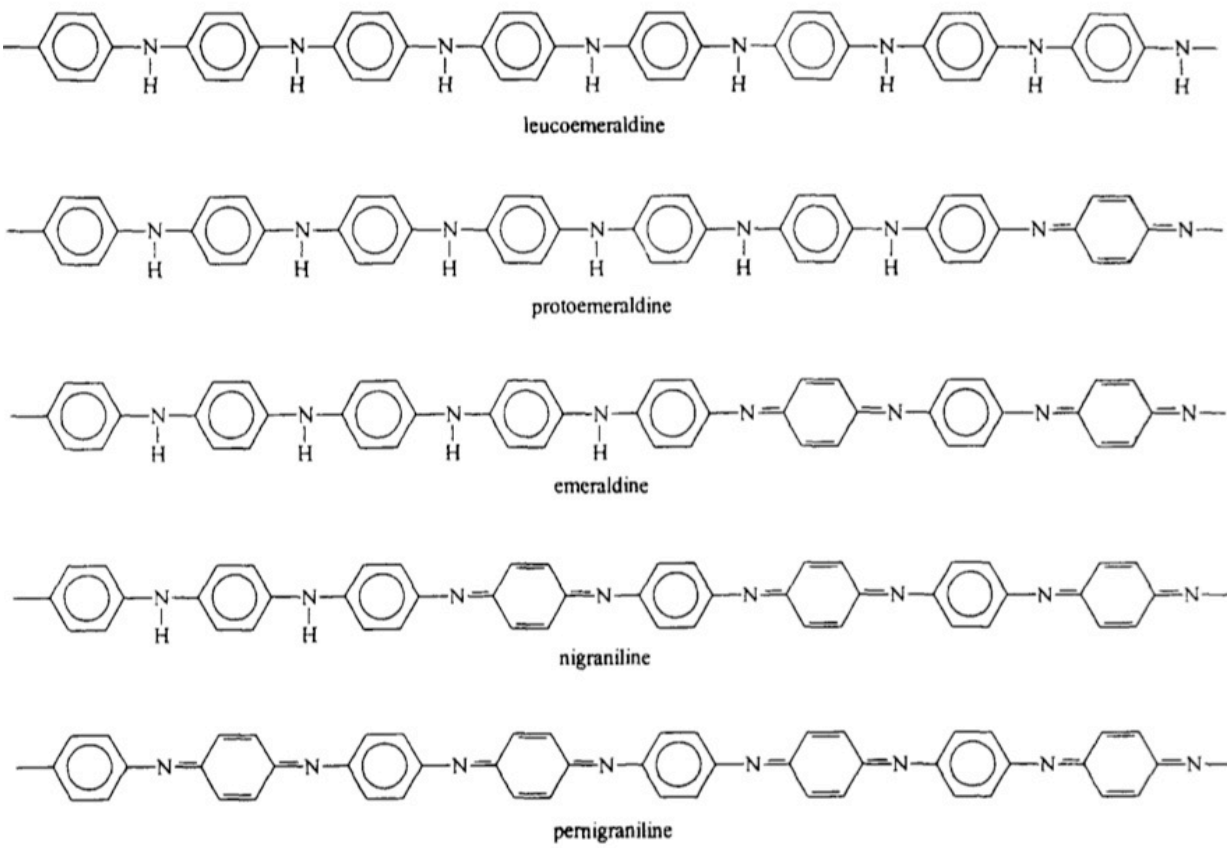

Figure 2.15: The five oxidation states of polyaniline (Feast et al., 1996).

Both PANI and its derivatives can be cross-linked by simply heating the emeraldine oxidation state. The cross-linking creates a more structured film, resulting in more spaces into which VOCs may be absorbed. The absorption of the VOCs causes a change in conductivity or weight and this change is what is detected (Feast et al., 1996).

PANI derivatives may be created by substituting some of the hydrogens on the aromatic ring with other functional groups, such as methyl (CH_3), ethyl (CH_2CH_3), methoxy (OCH_3) and ethoxy (OCH_2CH_3). This substitution may be done before the polymer synthesis (Nicolas-Debarnot and Poncin-Epaillard, 2003) and increases the solubility in organic solvents; however, it lowers conductivity (Liu et al., 2010). PANI's derivatives can be synthesized, cross-linked, and converted to conductive polymers in the same manner as PANI (Feast et al., 1996); however, PANI's derivatives were more soluble in organic solvents than PANI (Chen et al., 1997). The different functional groups on PANI and its derivatives may alter the sensing abilities of the film (See Figure 2.16).

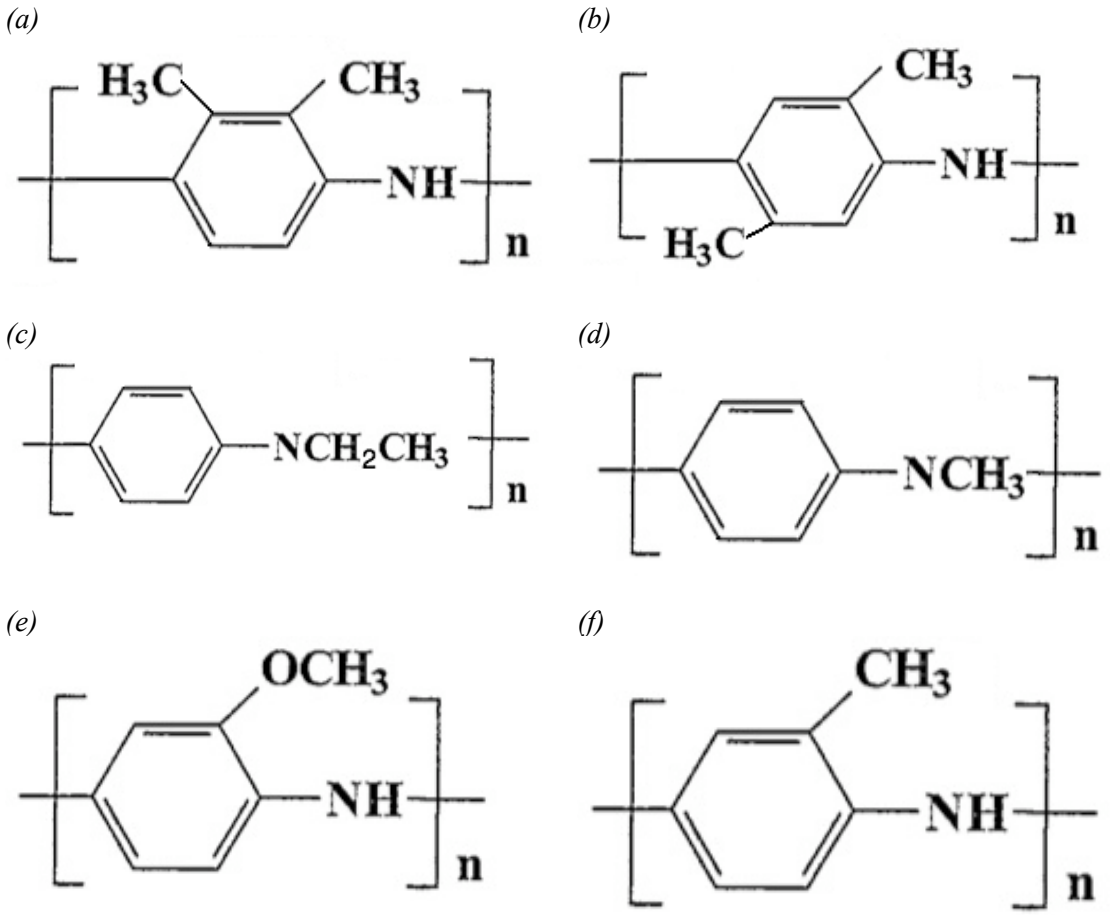

Figure 2.16: The general structure of PANI's derivatives: (a) poly (2,3-dimethyl aniline) (P2,3-DMA), (b) poly (2,5-dimethyl aniline) (P2,5-DMA), (c) poly (N-ethyl aniline) (PNEA), (d) poly (N-methyl aniline) (PNMA), (e) poly (o-anisidine) (PoANI), (f) poly (o-toluidene) (PoTol); Chen et al. (1997) and Feast et al. (1996).

PANI and its derivatives, PoANI, P2,5-DMA, and PNMA, are polymerized via oxidation of their monomers. This reaction propagates by a free radical mechanism (Nicolas-Debarnot and Poncin-Epaillard, 2003). The radical cations initially form in the pernigraniline oxidation state (Ayad et al., 2003). The radical may be found in three locations on the benzene ring (see Figure 2.17), but the *para* position to the nitro group ((2) in Figure 2.17) is the most reactive because of the lack of steric hindrance and inductive effects. Under acidic conditions, the "head-to-tail" reaction is favoured (Nicolas-Debarnot and Poncin-Epaillard, 2003); in other media, the "head-to-head" reaction is favoured (Hosseini et al., 2005).

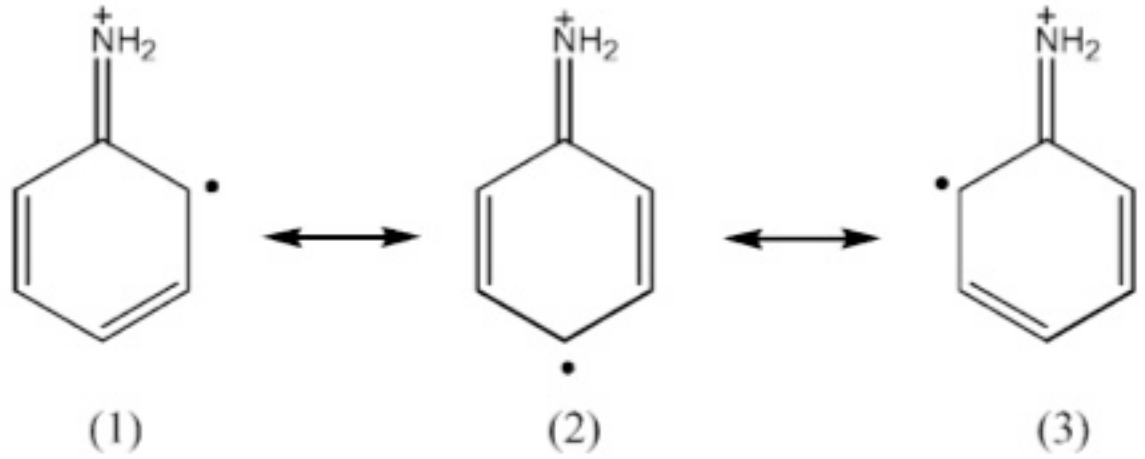

Figure 2.17: The resonance forms of the aniline radical cation. (2) is the most stable (Nicolas-Debarnot and Poncin-Epaillard, 2003).

PoANI is made from an *ortho* alkoxy substituted aniline monomer and is prepared in a similar fashion to PANI. *Ortho* substituted monomers react faster than *meta* substituted monomers, although both give the same polymer (Nicolas-Debarnot and Poncin-Epaillard, 2003).

PANI chain growth can follow a number of pathways (see Figure 2.18). Mechanisms 1 and 2 are via nucleophilic substitution, mechanism 3 is via radical addition and mechanisms 4 and 5 are via electrophilic addition of the two different oxidized forms of the aniline monomer. Due to the delocalization of charge densities, nucleophilic substitution (mechanisms 1 and 2) is less likely than the other mechanisms; however, as the film increases in thickness, the ohmic drop increases resulting in nucleophilic substitution being favoured over mechanisms 3 and 5. This explains the long polymer chains that result from the polymerization of aniline (Geniès et al., 1990).

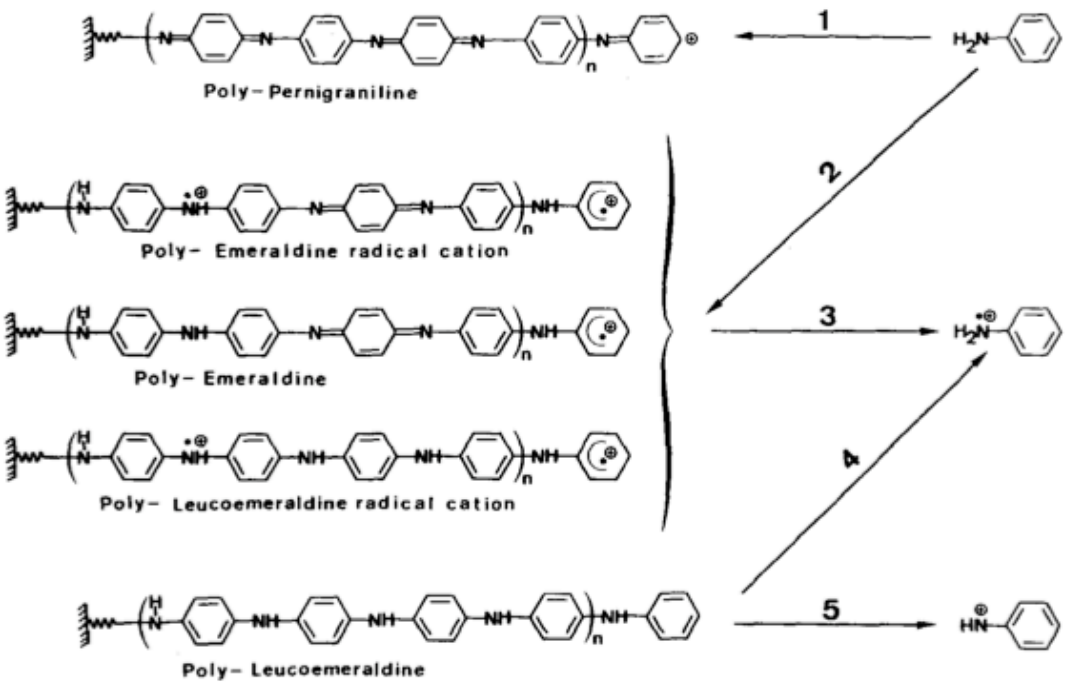

Figure 2.18: Reaction mechanisms for PANI (Geniès et al., 1990).

Polypyrrole (PPy) also polymerizes via oxidation and propagates via free radical reactions. The free radical exists in the 2- and 5-position on the ring. Due to steric hindrance, PPy is syndiotactic since the amine groups alternate sides (Koleli and Dundar, 2008); see Figure 2.19.

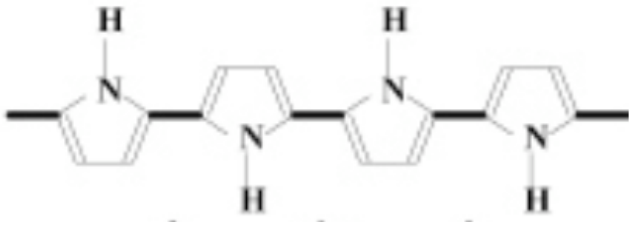

Figure 2.19: The structure of PPy (Hosono et al., 2005).

Some VOCs may also adsorb onto the surface of the PANI film, or its derivatives, via hydrogen bonding. The presence of a hydrogen attached to an electronegative nitrogen in all of the polymers allows for hydrogen bonding.

To detect VOCs in an indoor environment, a sensor must be able to function at room temperature. PANI and all of its derivatives are capable of detecting VOCs at room temperature (Itoh et al., 2008). A sensor must also be reusable. Therefore, the VOCs must be able to be removed from the polymer film. This is done easily by purging the system with either nitrogen or air and/or by heating the polymer film. Once the VOCs have been removed, the sensor can be reused (Itoh et al., 2007b).

The different functional groups attached to PANI affect sensitivity and selectivity. Various aliphatic alcohols have been used to compare PANI and its derivatives as sensing materials (see Table 2.5).

Table 2.5: Sensitivity Values of Polyaniline and its Derivatives for Different Alcohol Vapours

Polymer	**Methanol (± 1%)**	**Ethanol (± 1%)**	**Propanol (± 1%)**	**Butanol (± 1%)**	**Heptanol (± 1%)**
PANI	94.23	74.66	36.80	46.72	45.16
PoTol	90.00	60.00	8.82	31.14	15.24
PoANI	82.14	57.00	28.73	30.47	70.90
PNMA	73.91	40.00	17.60	6.39	38.09
PNEA	91.07	48.97	61.66	31.57	4.95
P2,3-DMA	95.93	61.53	29.07	26.47	97.91
P2,5-DMA	91.45	76.25	10.71	-	20.93
PDPA	83.87	54.45	37.50	32.14	55.55

Values >80% are considered high sensitivity (Athawale and Kulkarni, 2000).

PANI and most derivatives had high sensitivity towards methanol. This was primarily due to methanol's small size. None were highly sensitive to ethanol, propanol and butanol. As for selectivity, all but P2,3-DMA had high selectivity for methanol (Athawale and Kulkarni, 2000).

Layered organic/MoO_3 hybrid thin films made with PANI or one of its derivatives had excellent gas sensing properties, especially for aldehydes. Their sensitivity and selectivity could be controlled by the functional groups attached to the polymer. The advantage of these sensors was that they worked below 100°C and some also at room temperature (Itoh et al., 2008).

2.5 Sensitivity and Selectivity

2.5.1 Sensitivity

Sensitivity is defined as the ability of a sensor to produce a signal when low concentrations of a target analyte are present. The larger the signal, the more sensitive a sensor is. The sensitivity of a sensing material is defined as the concentration of analyte sorbed onto the sensing material divided by the total concentration of the analyte (see Equation 2.11). The

higher the concentration sorbed, the more sensitive the sensing material. A sensing material is deemed sensitive when the sensitivity is greater than 0.45.

$$Sensitivity = \frac{[Gas]_{Total} - [Gas]_{Residual}}{[Gas]_{Total}} \quad \text{(Equation 2.11)}$$

Depending on the VOC, detection levels may need to be as low as ppb. Therefore, high sensitivity is needed. Increasing the number of recognition (reaction or binding) sites for the VOC will increase sensitivity.

Itoh et al. (2008) were able to detect in the 25-400 ppb range for aldehydes. PANI/MoO_3 and PoANI/MoO_3 hybrids were made through an intercalation process, where insoluble polymers possessing a high degree of polymerization were filtered out. This removal allowed for the detection of formaldehyde and aldehydes in the ppb range.

Thin films and highly ordered structures increased sensitivity. These could be achieved by using the Langmuir-Blodgett (LB) technique. An increase in the number of layers in LB films increased sensitivity; however, the selectivity decreased. The increase in layers provided more sites into which the VOC could diffuse; however, these sites were not specific to any one VOC. Since the detector could not differentiate between the VOC signals, specificity was diminished (Chen et al., 1997).

2.5.2 Selectivity

Selectivity is a qualitative value that measures the difference in sensitivities. A ratio is taken between the concentration of two analytes that sorb onto the polymer (see Equation 2.12). The higher concentration is taken as the numerator (Gas 1). If the ratio is larger than 1.75, then the sensing material is selective towards Gas 1 (the target analyte), when Gas 2 is present as an interferent.

$$Selectivity = \frac{[Gas\ 1]}{[Gas\ 2]} \quad \text{(Equation 2.12)}$$

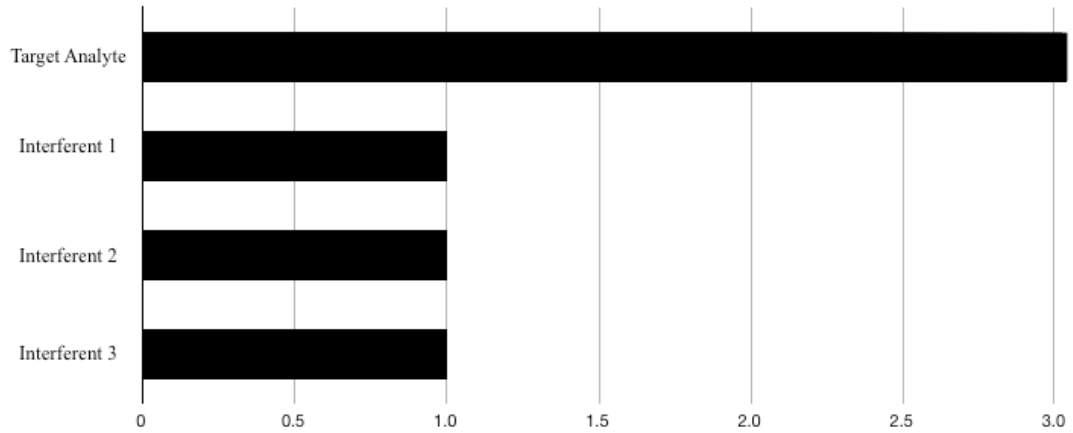

Figure 2.20: Ideal case for selectivity.

High selectivity is important for a sensor (see Figure 2.20). Itoh et al. (2007b) found that the selectivity of PANI could be controlled by the functional groups attached to it. Therefore, the use of one of PANI's derivatives may produce a more selective sensor for specific analytes.

PANI/MoO_3 hybrids displayed high sensitivity to formaldehyde, a moderate sensitivity to acetylaldehyde, and a weak sensitivity to the other VOCs measured. Therefore, there was high selectivity to aldehyde gases. This was most likely due to the presence of the H-C=O group which formed a hydrogen bond with Mo. There may also have been some nucleophilic interaction between the oxygen in MoO_3 and the carbon in the H-C=O. Since formaldehyde has two H-C=O groups, there should be a stronger interaction and thus a higher sensitivity (Wang et al., 2006); see also Figure 2.26.

P2,5-DMA/MoO_3 also had high selectivity for aldehyde gases; however, it had a higher sensitivity towards acetylaldehyde than formaldehyde (see Figure 2.21). This was because the solubility parameters of acetylaldehyde and P2,5-DMA are very close: 21.1$(MPa)^{1/2}$ and 21.0 $(MPa)^{1/2}$, respectively (Itoh et al., 2007a).

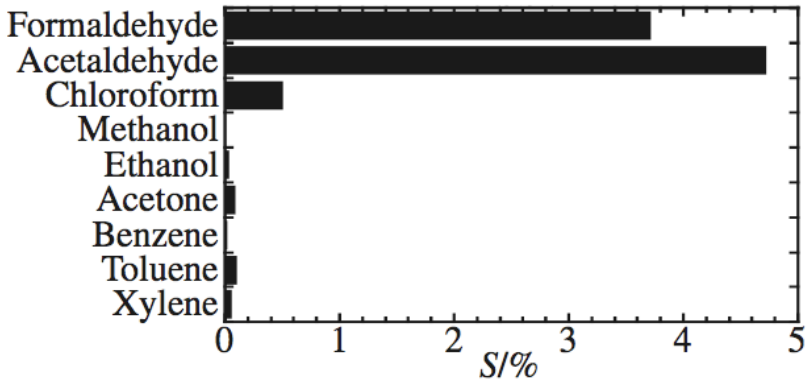

Figure 2.21: The sensitivity (S/%) of P2,5-DMA/MoO3 hybrid for various VOCs. Note the higher sensitivity for acetylaldehyde compared to formaldehyde (Itoh et al., 2007a).

2.6 Dopants

The sensitivity, selectivity, and response time of a sensor may be improved by adding a small amount of dopant (Nicolas-Debarnot and Poncin-Epillard, 2003). A dopant is defined as a trace amount of one material dispersed throughout a bulk material causing a significant change in one or more properties. The concentration, size, and shape of a dopant all affect the properties of the bulk sensing material (Choudhury, 2009). More than one dopant may be added into a bulk material at a time.

Dopants may be added to sensing materials to improve different properties. To increase the rigidity of flexible, organic, polymeric thin films, inorganic dopants are added. Inorganic dopants generally increase the thermal and mechanical stability of polymer sensing materials (Chen et al., 2009a). For gas sensors, metal and metal oxide dopants are used for both their electronic conductivities and their surface catalytic properties as oxidation catalysts (Dirksen et al., 2001).

Polyaniline (PANI) is not conductive unless it is doped with an HA type acid. By doing so, neutral PANI gains protons in an energetically favourable reaction (Kukla et al., 1996); see Equation 2.13 and Figure 2.22.

$$PANI + H\text{-}A \rightarrow PANI\text{-}H^+ + A^- \qquad \text{(Equation 2.13)}$$

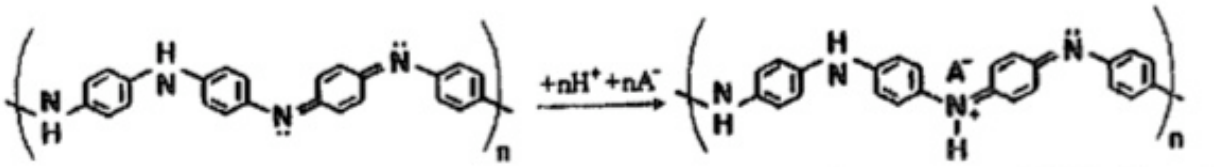

Figure 2.22: Schematic of PANI-acid doping mechanism seen in Equation 2.13 (Kukla et al., 1996).

This creates positively charged nitrogen (N) atoms, which creates holes, allowing valence electrons to jump from one hole, or positively charged nitrogen, to another. This creates p-type conduction. The current mechanism is similar to that of activated hopping conduction (Kukla et al., 1996).

2.7 Sensors for Other Volatile Organic Compounds (VOCs)

Volatile organic compounds (VOCs) are of great interest due to their environmental effects (Agbor et al., 1995), health effects (Endo et al., 2007), and use in industrial processes (Itoh et al., 2008). Classification of VOCs is based on their functionality. Sensors for detection of acids, alcohols, aldehydes and ketones, amines, and aromatics will be examined.

Generally, if inhaled, VOC symptoms include respiratory tract irritation, which can cause eyes and nose irritation, coughing, sneezing, choking, shortness of breath, headache and fatigue

(WHO, 2004). These symptoms occur at varying VOC concentrations. Although the toxicity levels of VOCs vary, they have an impact on human health. Thus, their detection is important.

Brown (2002) tested the indoor air quality of many buildings and found that the indoor concentration of VOCs was much higher than the VOC concentration of the outdoor air tested a few meters away from each building. This meant that there were many indoor sources of VOCs and that the VOC concentration did not come from outside sources.

It was found that newly manufactured materials emitted a significant amount of VOCs, which caused the indoor VOC concentration of new or newly renovated buildings to be one to two orders of magnitude higher than in older buildings. Over time, the amount of VOCs emitted from these materials exponentially diminished; however, the indoor VOC concentration never reached zero, but rather a basal concentration which could be seen in older buildings. It took many months to reach this basal concentration (Brown, 2002).

The VOCs did not solely impact the rooms in the building that were being renovated, but rather the entire building (Brown, 2002). Brown (2002) measured the VOC concentration in many rooms in several buildings and found that even rooms which were distant from, and even on a different floor than, the renovated room had much higher VOC concentrations than the basal concentration seen many weeks later. The distant rooms had a lower VOC concentration than the renovated room; however, this was only by approximately twenty to thirty percent.

2.7.1 Acids

Misra et al. (2004a) developed a thin film sensor for hydrogen chloride (HCl) vapour composed of an aniline and formaldehyde copolymer doped with a stoichiometric composition of iron-aluminum oxide (Fe-Al) (95:05). The Fe-Al induced a highly crystalized structure, which enhanced the sensitivity of the thin film. The thin film was used as a resistor in a circuit and the change in conductivity was used to determine the concentration of HCl. The sensor had a detection limit of 0.20 ppm which is below the short term exposure limit of 5 ppm. Compared to inorganic (oxide-based) sensors, the polymeric thin film had a much shorter response time of eight to ten seconds (see Figure 2.23), as opposed to one to two minutes, and operated at a lower temperature, room temperature, instead of 250-300ºC. The film was also stable and reusable since the HCl adsorbed onto, but did not chemically react with, the film.

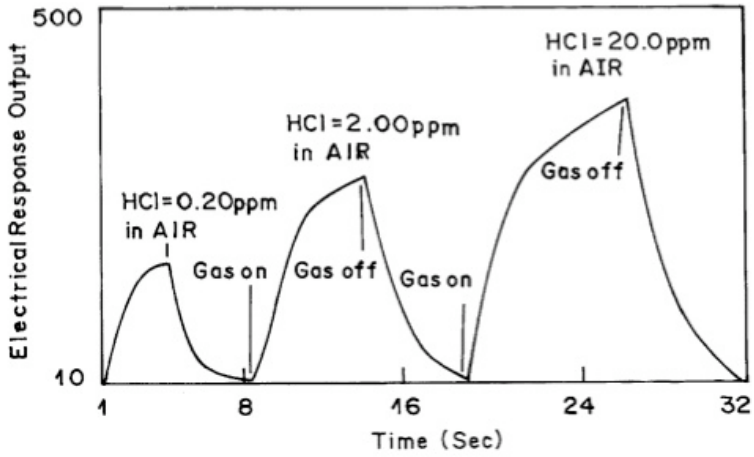

Figure 2.23: Response time of the sensor (Misra et al., 2004a).

Using a QCM with PoANI as the sensing layer, Chen et al. (1997) were able to detect organic acid vapours, including formic acid, acetic acid, propionic acid and butyric acid. The frequency shift was the measured quantity and was the result of added mass to the sensor. Therefore, butyric acid had the largest frequency shift given the same number of molecules of each organic acid attached to the sensor (see Figure 2.8). Steric hindrance was also a factor because formic acid was too small to provide much steric hindrance. Thus, more formic acid was able to attach to the sensor, increasing the frequency shift. Since there was a visible frequency shift for all of the organic acids tested (see Figure 2.8), the selectivity for the sensor was poor.

2.7.2 Alcohols

Athawale and Kulkarni (2000) compared different polymer pellets (PANI and its derivatives) as sensing materials for various aliphatic alcohols. The pellet was inserted into a circuit as a resistor and the change in resistance was measured, which was used to determine the concentration of the alcohol. The difference in chemical structure of the polymer, in conjunction with the chain length and dielectric nature of the alcohol, were the reasons for the different responses.

Methanol had a large change in resistance (high sensitivity) and a fast response time with P2,3-DMA pellets. The other polymer pellets (PANI, PoTol, PoANI, PNMA, P2,5-DMA, and PDPA) had high sensitivity, except PNMA, but long response times (Athawale and Kulkarni, 2000); see Table 2.5.

Mitsubayashi et al. (1994) developed a selective sensor for ethanol using a novel cell with both gas and liquid chambers separated by a porous membrane. The sensing material was an immobilized enzyme, alcohol oxidase (AOD), which was attached to the porous membrane and fully submerged in the liquid solution. The sensor was able to measure ethanol

concentrations of 0.348-1242 ppm depending on the size of the pores in the membrane. The disadvantage of this sensor was its short lifetime due to low enzyme and thermal stability.

PANI and many of its derivatives were tested for their sensitivity and selectivity for ethanol, propanol, butanol, and heptanol; however, none of the polymers tested were good sensing materials for ethanol, propanol and butanol. P2,3-DMA had very high sensitivity for heptanol, but it also had very high sensitivity for methanol (Athawale and Kulkarni, 2000); see Table 2.5. Thus, its selectivity was not very good. It may be possible to design a dual sensor that measures the concentration of methanol using a different material in conjunction with P2,3-DMA, thus enabling it to sense both methanol and heptanol to determine the concentration of heptanol.

2.7.3 Aldehydes and Ketones

Acetylaldehyde is the main interfering analyte when detecting formaldehyde since they are chemically similar. If a sensor is not selective enough for formaldehyde, it may be possible to use multiple sensing heads to simultaneously determine the concentration of acetylaldehyde and therefore, calculate the concentration of formaldehyde.

Some sensors for acetylaldehyde have been developed. Mitsubayashi et al. (2003) created a biosensor that used aldehyde dehydrogenase (ALDH) to selectively target acetylaldehyde (see Figure 2.24). The detection range was based on the pore size of the membrane: 0.525-20.0 ppm for the 1-2μm pore size and 0.105-5.25 ppm for the 20-30μm pore size.

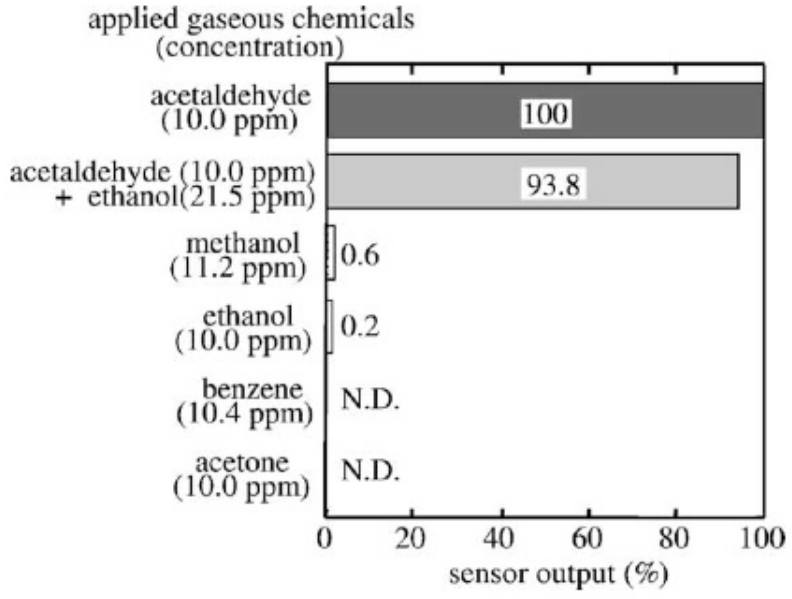

Figure 2.24: Selectivity of ALDH for various gases. Note the response for acetylaldehyde and ethanol is almost the same as for acetylaldehyde alone (Mitsubayashi et al., 2003).

A conductive, sensing, thin film of poly (5,6,7,8-tetrahydro-1-naphthylamine) (PTHNA) doped with MoO_3 was used to detect aldehydes. Above 50 ppb, acetylaldehyde produced a stronger signal than formaldehyde (Itoh et al., 2007c); see Figure 2.25.

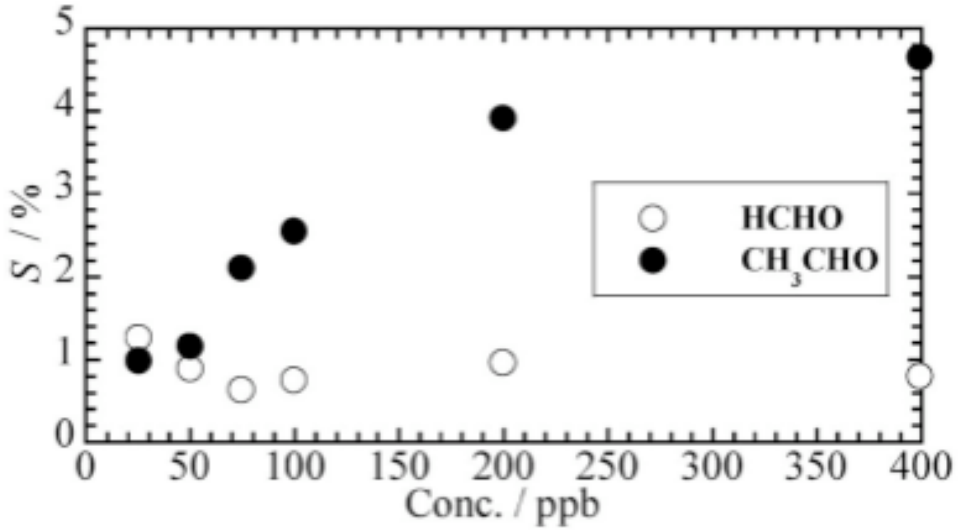

Figure 2.25: Response signals (S) to acetylaldehyde and formaldehyde below 400 ppb (Itoh et al., 2007c).

Using a polymer doped with MoO_3, Wang et al. (2006) designed a sensor for small aldehydes. This sensor used PANI intercalated with MoO_3 as the sensing material and the change in resistivity was measured. The sensor was more sensitive to formaldehyde than acetylaldehyde; however, it did not have the selectivity required for a sensor (Wang et al., 2006); see Figure 2.26.

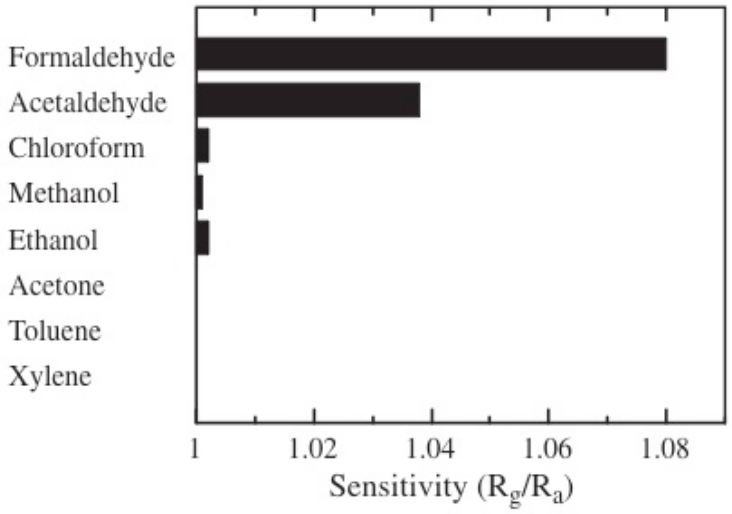

Figure 2.26: The sensitivity of PANI/MoO_3 in response to various VOCs, where the sensitivity is defined as the resistance of the gas interaction with the sensing material divided by the resistance in air (Wang et al., 2006).

Since the sensor created by Itoh et al. (2007c) was below the exposure limit of formaldehyde, this sensor could be used in conjunction with another sensor such as the one developed by Wang et al. (2006) to detect formaldehyde concentration. By cross referencing the outputs of both sensors, the concentration of both acetylaldehyde and formaldehyde could be determined.

A sensor for acetone based on electrical conductivity was developed by Ruangchuay et al. (2003) using a film of α-naphthalene sulfonate-doped polypyrrole/poly (methyl methacrylate) (PPy/α-NS^-/PMMA). When PPy /α-NS^-/PMMA interacts with the acetone, it swells, which results in a change in electrical conductivity, which is measured. Acetone is highly flammable and thus, its detection should be between its explosive limits: 2.5-12.8 vol.%; however, only saturation values of acetone were recorded at 30.3 vol.% at 25°C.

The main interferences for the acetone sensor were acetic acid and water. PPy/α-NS^- improved the selectivity for acetone because it interacted differently with acetone and acetic acid. Acetone formed a hydrogen bond with the N-H group in PPy that was reversible, whereas acetic acid protonated the =N- group of the PPy/α-NS^- permanently under the conditions studied. Since acetic acid formed a stronger bond, PPy/α-NS^- swelled less, and thus produced a smaller signal. Water would have increased the signal by increasing the ionic conductivity. PMMA reduced the effect of humidity since it sheltered the PPY/α-NS^- from water. The sensor was stable over a range of relative humidity (RH), 20-70%; however, as RH increased, so did the sensing time, which went from 10 to 50 minutes (Ruangchuay et al., 2003).

2.7.4 Amines

Ai et al. (2007) designed a fiber sensor used to detect ammonia gas. The sensor used an etched superstructure fiber Bragg grating (SFBG) cladded in PANI (sensing head); see Figure 2.27. As the ammonia gas reacted with the PANI coating, the refractive index of the cladding layer changed and resulted in a Bragg wavelength shift. The shift in wavelength was measured by a spectrometer (see Figure 2.28).

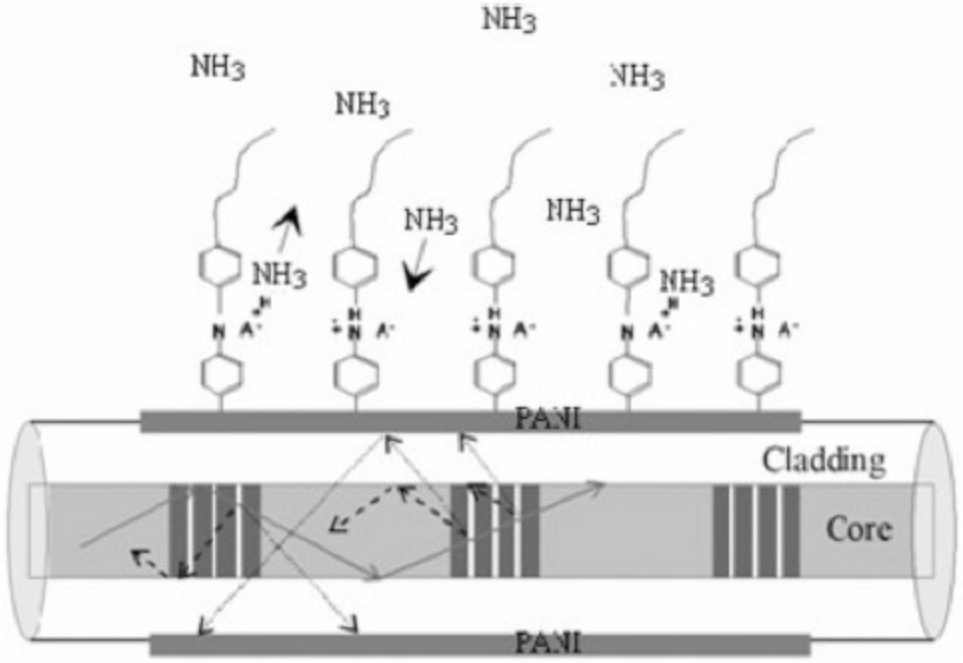

Figure 2.27: A schematic of the SFBG sensing head (Ai et al., 2007).

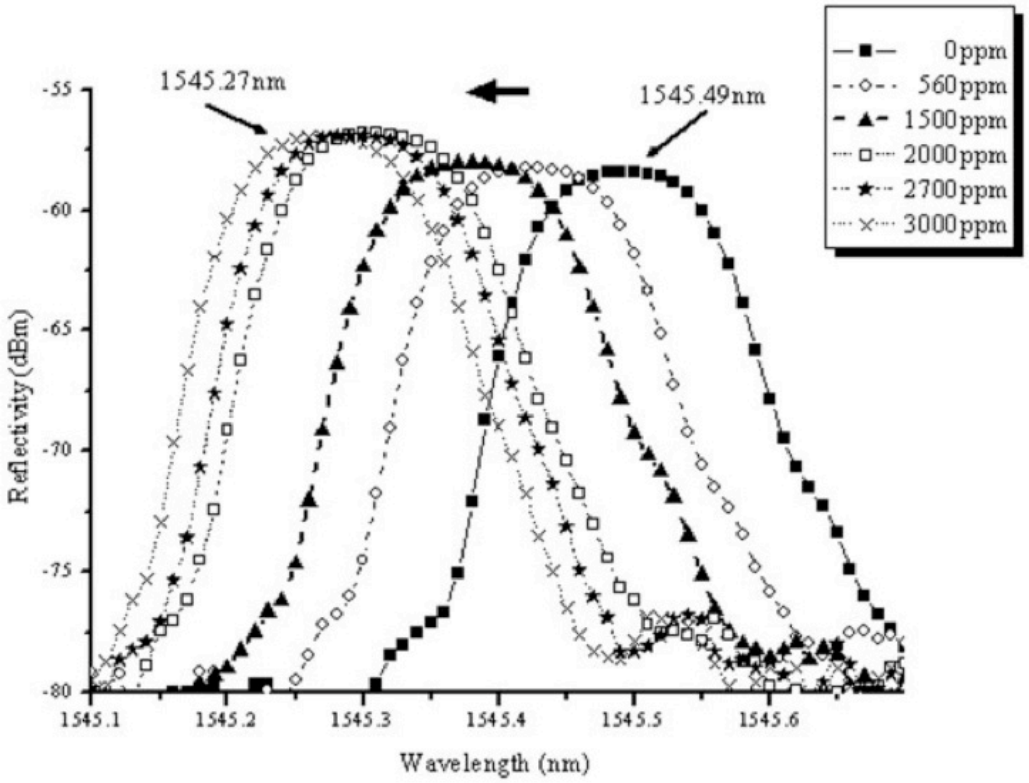

Figure 2.28: The sensor reflection spectra for different concentrations of ammonia gas (Ai et al., 2007).

To keep the SFBG sensing head straight during the measurements, it was fixed to a fiber holder. This ensured an accurate measurement of the wavelength shift since bending of the SFBG sensing head would have bent the light and affected the measurement. It took several minutes to return the sensor to its original state by passing pure nitrogen gas over the cladding. This removed ammonia from the sensor (Ai et al., 2007).

Another ammonia sensor was designed by Kukla et al. (1996) that used an acid doped polyaniline (PANI) as the sensing layer. The change in resistance caused by the chemiadsorption of ammonia onto PANI was measured. This sensor was able to reproducibly detect ammonia over a wide range of concentrations (5-2000 ppm), over a short response time, and had a moderately short recovery time; see Figure 2.29 for response and recovery times.

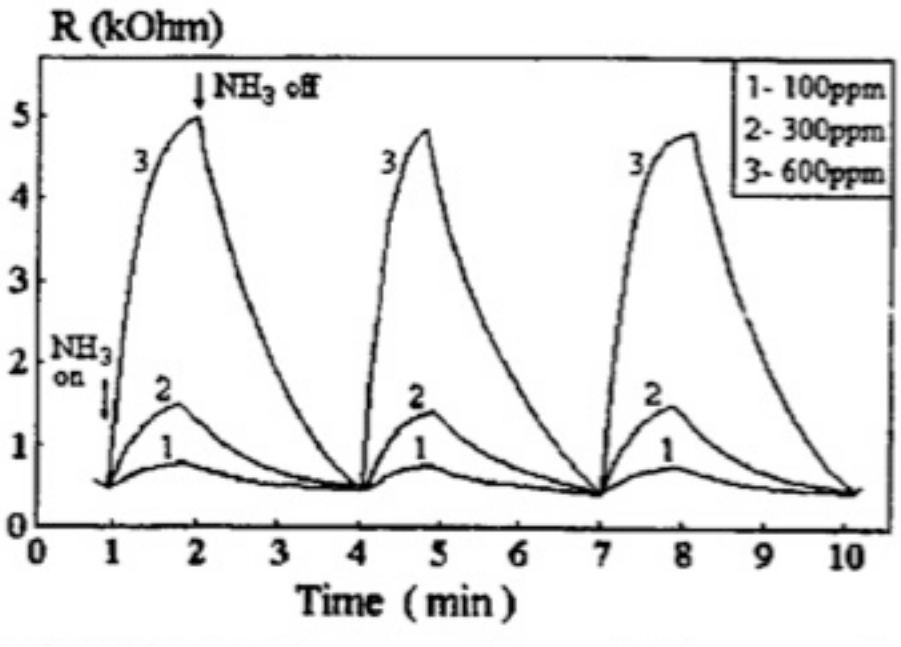

Figure 2.29: The response and recovery times of ammonia at different concentrations (Kukla et al., 1996).

Both the response and recovery times were a little longer for higher concentrations of ammonia. The recovery time was shortened by heating the PANI film to 104°C; however, if PANI remained in a high concentration of ammonia for more than an hour, then it would not be possible to return the PANI sensor to its original state (Kukla et al., 1996).

Trimethyl amine (TMA), which causes fish odour, is toxic at elevated levels causing respiratory irritation. Its exposure limit is 5.0 ppm (Mitsubayashi and Hashimoto, 2002a). Mitsubayashi and Hashimoto (2002a) designed a selective biosensor which used flavin-containing monooxygenase 3 (FCO3) to detect the concentration of TMA (see Figure 2.30). The sensor had a detection limit of 0.52 ppm, which was below the exposure limit. The sensor was reusable and the sample time was five minutes (see Figure 2.31).

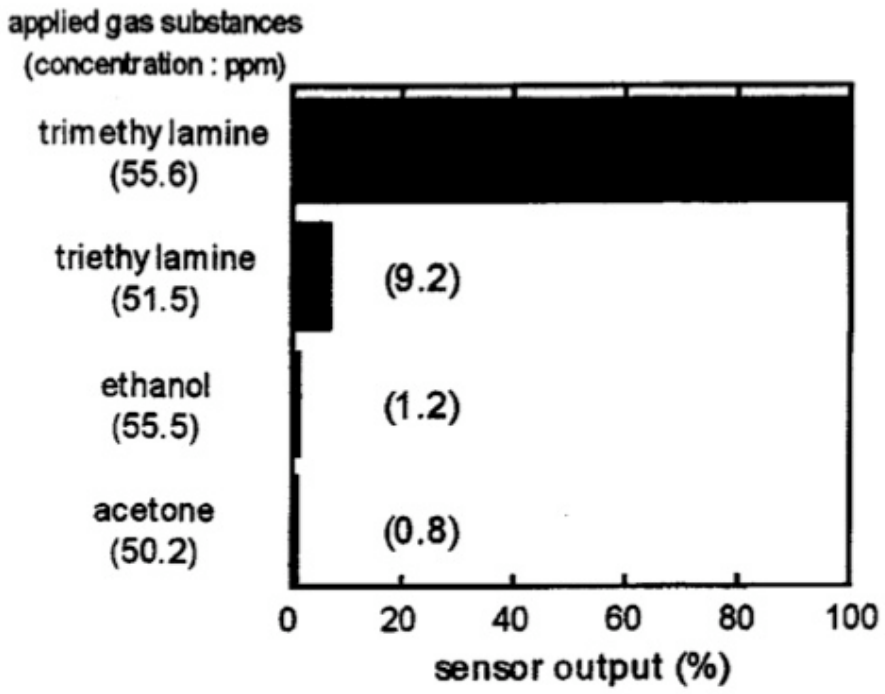

Figure 2.30: Selectivity of FCO3 biosensor for various VOCs (TMA: 55.6 ppm, triethylamine: 51.5 ppm, ethanol: 55.5 ppm, and acetone: 50.2 ppm); Mitsubayashi and Hashimoto (2002a).

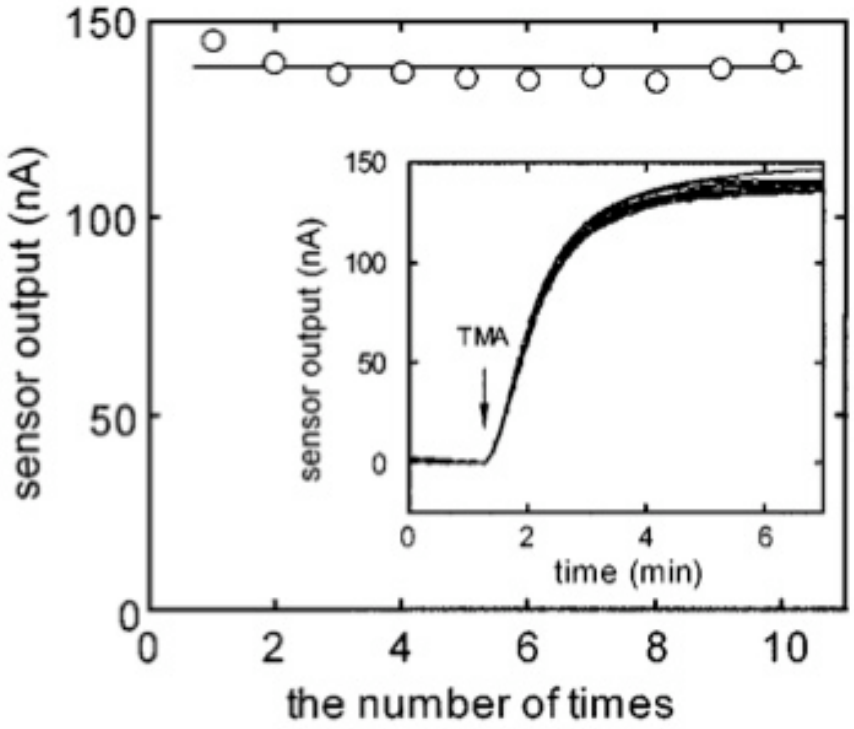

Figure 2.31: FCO3 biosensor reproducibility for n = 10. Inset: 10 trials of the device for 55.6 ppm TMA vapour (Mitsubayashi and Hashimoto, 2002a).

2.7.5 Aromatics

A poly (dimethyl siloxane) with 2.0% (w/v) polystyrene (PDMS/PS) colloidal crystal-based sensor for aromatic (benzene, toluene, and xylene) solutions was developed. The PDMS/PS swelled upon the introduction of the aromatic solutions which resulted in a wavelength shift. A spectrometer was used to measure the wavelength shift; however, the shift was visible to the naked eye via a colour change (Endo et al., 2007).

PDMS/PS, the colloidal crystal, was highly selective for aromatic solutions since it swelled to a much greater extent in non-polar organic solvents (see Figure 2.32). Once the aromatic solution was removed from the matrix, by allowing it to dry in air, the PDMS/PS colloidal crystal shrank and the wavelength returned to its original value. This meant that the sensor was reusable. The detection limits of the aromatic solutions were 10ng/mL for benzene, 1 ng/mL for toluene, and 10 pg/mL for xylene (Endo et al., 2007).

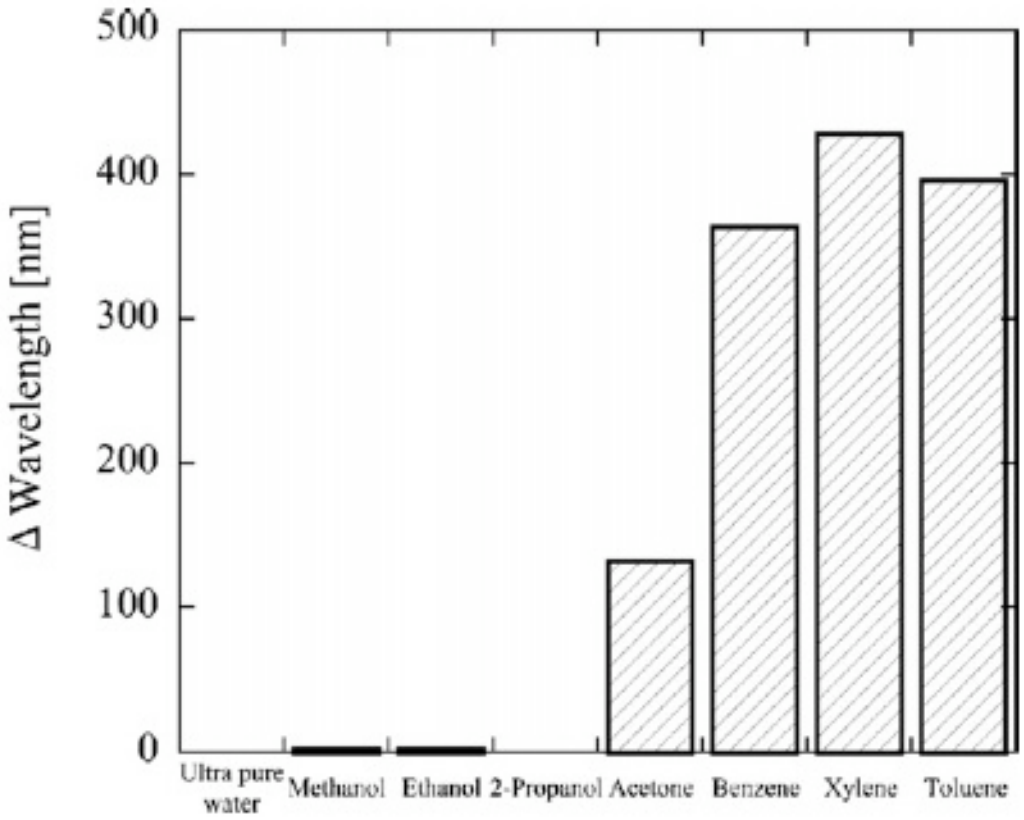

Figure 2.32: Selectivity for different kinds of organic solvents using the PDMS/PS colloidal crystal-based sensor (Endo et al., 2007).

2.8 Inorganic Sensors

2.8.1 Carbon Dioxide (CO_2) Sensors

Carbonate type electrodes are a good option for CO_2 detection (Fergus, 2008). Figueroa et al. (2005) used a Li_2CO_3 sensing electrode coupled with a Li_3PO_4 solid-electrode and a Li_2TiO_3 + TiO_2 reference electrode to detect CO_2 at temperatures from 400°C to 500°C. A range of 500 ppm to 50% was tested; however, it was found that the sensing ability suffered from particulate contamination and thus a filter was recommended to improve the sensing ability.

2.8.2 Carbon Monoxide (CO) Sensors

Traditional carbon monoxide (CO) sensors use the reducing properties of CO on an n-type semiconductor. The main problem with n-type semiconductors such as tin oxide (SnO_2) is their lack of selectivity (Aruna et al., 2009). P-type sensors are generally doped and have improved selectivity as well as sensitivity. Therefore, P-type semiconductor sensors have been developped (Zhuiykov and Dowling, 2008).

2.8.2.1 High Temperature Sensors (Above 100°C)

Tischner et al. (2009) developed a SnO_2 ultra thin film sensor for the detection of CO at 300°C. The sensor was able to detect CO at 4 ppm; however, the sensor had poor stability and selectivity. To improve the stability, SnO_2 nanowires were used since they have less signal drift over time and thus greater stability. To improve the selectivity, platinum was sputtered onto the nanowires which resulted in greater selectivity and sensitivity, by reducing the signal caused by humidity, and lowering the detection limit to 3 ppm.

Aruna et al. (2009) used monodispersed tin oxide: palladium (SnO_x:Pd) mixed nanoparticle layers which allowed for the detection of CO at 10 ppb at an optimum temperature of 573K. The addition of the Pd created a p-type semiconductor and improved both the sensitivity and selectivity of the sensor (See Figure 2.33).

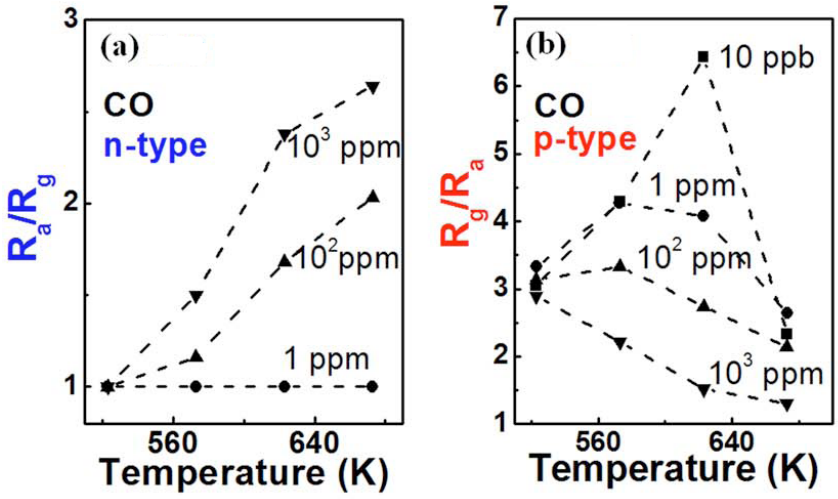

Figure 2.33: The signal (R_a/R_g) for varying concentrations of CO at different temperatures for (a) an n-type sensor (SnO_x) and (b) a p-type sensor (SnO_x:Pd); Aruna et al., (2009).

2.8.2.2 Low Temperature Sensors (Less than 100°C)

Zhuiykov and Dowling (2008) made a low temperature CO sensor using 0.05% gold-loaded cobalt oxyhydroxyide (Au-CoOOH) nanostructures. The sensor had an optimum sensing temperature at 80°C for 10 ppm. The Au-CoOOH had very good selectivity.

Galdikas et al. (1996) created resistance switching in SnO_2/ultrathin platinum (Pt), which was induced by the interaction with CO. The change in resistance of the Pt was measured. The sensor had a detection in the range of 10 - 40 ppm below 100°C.

2.8.3 Humidity (H_2O) Sensors

2.8.3.1 Low Temperature (Below 100°C) Sensors

Zhang et al. (2007) designed a relative humidity sensor based on poly(m-aminobenzene sulfonic acid) functionalized single-wall carbon nanotubes (SWCNTs). The sensor had a linear response between 10% and 70% relative humidity at room temperature. The response was based on an increased resistance as the water molecules adsorbed onto the surface of the SWCNTs.

Wiedijk (1980) created a humidity sensor for glove boxes. It consisted of a small alumina substrate with two rhodium electrodes. The change in current was measured since it was directly proportional to the water vapour pressure. At atmospheric pressure, the sensor worked between 20°C and 70°C, whereas in vacuum, the sensor worked at 20°C up to about 150°C.

2.8.3.2 High Temperature (Above 100°C) Sensors

Chen et al. (2009b) designed a humidity sensor that operated at 400°C which was made of Y-doped $BaZrO_3$. Water vapour dissolved into the Y-doped $BaZrO_3$ lattice and filled the oxygen vacancies that were created by the doping of Ba with lower valence ions such as Y^{3+} and Zr^{4+}. As water vapour filled these vacancies, protons were released into the lattice which increased the conductivity, which was measured. This sensor had high selectivity as it showed no response to NO_2, NH_3, or O_2.

Zhou and Ahmad (2008) created a $CaZrO_3$ doped with 10 mol% In sensor for humidity and hydrogen, with an optimum operating temperature of 700°C. Doping with In increased the oxygen ion conductivity and thus the sensitivity towards water vapour and hydrogen. The sensor was produced by sol-gel processing and the most porous In-doped $CaZrO_3$ was used, which increased the exposed surface area and allowed more interaction with the water vapour.

2.8.4 Mercaptan Sensors

Biosensors have been discussed in detail in Section 2.2.6. The biosensor developed by Mitsubayashi et al. (2003) was modified to detect methyl mercaptan using the xenobiotic metabolizing enzyme flavin-containing monooxygenase (Mitsubayashi and Hashimoto, 2002b).

2.8.5 Nitrogen Oxide (NO_x) Sensors

Polymeric materials are not used for the detection of NO_x. Instead, NiO and/or ZrO_2 are the most common sensing materials (Plashnitsa et al., 2010). Plashnitsa et al. (2010) used a NiO sensing electrode on a yttria-stabilized-zirconia (YSZ) electrolyte to sense NO_2. The sensor was able to detect down to 50 ppm at 800°C; however, it had poor selectivity towards NO_2, since a large signal was also produced for CH_4.

Sekhar et al. (2010) used a $La_{0.8}Sr_{0.2}CrO_3$ working electrode in a mixed potential sensor to detect NO_x down to 100 ppm at 600°C. A positive current bias was used to improve selectivity towards NO_x; however, the stability of the sensor was poorer with the positive current bias which caused a baseline drift over time.

Yang et al. (2008) designed a potentiometric NO_x sensor that used Pt electrodes on a yttria-stabilized-zirconia (YSZ) electrolyte. Pt-loaded zeolite (PtY) was used as a filter to remove interferents such as CO, propane, and NH_3. The sensor was highly selective due to the added filter and had an optimum operating temperature of 500°C. The sensor was also very sensitive and could detect NO_x down to 1 ppm. There was, however, baseline drift over time.

Figueroa et al. (2005) also used a Pt-loaded zeolite Y as a catalyst with a Pt reference electrode to detect NO_x. A filter was used to catalyze the ionization of NO_x. The sensor was

tested over a range of 100-400 ppm at temperatures between 300°C and 500°C. This sensor had high selectivity due to the filter used.

2.8.6 Radon (Rn) Sensors

Radon (Rn) is not measured directly. Instead the alpha particles given off during its decay are measured. Passive samplers are also generally used due to their low cost (Degerlier and Celebi, 2008).

The main problem with Rn sensors is interference due to humidity. Water droplets may come into contact with the sensor, thus restricting access of the Rn to the sensor. Miles et al. (2009) encased a passive sampler in a heat sealed polyethylene bag that allowed Rn to pass through, but not water nor the decay products of Rn.

2.8.7 Sulfur Oxide (SO_x) Sensors

Qin et al. (2005) created a sensor for SO_2 similar to the CO sensor. They used a Au patterned electrode on PTFE to detect down to 100 ppm SO_2. Their sensor had poor response and recovery times of six to eleven seconds, although it did have high stability.

Shimizu et al. (2006) tested many different metal sulfides for the detection of SO_2 and found that there was no response for any of them between 150°C and 250°C. There was, however, a response above 400°C. The largest response was given by CdS, which also had one of the shortest response times of four minutes for 100 ppm, which is too slow for online monitoring. $Pb_{0.9}Cd_{0.1}S$ had the shortest response time of three minutes, but had a lower signal response and the response time was too slow.

2.9 Formaldehyde Sensor Applications

The main application for formaldehyde sensors is monitoring indoor air quality. This can be done either by using a portable sensing device or including a sensing device in heating, ventilation and air conditioning (HVAC) systems. Portable sensing devices can be used in either industrial, commercial, or residential applications. For example, the sensors can be used to monitor environmental air quality (Agbor et al., 1995) as well as headspaces in reactors (Li et al., 2008). Incorporating a sensor into an HVAC system will allow for continuous detection. When the sensor detects a concentration of formaldehyde above the recommended amount, the ventilation system can flush the building with fresh air from outside. This will reduce the concentration of formaldehyde inside the building and the ventilation can be shut off once acceptable levels of formaldehyde have been reached. A system set up like this ensures optimal indoor air quality and can be expanded to other irritating or toxic gases (Itoh et al., 2007a; Yang et al., 2009).

Chapter 3: Experimental

3.1 Sensor Constraints

The most important component of the sensor is the sensing layer. To determine which material(s) is the most appropriate for the sensing layer, many factors must be taken into consideration. Above all, the sensing layer must both selectively interact with and be sensitive to low concentrations of formaldehyde.

For the sensor to be reusable, it must be able to be regenerated. This can be done by either passing fresh, non-contaminated (formaldehyde free) air over the sensing layer to allow the formaldehyde to diffuse from the sensing layer into the stream of fresh air, and/or by heating the sensing layer, which provides energy to the formaldehyde, making it easier for the formaldehyde to remove itself from the sensing layer. Heating the sensing layer increases the rate at which formaldehyde is removed, and thus reduces the recovery time of the sensor (Nicolas-Debarnot and Poncin-Epaillard, 2003).

A larger surface area for the sensing layer increases the sensitivity of the sensor (Wang et al., 2008b); however, the surface area is constrained by the area available on the sensor. The application of a thin film of sensing material to the sensor improves the sensing ability of the sensor (Lee et al., 2007).

3.2 Material Selection

3.2.1 Sensing Materials

Polymers are good sensing materials since they work at low temperatures (Mabrook and Hawkins, 2001), possess high toughness, and are recyclable (Yi et al., 2008). Of the many polymeric materials available, polyaniline (PANI) and its derivatives are particularly sensitive to formaldehyde (Itoh et al., 2008).

PANI was chosen for this project because of its sensitivity to formaldehyde, low temperature operation (Itoh et al., 2008), and its high stability, especially in oxidizing environments (Kukla et al., 1996). PANI begins to decompose at 107°C, which means a sensor based on PANI may be operated at elevated temperatures and the sensor may be heated to speed up the regeneration of the sensor. This is especially important since PANI forms strong dipole-dipole interactions with formaldehyde, which can increase response and regeneration times (Athawale and Kulkarni, 2000).

The sensitivity, selectivity, and response time of a sensor may be improved by adding a small amount of dopant (Nicolas-Debarnot and Poncon-Epillard, 2003). Nanoparticles provide

better dopants due to their larger surface area with respect to volume, which gives an analyte more chance to adsorb and desorb to the nanoparticle, thus inducing a larger signal (Wang et al., 2009c). If dopants are used, they should be homogeneously dispersed throughout the film to improve the sensing properties of the sensing film (Lee et al., 2009).

Generally, PANI is doped with an acid to improve the conductivity of the polymer. If the conductivity of PANI is not being exploited, using an acid dopant may be more harmful than beneficial to the sensor. This is because acid dopants, even some mild Lewis acids, may be reactive enough to damage the electronic components of the sensor, thereby reducing a sensor's stability and thus, shortening a sensor's lifetime. Therefore, it is better to use metal dopants (Misra et al., 2004b).

Doping PANI with an acid also increases its crystallinity. High crystallinity (more ordered films), leads to higher sensitivity towards analytes (Mädler et al., 2006). Although doping PANI with an acid, such as hydrochloric acid (HCl), tends to create more ordered films, this can also be achieved by increasing the concentration of aniline during the polymerization (Tang et al., 2009).

For gas sensors, metal and metal oxide dopants are sometimes used for both their electronic conductivities and their surface catalytic properties as oxidation catalysts (Dirksen et al., 2001). The specific area of a conductive polymer is increased by the addition of metal particles, which improves the catalytic efficiency of the sensing material (Choudhury, 2009). The smaller the grain size of the metal dopant, the better the sensitivity and selectivity due to the increased surface area of the dopant in contact with the gas (Lee et al., 2007).

SnO_2 is a commonly used sensing material for small organic molecules that are reducing in nature (Zhang et al., 2005). SnO_2 on its own is not very selective. Therefore, dopants can be added to improve its selectivity. Both Pt- and Pd-doped SnO_2 showed higher sensitivity towards ethanol, rather than formaldehyde (Lee et al., 2009 and Wang et al., 2009b).

Wieckowski et al. (2003) compared Pt-Sn, Pt-Ru, and Pt-Ru-Sn and found that Pt-Sn was the best electro-oxidation of formaldehyde, which meant that Pt-Sn had the greatest affinity towards formaldehyde compared to the others. This was, however, in solution and both Pt and Sn were not very selective for a sensor.

Many of the sensors that use Pt nanoparticles work well for low concentrations of formaldehyde in acidic solutions (Mascaro et al., 2004). The incorporation of Pt into PANI increases the conversion rate between conductor and insulator, thereby decreasing the response and recovery time (Ulmann et al., 1992). Although Pt is catalytically active and converts small organic molecules to CO and CO_2, this causes a problem since CO poisons the Pt, rendering it inactive (Wu et al., 2005).

Lv et al. (2007) created a sensor array to detect formaldehyde that used SnO_2 thin film sensors with Au, Cu, Pt, and Pd as metal catalysts. The sensor was able to detect formaldehyde selectively down to 0.06 ppm (see Figure 3.1).

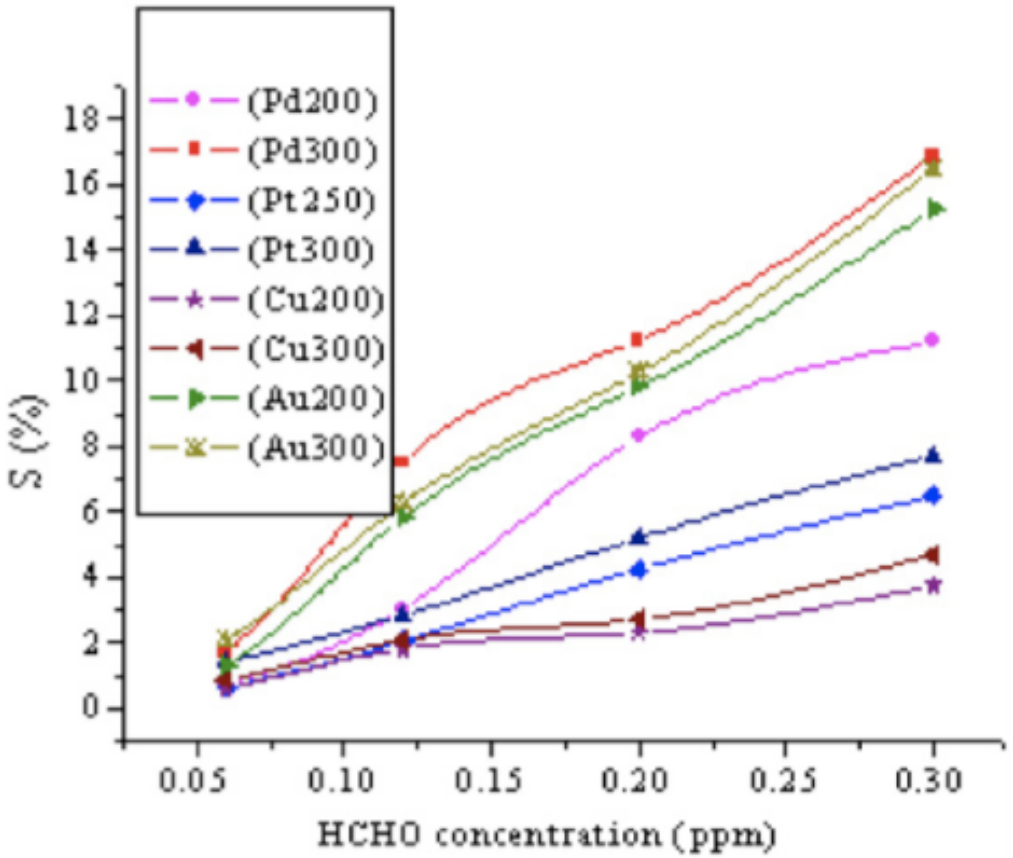

Figure 3.1: Signal response of each sensor in the sensor array (Lv et al., 2007).

Pd and Au showed the highest signal response towards formaldehyde; however, the sensor worked between 150°C and 300°C. There were issues separating signals of gas mixtures which made it difficult to determine concentrations and components of mixed gases (Lv et al., 2007).

Over time, some metals become inactive, and thus no longer offer the catalytic effects that improve the sensing properties of the sensor. When a metal is rendered inactive, it is considered to be poisoned. Pt, and to a lesser extent Pd, are poisoned by carbon monoxide (CO), which can be produced during the oxidation of formaldehyde (Wu et al., 2005 and Safavi et al., 2009), although Pt is less likely to become poisoned when dispersed throughout the PANI film. This, however, does not completely stop the poisoning from occurring, especially near the surface of the film (Ulmann et al., 1992). Another way to reduce poisoning is by mixing Pt and Pd in a 1:1 ratio before dispersing the nanoparticles throughout the film, which minimizes poisoning by CO (Zhou et al., 2009). Due to the possibility of poisoning, Pt and Pd have not been selected.

Many different metal and metal oxides were considered and it was concluded that NiO would be the best option for doping PANI to detect formaldehyde for study. Ni is in the same group as Pt and Pd, which are both good oxidation catalysts for small organic molecules (Safavi et al., 2009). Dirksen et al. (2001) compared the catalytic activity towards the oxidation of formaldehyde of many metals (including Pt and Pd) and metal oxides and determined that NiO had the highest catalytic activity towards formaldehyde.

NiO catalytically converts formaldehyde to formic acid in solution, which results in a measurable change in pH. This reaction changes the oxide surface and thus can also be measured potentiometrically. The main drawbacks of this method are that the gas must first dissolve into a liquid and the volume of air being sampled must be known, although the volume can be obtained through the use of pumps or gas traps (Campanella et al., 2006).

Lee et al. (2007) designed a self-heating, NiO thin film sensor that had high sensitivity towards formaldehyde. This sensor had response and recovery times on the order of seconds and a low detection limit of 0.8 ppm.

The surface catalytic properties of NiO and Al_2O_3 were exploited for their selectivity towards formaldehyde by Wang et al. (2008b). By using a nanometer scale grain size, the sensitivity of the sensor increased since a larger area was available to interact with the formaldehyde. The sensor was able to detect down to 0.04 ppm.

Wang et al. (2008b) found that Al_2O_3 increased the sensitivity towards formaldehyde; however, the selectivity was decreased. This disagrees with Campanella et al. (2006), who found that Al_2O_3 was selective towards formaldehyde.

Both Itoh et al. (2008) and Wang et al. (2006) developed a formaldehyde sensor based on intercalated layers of MoO_3 and polyaniline. Although both sensors were able to detect formaldehyde in the ppb range at room temperature, the sensors were also responsive to acetaldehyde as well, thus making the sensor not very selective.

More exotic metal combinations have also been used for the detection of formaldehyde, including: Ag doped-In_2O_3 (Wang et al., 2009a), $BiCuVO_x$ (Kida et al., 2009), Ga doped-ZnO Han et al., 2009), and $La_{0.68}Pb_{0.32}FeO_3$ (Zhang et al., 2005). Ag doped-In_2O_3 had a detection limit of 2 ppm; however, it was at a temperature of 100°C, which is too high (Wang et al., 2009a). Although $BiCuVO_x$ had moderate sensitivity to formaldehyde, it had high sensitivity to ethanol, and thus was more selective to ethanol (Kida et al., 2009). This was also the case for In_2O_3 (Wang et al., 2009c). The Ga doped-ZnO sensor was not very sensitive towards formaldehyde, with a detection limit of only 32 ppm; however, it a had moderate response and recovery time on the order of minutes (Han et al., 2009). $La_{0.68}Pb_{0.32}FeO_3$ was tested to 10 ppm and had an optimum operating temperature of 180°C, both of which are too high for the targeted application (Zhang et al., 2005). Since these all had poor sensitivity and/or selectivity towards formaldehyde, at room temperature, none were chosen as potential dopants.

After considering and critically evaluating the literature on possible dopants, it was concluded that doping PANI with either NiO or NiO and Al_2O_3 would be the best for a formaldehyde sensor. These dopants would yield the targeted low detection limits (high sensitivity) and potential higher selectivity.

3.2.2 Polyaniline/NiO Interaction

Ni coordinates with the nitrogen of the quinoid rings causing the quinoid rings to convert the rings in the structure from a chair conformation to a boat conformation. This changes the morphology of PANI, resulting in a more crystalline material. The nitrogen electron cloud density of the quinoid rings is stronger than that in the benzoid rings, which results in the coordination of nitrogen, from the quinoid rings to Ni (Han et al., 2006); see Figure 3.2.

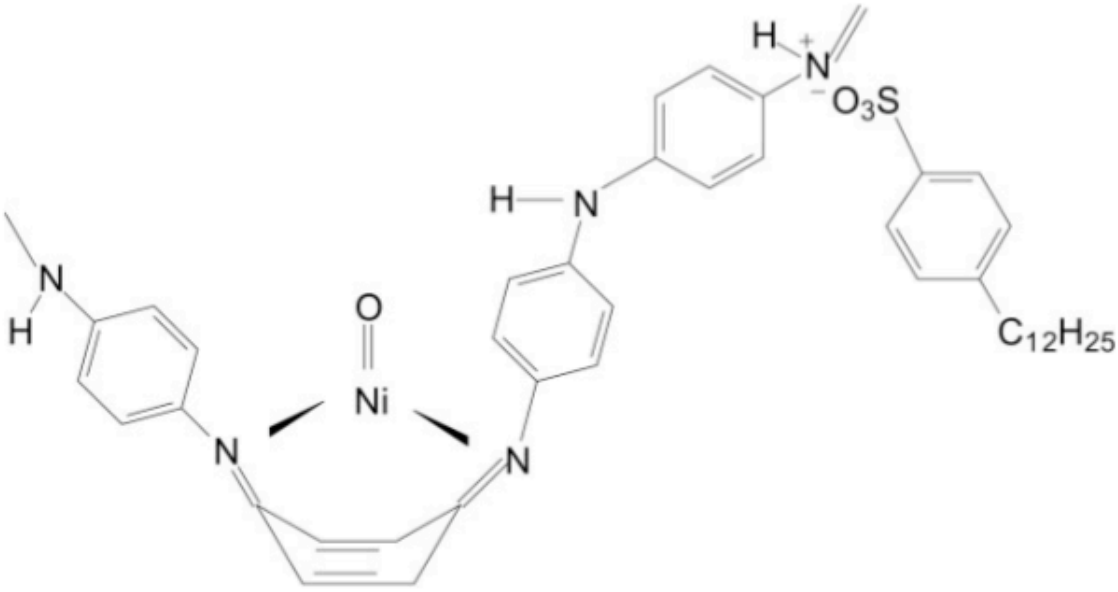

Figure 3.2: Ni coordination to the nitrogens in the quinoid ring (Han et al., 2006).

The boat conformation, as a result of the Ni-N interaction that occurrs between the NiO and PANI, was confirmed by the shift in the N-H stretching frequency in the infrared spectrum of the material. This change in conformation resulted in the N-H stretch vibrating at a different frequency, which was seen as a shift in the absorbance portion of the infrared spectrum (Song et al., 2007); see Figure 3.3.

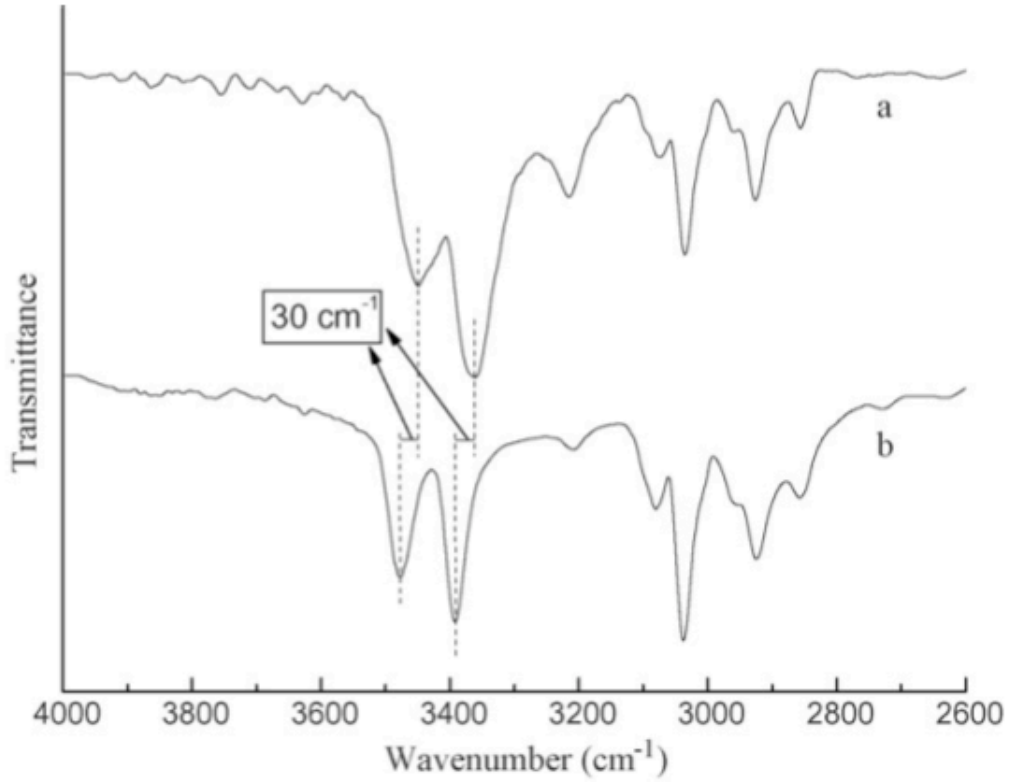

Figure 3.3: Shift in N-H absorbance in the infrared spectrum as N-Ni coordination confirmation (Song et al., 2007).

3.3 Experimental Steps

3.3.1 Polymer Synthesis

PANI was synthesized by mixing aniline, ammonium persulfate, and, if present, the dopants in deionized water. 0.39 mL of aniline (A.C.S. reagent, Sigma-Aldrich) was added to 20 mL of deionized water and then mixed using a sonicator for 30 minutes. This solution was then cooled to -1°C before the addition of a solution containing 1.0g of ammonium persulphate (A.C.S. Reagent, Sigma-Aldrich) in 5 mL of deionized water. The solution was mixed using a sonicator for one minute to ensure everything was throughly combined and the solution was left to react at -1°C for 24 hours. The polymerization was done at a low temperature to produce a polymer with a higher molecular weight and more crystallinity (Steiskal and Gilbert, 2002). The polymer was filtered out using a Büchner funnel and Wattman #5 filter paper and left overnight. The polymer was then washed with methanol, ethanol, and acetone until the liquid ran clear. The polymer was scraped into a glass vial for storage.

To obtain modified PANI, aniline was polymerized with the dopant suspended in the starting solution. The dopant was added up to 20% by weight to the aniline before the solution was initially cooled prior to the addition of the ammonium persulphate. The NiO (99.8%,

Sigma-Aldrich) came in powder form and was weighed, whereas the Al_2O_3 (10 wt. % in H_2O, Sigma-Aldrich) came in a solution and thus the weight percent was converted into a volume. Other than the addition of the dopant, which was nickel oxide (NiO) and/or aluminum oxide (Al_2O_3), the polymerization procedure was the same as for PANI. The dopant compositions prepared are listed in Table 3.1.

Table 3.1: PANI/Dopant Composition by Weight

PANI Composition (%)	**Dopant**	**Dopant Composition (%)**
100	None	0
95	NiO	5
90	NiO	10
85	NiO	15
80	NiO	20
80	NiO/Al_2O_3	5/15
80	NiO/Al_2O_3	10/10
80	NiO/Al_2O_3	15/5

3.3.2 Experimental Apparatus

In order to assess the polymeric materials prepared as bases for the formaldehyde sensor, a specific apparatus was constructed to allow exposure of the sensor to the analytes. In addition, a specialized gas chromatograph (GC) was used for determining residual analyte after exposure to the sensor material. It should be noted that the generic term polymer will henceforth refer to both PANI and doped PANI.

Four gaseous analytes (formaldehyde, acetylaldehyde, ethanol, and benzene) were used to evaluate both the sensitivity and selectivity of the sensing material. These gases (all certified standards from Praxair), whose concentrations were approximately 5 ppm in nitrogen, were mixed in a mixing chamber (1 m length by 2.5 cm in diameter) where they were also diluted, with nitrogen (Praxair, 5.0 grade), down to the desired concentration without much waste. Various concentrations of gases and gas mixtures were tested.

Acetaldehyde, ethanol and benzene were chosen as interferents because they have a variety of functional groups. Acetaldehyde was chosen since it is chemically very similar to

formaldehyde. Ethanol was chosen to represent alcohols, in which hydrogen bonding may present an issue since the sensing material also contains hydrogen bonds. Benzene was chosen since it represents aromatics and shows the effect of a non-polar interferent.

The test system (see Figure 3.4) was set up so that the gases would pass through an empty flask en route to the specialized gas chromatograph (GC) to determine the initial concentration of gas. A flask that contained 0.20 g of polymer replaced the empty flask, which allowed the sensing material to be saturated with the gas. The difference between the concentrations measured was the amount of analyte that interacted with the sensing film. The GC was used as a standard or reference to determine the concentrations of the gases. The GC used (described later in Section 3.3.3) could detect into the ppb range and was able to differentiate between formaldehyde and acetaldehyde and other volatile organic compounds.

Tygon® tubing was used to transport the gases since the gases were less likely to adsorb onto the inside of the tubing. The mixing chamber was made of glass. MKS RS-485 mass flow controllers were used to control the flow rate of the gases, which in turn controlled the concentration of the gases being tested.

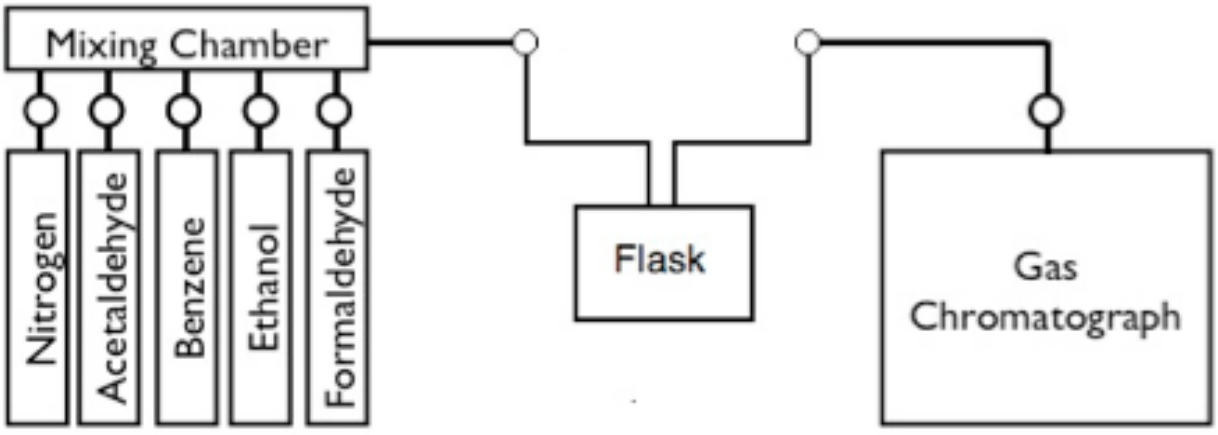

Figure 3.4: Sensing material test system. It should be noted that the gases listed in the figure are approximately 5 ppm in nitrogen.

PANI and PANI doped with NiO or NiO/Al_2O_3 were synthesized as stated above. After filtering the polymer, it was allowed to air dry and was then transferred to a 100mL round bottom flask. The round bottom flask was heated in a water bath at 65°C and purged with nitrogen for 40 minutes, then attached to the test system.

3.3.3 Gas Chromatograph (GC)

A gas chromatograph (GC) is used to qualitatively and quantitatively identify components in either a liquid or a gas sample. The components of a sample are separated as they flow through a column, which contains a suitable packing material. The packing material is

chosen based on what components are known to be in the sample. As the components of a sample pass through the column, they adsorb or absorb (sorb) onto the packing material at different rates resulting in each component having their own retention time. The components of the sample are thereby separated based on their retention times. The retention time indicates qualitatively which components are in a sample. The data of a gas chromatograph can be represented graphically and appear as peaks on a voltage versus time graph. The peaks are integrated and compared to an internal standard to determine quantitatively the concentration of each component in a sample (Grob and Barry, 2004).

The specialized gas chromatograph used in this study needed to be able to separate very chemically similar compounds and detect very low concentrations. The separation was achieved using a Varian CP-Sil 5 CB for formaldehyde with a capillary column of dimensions 60 m x 0.32 mm x 8 μm (CP-Sil 5 CB is the column packing identifier).

The GC uses a pulsed discharge helium ionization detector (PDHID) which is very sensitive and can detect in the parts per billion (ppb) range. Pulsed direct current (DC) discharge causes the helium to ionize. As the helium returns to its natural state, photons are released and ionize the sample as it flows down the column, producing electrons. These electrons are forced towards the detector and generate a response. This detector is virtually non-destructive to the sample and very sensitive. Because of the sensitivity of the detector, the detector is encased in helium to limit interferents from the atmosphere (Agilent Technologies, 2006).

3.4 Experimental Data

The GC produced chromatograms from which the concentration of residual gas (i.e. gas that was not sorbed onto the sensing material) was determined (see Figure 3.5). This value was subtracted from the initial concentration of gas that flowed through the system to determine the amount of gas adsorbed onto the sensing material (see Equation 3.1).

$$[Gas]_{Sorbed} = [Gas]_{Initial} - [Gas]_{Residual} \quad \text{(Equation 3.1)}$$

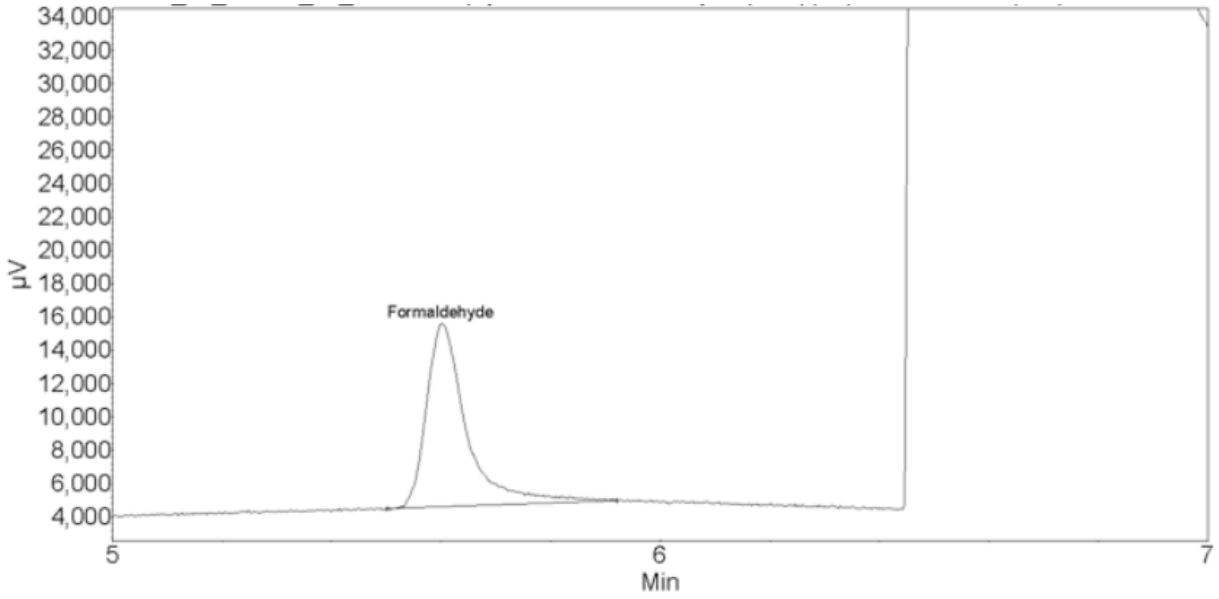

Figure 3.5: Gas chromatogram for formaldehyde at 5.05 ppm.

The concentrations of the gases sorbed onto the polymer are listed in Table 3.2 and Table 3.3. Ideally, the polymer would sorb a high concentration of formaldehyde and a low concentration of the other gases. The ppm amounts following (in brackets) the gas headings of each of the four columns of Table 3.2 (and the bolded ppm concentrations at the top of the three columns of Table 3.3) represent the actual concentration of each gas that entered the test system and was supposed to be detected (sorbed onto the polymer) under ideal conditions (essentially, a target concentration). There are three numbers reported per cell (in Tables 3.2 and 3.3). These three numbers represent completely independent replicates of each treatment, thus allowing a reliable estimation of the corresponding inherent error.

At the bottom of both Tables 3.2 and 3.3, blanks are listed. The blanks were taken both before and after the polymers were tested (for a specific analyte at a specified concentration) to verify that the concentration tested was the same for all the polymers measured. A "blank" means that an empty flask was used without any absorbent polymer in it and left to run overnight or for a sufficiently long period. For the ideal case, the expected response from the blank should be equal to zero, which means that all the gas passed through (and thus did not sorb onto) the test system at the appropriate concentration. These were used to ensure there was no baseline drift throughout the measurements. Had there been baseline drift, there would have been large fluctuations between the blank measurements resulting in a high variance (s^2).

The equations for the average ($\overline{x}$) and the variance are given below (see Equation 3.2 and 3.3), where x is the measured variable and n specific sample size.

$$\bar{x} = \sum \frac{x}{n} \qquad \text{(Equation 3.2)}$$

$$s^2 = \frac{1}{n-1}\left(\sum(x^2) - \frac{1}{n}(\sum x)^2\right)$$ (Equation 3.3)

The data have also been presented in graphical form for better visualization (see Figure 3.6 through 3.11). More sample chromatograms are available in Appendix A. All of the data collected during this thesis are available on disk from professor A. Penlidis. The data entries of Tables 3.2 and 3.3 (plotted in Figures 3.6 to 3.11) are discussed in detail in Chapter 4.

The estimates of s^2 from the replicated blanks give an indication of the underlying (inherent) errors (per column of Tables 3.2 and 3.3). These inherent error estimates are consistent and comparable, and of a similar order of magnitude as estimated s^2 from the independently replicated actual runs with the analytes.

Table 3.2: Concentration of Gas Sorbed onto the Polymer Sensor for Different Gases Tested

Polymer Sample	Concentration of Gas Sorbed (ppm)			
	Formaldehyde (5.05 ppm)	Ethanol (5.00 ppm)	Acetaldehyde (4.96 ppm)	Benzene (5.10 ppm)
PANI 1	3.00	2.74	2.03	1.73
PANI 2	2.94	2.61	2.25	1.53
PANI 3	2.86	2.66	1.99	1.79
Average	2.93	2.67	2.09	1.68
s^2	0.005	0.004	0.020	0.019
PANI 5% NiO 1	2.33	2.01	1.68	0.40
PANI 5% NiO 2	2.35	2.02	1.75	0.46
PANI 5% NiO 3	2.23	2.08	1.99	0.34
Average	2.30	2.04	1.81	0.40
s^2	0.004	0.001	0.026	0.004
PANI 10% NiO 1	2.30	2.53	2.12	0.59
PANI 10% NiO 2	2.69	2.89	2.19	0.37
PANI 10% NiO 3	2.38	2.44	2.23	0.31
Average	2.46	2.62	2.18	0.42
s^2	0.042	0.057	0.003	0.022
PANI 15% NiO 1	2.77	1.72	1.92	1.81
PANI 15% NiO 2	2.87	1.72	2.17	1.80
PANI 15% NiO 3	2.72	1.68	1.89	1.61
Average	2.79	1.71	1.99	1.74
s^2	0.006	0.001	0.024	0.013
PANI 20% NiO 1	2.77	2.32	1.97	1.55
PANI 20% NiO 2	2.89	2.43	1.75	1.88
PANI 20% NiO 3	2.71	2.41	1.89	1.45
Average	2.79	2.39	1.87	1.63
s^2	0.008	0.003	0.012	0.051
PANI 5% NiO 15% Al_2O_3 1	2.47	1.26	1.53	0.95
PANI 5% NiO 15% Al_2O_3 2	2.29	1.40	1.49	1.22
PANI 5% NiO 15% Al_2O_3 3	2.45	1.22	1.00	1.24
Average	2.40	1.29	1.34	1.14
s^2	0.010	0.009	0.087	0.026
PANI 10% NiO 10% Al_2O_3 1	2.71	2.46	2.15	2.07
PANI 10% NiO 10% Al_2O_3 2	2.86	2.53	2.21	1.92
PANI 10% NiO 10% Al_2O_3 3	2.75	2.45	2.11	2.20
Average	2.77	2.48	2.16	2.06
s^2	0.006	0.002	0.003	0.020
PANI 15% NiO 5% Al_2O_3 1	2.95	2.44	2.58	2.09
PANI 15% NiO 5% Al_2O_3 2	2.65	2.66	2.61	2.22
PANI 15% NiO 5% Al_2O_3 3	2.65	2.28	2.23	2.35
Average	2.75	2.46	2.47	2.22
s^2	0.030	0.036	0.045	0.017
Blank 1	0.14	0.02	0.00	0.00
Blank 2	0.00	0.08	0.15	0.19
Blank 3	0.00	0.00	0.00	0.00
Average	0.05	0.03	0.05	0.06
s^2	0.007	0.002	0.008	0.012

Table 3.3: Concentration of Gas Sorbed onto the Polymer Sensor for Different Concentrations of Formaldehyde Tested

Polymer Sample	**Concentration of Formaldehyde Gas Sorbed (ppm)**		
	5.05	**0.73**	**0.09**
PANI 1	3.00	0.36	0.03
PANI 2	2.94	0.42	0.06
PANI 3	2.86	0.40	0.04
Average	2.93	0.39	0.04
s^2	0.005	0.001	0.0002
PANI 5% NiO 1	2.33	0.26	0.02
PANI 5% NiO 2	2.35	0.33	0.05
PANI 5% NiO 3	2.23	0.43	0.03
Average	2.30	0.34	0.03
s^2	0.004	0.007	0.0002
PANI 10% NiO 1	2.30	0.34	0.05
PANI 10% NiO 2	2.69	0.34	0.03
PANI 10% NiO 3	2.38	0.35	0.05
Average	2.46	0.34	0.04
s^2	0.042	0.000	0.0001
PANI 15% NiO 1	2.77	0.41	0.05
PANI 15% NiO 2	2.87	0.08	0.04
PANI 15% NiO 3	2.72	0.28	0.05
Average	2.79	0.26	0.05
s^2	0.006	0.028	0.0000
PANI 20% NiO 1	2.77	0.35	0.05
PANI 20% NiO 2	2.89	0.31	0.03
PANI 20% NiO 3	2.71	0.33	0.02
Average	2.79	0.33	0.03
s^2	0.008	0.000	0.0002
PANI 5% NiO 15% Al_2O_3 1	2.47	0.14	0.00
PANI 5% NiO 15% Al_2O_3 2	2.29	0.36	0.01
PANI 5% NiO 15% Al_2O_3 3	2.45	0.21	0.01
Average	2.40	0.24	0.01
s^2	0.010	0.013	0.0000
PANI 10% NiO 10% Al_2O_3 1	2.71	0.13	0.04
PANI 10% NiO 10% Al_2O_3 2	2.86	0.40	0.05
PANI 10% NiO 10% Al_2O_3 3	2.75	0.37	0.03
Average	2.77	0.30	0.04
s^2	0.006	0.022	0.0001
PANI 15% NiO 5% Al_2O_3 1	2.95	0.21	0.04
PANI 15% NiO 5% Al_2O_3 2	2.65	0.40	0.05
PANI 15% NiO 5% Al_2O_3 3	2.65	0.15	0.02
Average	2.75	0.25	0.04
s^2	0.030	0.017	0.0002
Blank 1	0.14	0.09	0.00
Blank 2	0.00	0.00	0.00
Blank 3	0.00	0.00	0.00
Average	0.05	0.03	0.00
s^2	0.007	0.003	0.0000

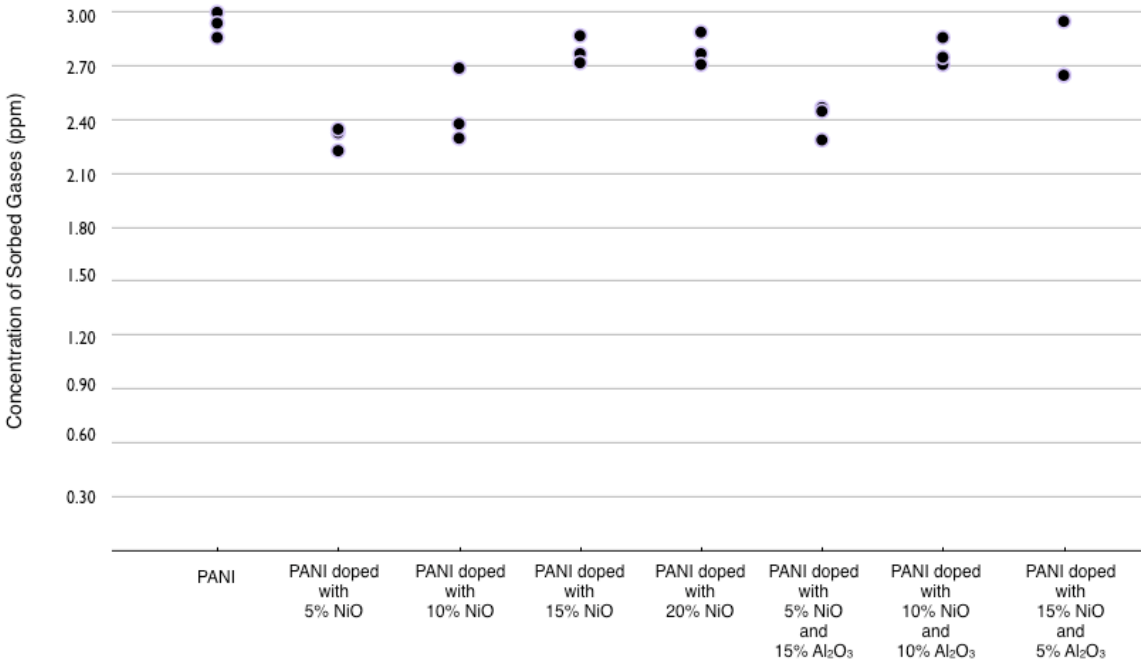

Figure 3.6: Sorbed formaldehyde for each polymer at a concentration of 5.05 ppm.

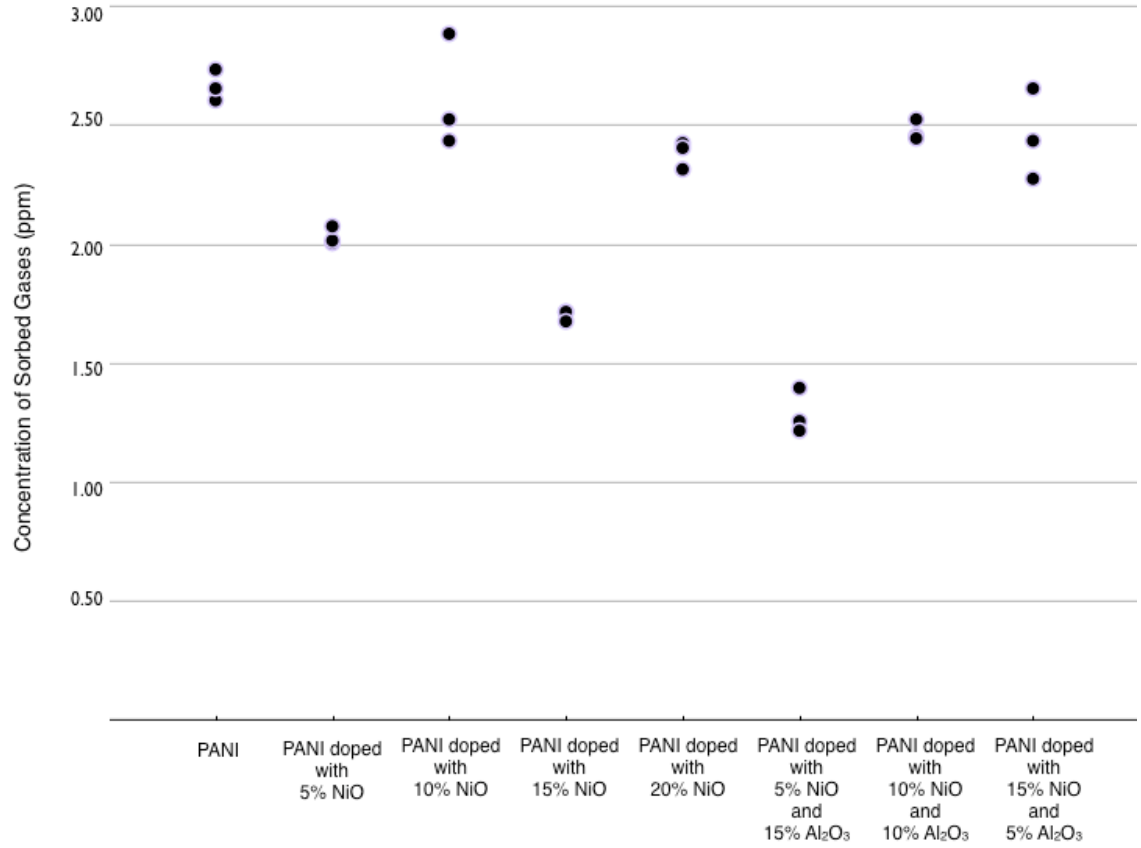

Figure 3.7: Sorbed ethanol for each polymer at a concentration of 5.00 ppm.

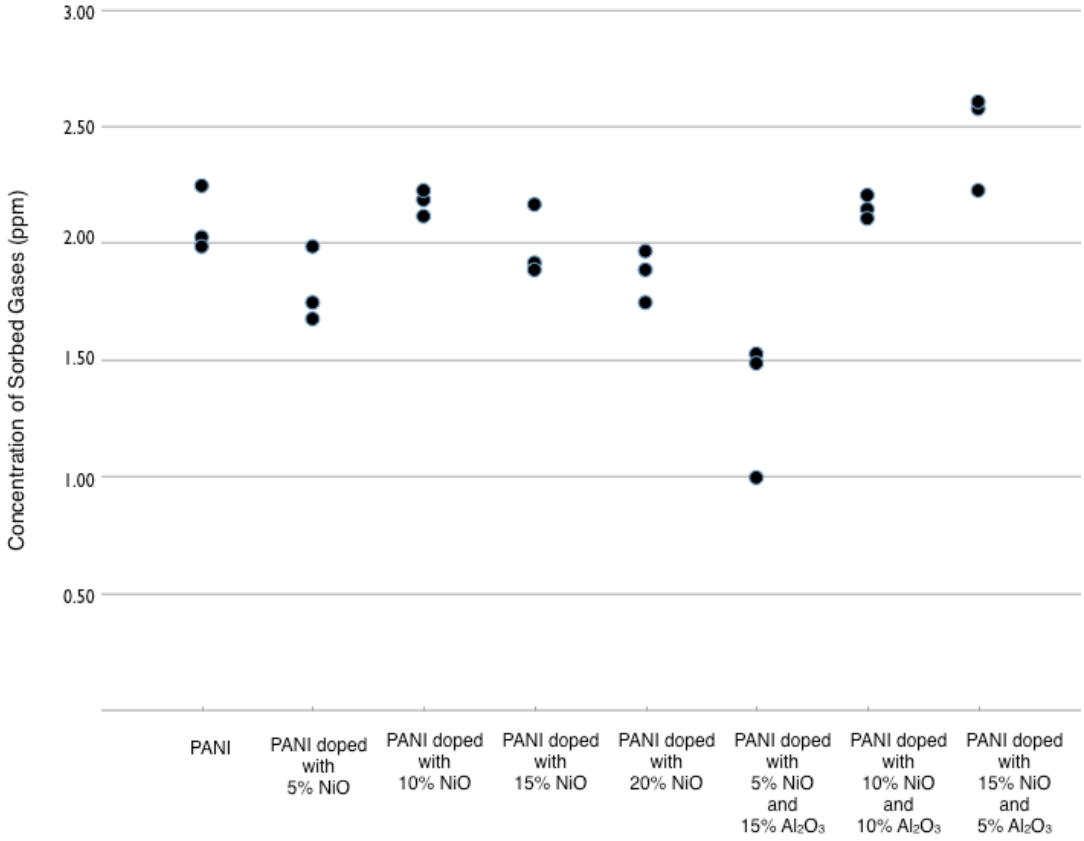

Figure 3.8: Sorbed acetaldehyde for each polymer at a concentration of 4.96 ppm.

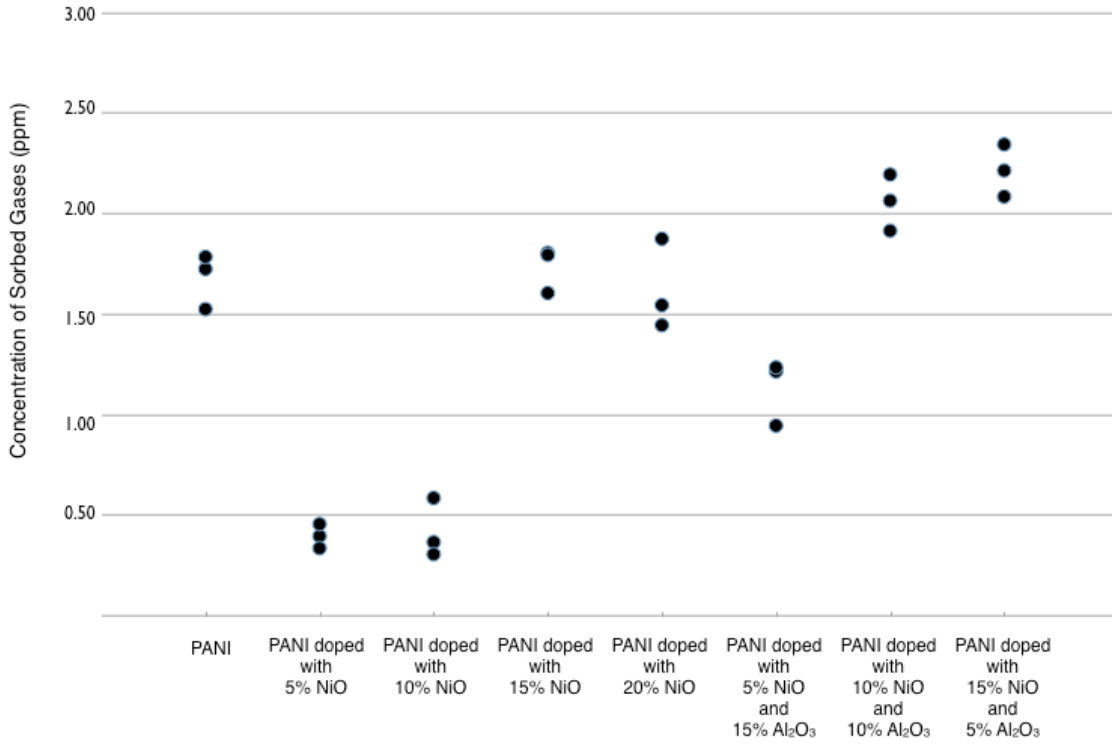

Figure 3.9: Sorbed benzene for each polymer at a concentration of 5.10 ppm.

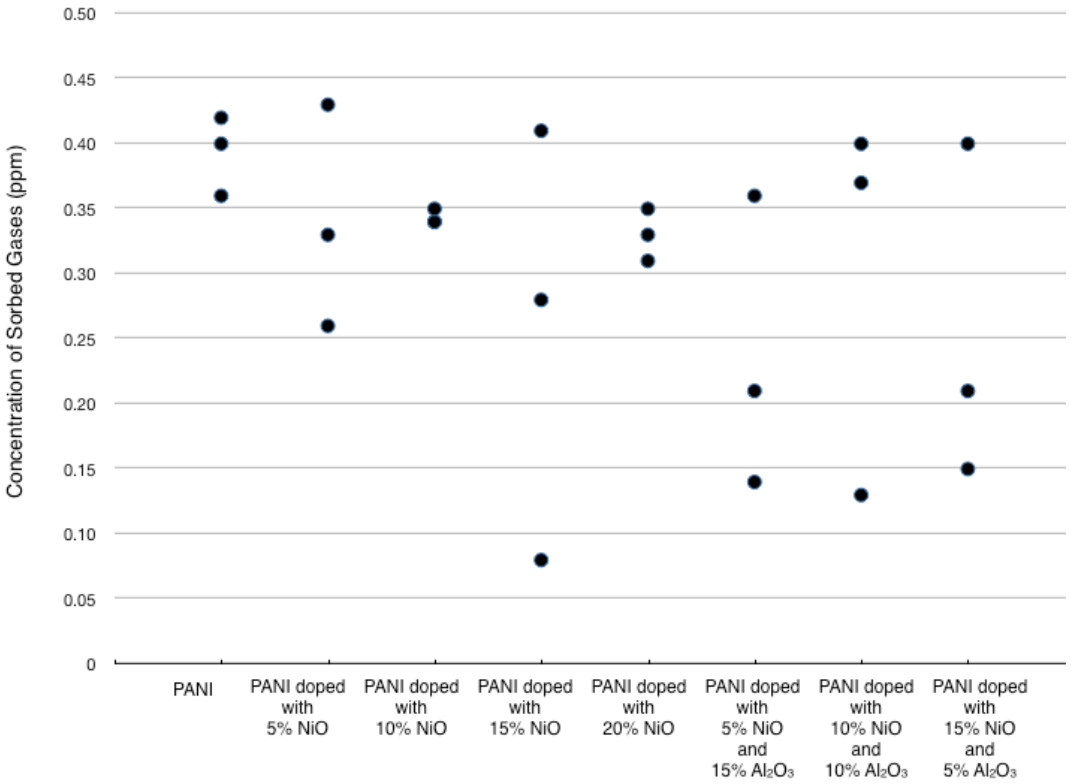

Figure 3.10: Sorbed formaldehyde for each polymer at a concentration of 0.73 ppm.

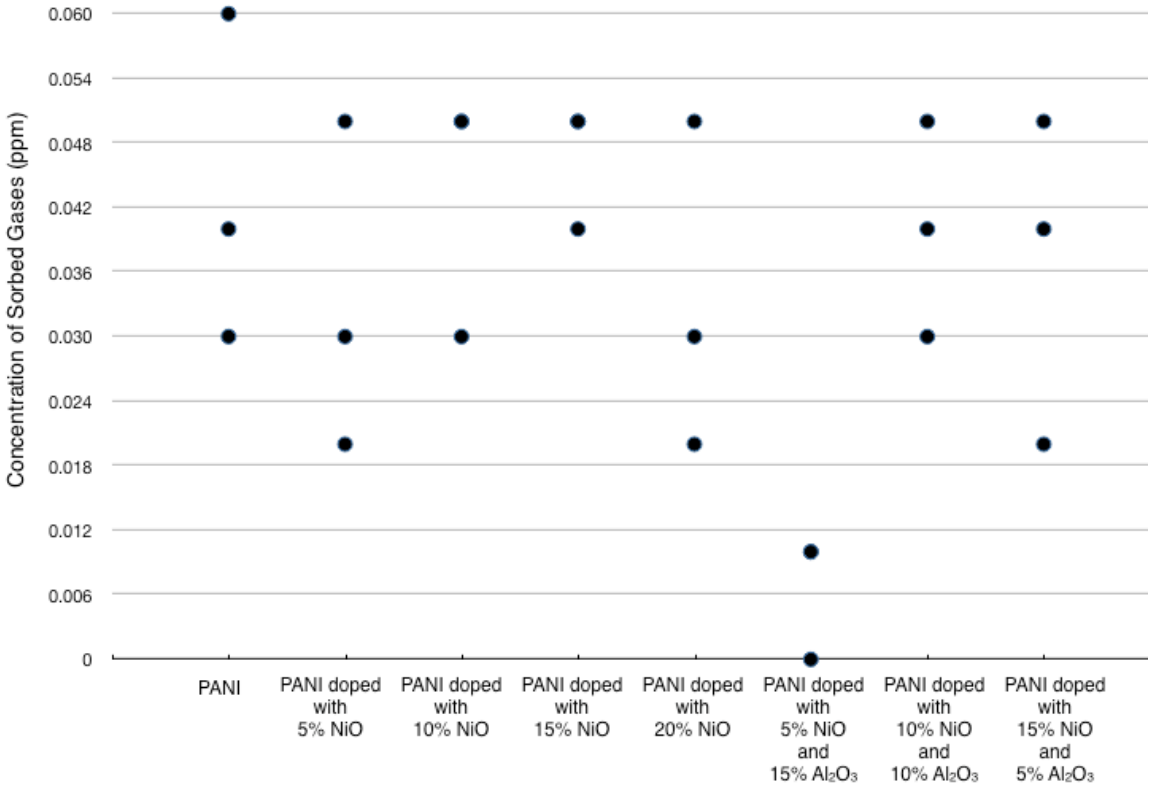

Figure 3.11: Sorbed formaldehyde for each polymer at a concentration of 0.09 ppm.

Chapter 4: Results and Discussion

4.1 Evaluation of Gas Chromatograph (GC)

4.1.1 Reproducibility of Results

It can be seen from the data in the previous chapter (see Tables 3.2 and 3.3) that the variance in the concentrations obtained by the gas chromatograph (GC) was very small. The manufacturer of this very specialized GC states that the GC has an error of 1%, which accounts for some of the variance. The rest of the variance (if at all present) is due to other sources of uncertainty that contribute to overall variability.

The polymer samples tested were independent replicates. The error within the replicates was expressed as the coefficient of variation (CV); see Equation 4.1. The coefficient of variation, which is a ratio between the standard deviation (s) and the mean ($\overline{x}$), is a normalized measure that can be used as an indicator of the overall error.

$$Coefficient\ of\ Variation\ (CV) = \frac{s}{\bar{x}} \qquad \text{(Equation 4.1)}$$

The CV values for each polymer at each concentration for each gas were determined from the concentration measured by the GC (residual) and not the concentration sorbed onto the polymer (see Table 4.1). At higher concentrations, above 1 ppm, for many of the polymers for each gas, the coefficient of variation was 0.05 or less. This means the error between the replicates was 5% or less and thus the GC had extremely reproducible results. A few polymers had a higher error, such as PANI doped with 15% NiO and 5% Al_2O_3 that had an error of up to 8% for all gases except benzene and PANI doped with 10% NiO that had an error of 10% for ethanol. Overall, at higher concentrations, the polymers exhibited low error and extremely reproducible results.

There was much higher error at low concentrations of formaldehyde (see Table 4.1). Generally, as the concentration decreased, the error increased. The coefficient of variation increased mainly due to the poorer signals obtained from the GC at lower concentrations. The poorer signals were the result of the signal being lost in the noise of the baseline (see Section 4.1.2).

Table 4.1: Coefficient of Variation (CV) Values for Each Polymer

Polymer Sample	**Coefficient of Variation**					
	Ethanol (5.00 ppm)	Acetaldehyde (4.96 ppm)	Benzene (5.10 ppm)	Formaldehyde (5.05 ppm)	Formaldehyde (0.73 ppm)	Formaldehyde (0.09 ppm)
PANI	0.03	0.05	0.04	0.03	0.09	0.33
PANI 5% NiO	0.01	0.05	0.01	0.02	0.22	0.27
PANI 10% NiO	0.10	0.02	0.03	0.08	0.01	0.25
PANI 15% NiO	0.01	0.05	0.03	0.03	0.35	0.13
PANI 20% NiO	0.02	0.04	0.06	0.04	0.05	0.27
PANI 5% NiO 15% Al_2O_3	0.03	0.08	0.04	0.04	0.23	0.13
PANI 10% NiO 10% Al_2O_3	0.02	0.02	0.05	0.03	0.34	0.20
PANI 15% NiO 5% Al_2O_3	0.08	0.08	0.05	0.08	0.27	0.29
Blank	0.01	0.02	0.03	0.02	0.10	0.06
Average	0.03	0.05	0.04	0.04	0.18	0.21

Baseline drift was observed over time, which may have been the result of either the depletion of gas in the gas cylinders or inherent in the GC. This was easily corrected by recalibrating the GC with a standard. Since the gases tested were standard grade, they were used as standards without dilution.

4.1.2 Signal-to-Noise Ratio

Signal-to-noise ratio is measured as the ratio between the signal, in this case the peak, and the noise from the baseline (see Equation 4.2, where A represents the amplitude under the chromatogram peak for either the signal, the analyte being tested, or the noise from the baseline). At higher concentrations, where the peak is large compared to the baseline, signal-to-noise ratio is much less of a concern (see Figure 4.1). The lower initial concentrations of formaldehyde had higher signal-to-noise ratios on the chromatogram (see Figure 4.2). The noise was measured through the first minute of the chromatogram, where no peaks were present, and compared to the signal, or peak response for each analyte. A signal-to-noise ratio of more than 3 is an indicator

of good performance (see Table 4.2). It can be seen from Table 4.2 (from the highlighted entries) that occurrences of signal-to-noise ratio less than 3 appeared only 40% of the time, when the target formaldehyde was at its lowest level (0.09 ppm or 90 ppb).

$$signal - to - noise = \frac{A_{Signal}}{A_{Noise}} \qquad \text{(Equation 4.2)}$$

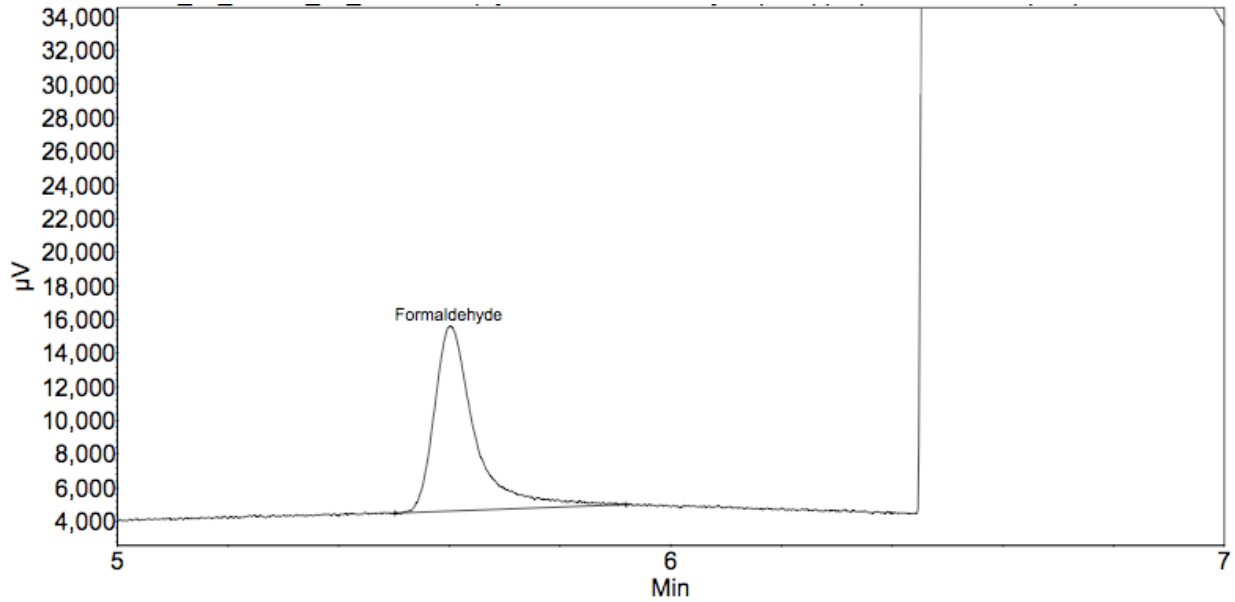

Figure 4.1: Chromatogram of formaldehyde at 5.05 ppm.

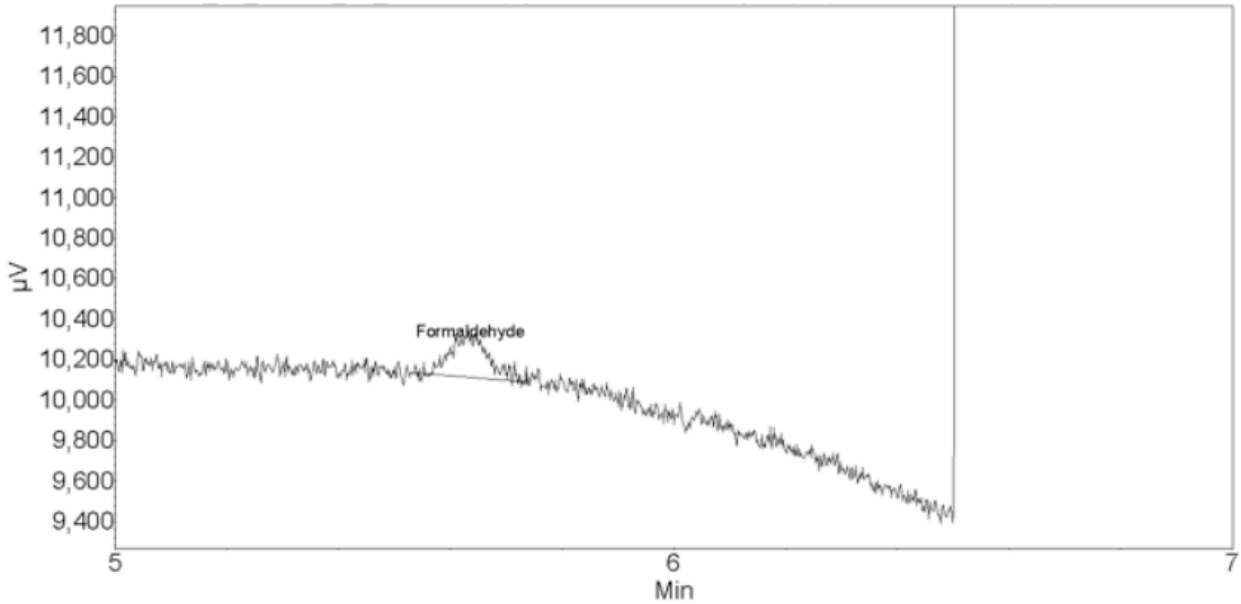

Figure 4.2: Chromatogram of formaldehyde at 0.09 ppm.

Table 4.2: Signal-to-Noise Ratios for all Gas Concentrations for Each Polymer

Polymer Sample	Signal-To-Noise Ratio for Gas Sorbed					
	Form-aldhyde (5.05 ppm)	Ethanol (5.00 ppm)	Acetal-dehyde (5.10 ppm)	Benzene (5.10 ppm)	Form-aldehyde (0.73 ppm)	Form-aldehyde (0.09 ppm)
PANI 1	107.35	151.12	176.93	1096.71	19.08	4.13
PANI 2	100.40	146.60	204.78	1417.28	19.71	2.07
PANI 3	129.22	118.82	225.82	930.71	17.82	3.32
PANI 5% NiO 1	117.03	162.72	243.74	1292.57	27.83	4.85
PANI 5% NiO 2	147.36	158.74	238.32	1722.13	19.09	2.69
PANI 5% NiO 3	108.96	123.12	220.38	1319.91	16.54	2.13
PANI 10% NiO 1	102.01	130.38	251.88	1627.03	19.60	2.51
PANI 10% NiO 2	132.15	156.17	179.17	1638.91	24.62	3.87
PANI 10% NiO 3	151.63	184.60	182.55	990.36	21.33	2.12
PANI 15% NiO 1	127.56	249.52	182.55	1054.42	16.17	2.51
PANI 15% NiO 2	121.88	259.42	200.39	1301.54	17.63	3.87
PANI 15% NiO 3	140.30	277.26	241.13	1191.68	13.99	2.12
PANI 20% NiO 1	128.95	218.22	229.66	1318.41	24.01	2.24
PANI 20% NiO 2	98.25	188.43	207.85	954.15	24.12	3.24
PANI 20% NiO 3	110.13	248.04	199.51	1119.03	25.58	3.46
PANI 5% NiO 15% Al_2O_3 1	168.78	299.38	238.02	1585.25	34.46	2.62
PANI 5% NiO 15% Al_2O_3 2	162.68	293.26	270.33	1196.24	20.92	3.89
PANI 5% NiO 15% Al_2O_3 3	152.32	229.92	264.76	1399.41	28.39	4.41
PANI 10% NiO 10% Al_2O_3 1	134.69	176.48	217.06	811.61	37.16	5.06
PANI 10% NiO 10% Al_2O_3 2	138.45	198.09	163.44	1140.88	17.87	4.24
PANI 10% NiO 10% Al_2O_3 3	142.16	204.03	201.37	859.88	17.72	5.58
PANI 15% NiO 5% Al_2O_3 1	108.35	152.74	160.58	1023.20	26.32	2.94
PANI 15% NiO 5% Al_2O_3 2	86.75	187.46	196.48	782.42	20.77	2.46
PANI 15% NiO 5% Al_2O_3 3	135.27	206.76	193.66	1033.81	33.87	3.25
Blank 1	297.35	312.30	387.55	1498.51	39.61	3.05
Blank 2	244.23	310.07	363.10	1694.19	43.44	2.23
Blank 3	294.21	255.93	355.11	1736.30	41.22	6.04

The highlighted signal-to-noise ratios are below 3.

4.1.3 Limit of Detection

The limit of detection, or detection limit, is the lowest signal that can be detected, which is not buried in the noise of the baseline and is calculated from the signal-to-noise ratio. Generally, a signal-to-noise ratio of 3 is used to find the limit of detection. This ensures that the signal is not lost within the noise of the baseline exhibited by the sensor; however, the signal

may still be present and detectable (discernible). The limit of detection for formaldehyde for the gas chromatograph (GC) used was 0.05 ppm, which was calculated from a signal-to-noise ratio of 3 (see Equation 4.3 and Equation 4.4).

$$A_{Signal} = 3 \times A_{Noise} \quad \text{(Equation 4.3)}$$

$$Detection\ Limit = \frac{A_{Signal} - [Analyte]_{Concentration\ of\ Standard}}{A_{Concentration\ of\ Standard}} \quad \text{(Equation 4.4)}$$

It was possible to see a signal at a concentration less than 0.05 ppm, but the signal is considered to be buried in the noise. In both Figures 4.3 and 4.4, the chromatograms show the residual concentration (of formaldehyde) not sorbed by the polymer. The peak (signal) shown in Figure 4.3 is 0.05 ppm, which is 3 times the signal of the noise. Therefore, the peak is not buried in the noise and can be easily seen. On the other hand, in Figure 4.4, the peak (signal) (corresponding to a concentration of 0.03 ppm) is only 2 times the noise signal and thus, overall, the signal-to-noise ratio is below 3. It can be seen that the signal is harder to see since its amplitude (or height) is not much greater (stronger) than the noise of the baseline. Although the signal can still be discerned (or seen) in Figure 4.4, it is considered to be buried within the noise.

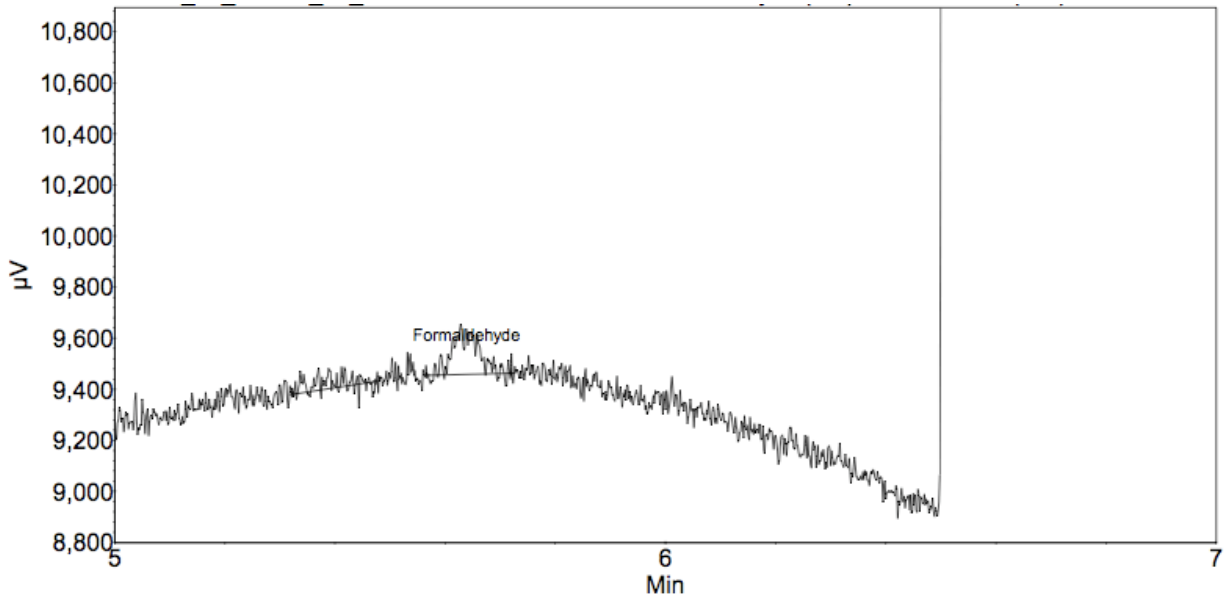

Figure 4.3: Chromatogram of PANI doped with 15% NiO 2 for formaldehyde at a concentration of 0.05 ppm.

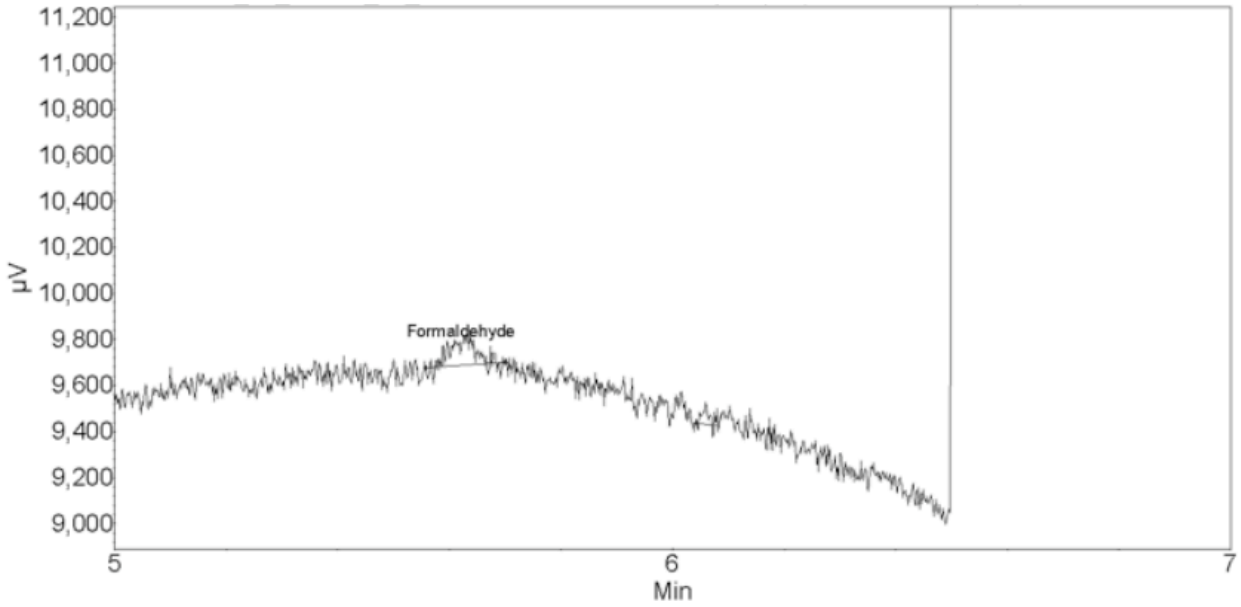

Figure 4.4: Chromatogram of PANI 2 for formaldehyde at a concentration of 0.03 ppm.

4.2 Determining the Percentage of Sorbed Formaldehyde on the Polymers

To predict the percentage of sorbed formaldehyde, the number of active sites on the polymer (substrate, which is essentially the polymeric sensor) must be considered. An active site is a spot on the polymer where an analyte may adsorb or absorb (hence, sorb). A steady state or equilibrium is reached when the concentration of analytes sorbing onto the sensing film equals the concentration that is released back into the air and limits the analyte concentration a sensing film or layer can detect. Once a steady state is reached, the active sites cannot sorb more analyte than is being released back into the air and thus, the sensor cannot detect a higher concentration. Before a steady state is reached, more analyte will sorb onto the sensing film than is released back into the air. Doping PANI with NiO and Al_2O_3 did not seem to change the percentage of formaldehyde sorbed. The percentage of sorbed formaldehyde varied between high and low target concentrations of formaldehyde.

4.2.1 High Concentrations (Above 1 ppm) of Formaldehyde

At higher target concentrations, above 1 ppm, a larger percentage of formaldehyde was sorbed onto the polymers. The concentration was determined by dividing the concentration sorbed by the actual (target) concentration tested (see Equation 4.5 and Table 4.3). The analyte in Equation 4.5 is formaldehyde for this case.

$$Fraction\ Sorbed = \frac{[Analyte]_{Sorbed}}{[Analyte]_{Actual}} \qquad \text{(Equation 4.5)}$$

Table 4.3: Fraction of Formaldehyde Sorbed for Each Polymer Tested at High Concentration

Polymer	Fraction of Formaldehyde Sorbed at 5.05 ppm
PANI	0.58
PANI 5% NiO	0.46
PANI 10% NiO	0.49
PANI 15% NiO	0.55
PANI 20% NiO	0.55
PANI 5% NiO 15% Al_2O_3	0.48
PANI 10% NiO 10% Al_2O_3	0.55
PANI 15% NiO 5% Al_2O_3	0.54
Average	0.52
s^2	0.002

The average fraction of formaldehyde sorbed was 0.52. Therefore, for higher concentrations of formaldehyde, and below the saturation point, 52% of the formaldehyde concentration in the air sorbed onto the polymer. Hence, the amount of formaldehyde sorbed could be determined as per Equation 4.6:

$$[Formaldehyde]_{Sorbed} = 0.52 \times [Formaldehyde]_{Actual} \quad \text{(Equation 4.6)}$$

4.2.2 Low Concentrations (Below 1 ppm) of Formaldehyde

At lower concentrations of formaldehyde, below 1 ppm, the percentage sorbed was reduced (see Equation 4.7) and, as discussed earlier, the corresponding s^2 was larger by about 5-7 times. This may be due to a reduced concentration that comes into contact with the polymer. The percentage of formaldehyde sorbed onto the polymers at low concentrations was averaged over both low target concentrations of formaldehyde tested. At low concentrations, below 1 ppm, the concentration of sorbed formaldehyde can be determined as per Equation 4.7. The calculations are presented in Table 4.4 It is also interesting to note that the data in both Tables 4.3 and 4.4, show that PANI seems to perform better when there are no dopants.

$$[Formaldehyde]_{Sorbed} = 0.40 \times [Formaldehyde]_{Actual} \quad \text{(Equation 4.7)}$$

Table 4.4: Fraction of Formaldehyde Sorbed for Each Polymer Tested at Low Concentration

Polymer	Fraction of Formaldehyde Sorbed at 0.73 ppm	Fraction of Formaldehyde Sorbed at 0.09 ppm
PANI	0.54	0.48
PANI 5% NiO	0.47	0.37
PANI 10% NiO	0.47	0.48
PANI 15% NiO	0.35	0.52
PANI 20% NiO	0.45	0.37
PANI 5% NiO 15% Al_2O_3	0.32	0.04
PANI 10% NiO 10% Al_2O_3	0.41	0.44
PANI 15% NiO 5% Al_2O_3	0.35	0.42
Average	0.40	
s^2	0.014	

4.3 Comparison of Polymer Sorption Averages

4.3.1 Analysis of Variance (ANOVA)

By comparing the polymer gas sorption means for different materials, (μ_t) from Tables 3.2 and 3.3, it is possible to determine if the variation between polymer types or substrates (effectively, the treatments) is significantly larger than the variation within each polymer. This is done by constructing an analysis of variance (ANOVA) table in which the $F_{Observed}$ value is calculated. This F-value is compared to the $F_{Tabulated}$ from the corresponding F-Table. $F_{Tabulated}$ is based on the degrees of freedom (df) of both the signal and the noise or error (to be discussed shortly). If the $F_{Observed}$ is greater than the $F_{Tabulated}$, then H_0 is rejected. H_0 and H_1 are listed in Equations 4.8 and 4.9.

H_0: $\tau_1 = \tau_2 = \tau_3 = \tau_4 = \tau_5 = \tau_6 = \tau_7 = \tau_8 = 0$ (Equation 4.8)

H_1: $\tau_t \neq 0$ for at least one of t = 1, 2, 3, 4, 5, 6, 7, 8 (Equation 4.9)

where τ is the deviation of the treatment mean (μ_t) for each polymer from the overall mean (μ) of the polymer for the gas tested (see Equation 4.10).

$$\tau_t = \mu_t - \mu \quad \text{(Equation 4.10)}$$

ANOVA tables were used to compare the polymers for each gas tested (see Tables 4.5 through to 4.10). If H_0 is rejected, then H_1 is true (see Equation 4.9), hence it can be seen that

some polymers do a better job at sorbing and thus detecting formaldehyde. Equations 4.11 through to 4.19 were used to determine the entries in the ANOVA tables.

$$SS_{Total} = \sum_k \sum_n y^2 - \frac{1}{\sum_k n}(\sum_k \sum_n y)^2 \quad \text{(Equation 4.11)}$$

$$df_{Total} = \sum_k n - 1 \quad \text{(Equation 4.12)}$$

$$SS_{Between} = \sum_k \frac{(\sum_n y)^2}{n} - \frac{1}{\sum_k n}(\sum_k \sum_n y)^2 \quad \text{(Equation 4.13)}$$

$$df_{Between} = k - 1 \quad \text{(Equation 4.14)}$$

$$SS_{Within} = SS_{Total} - SS_{Between} \quad \text{(Equation 4.15)}$$

$$df_{Within} = df_{Total} - dfS_{Between} \quad \text{(Equation 4.16)}$$

$$MS_{Between} = \frac{SS_{Between}}{df_{Between}} \quad \text{(Equation 4.17)}$$

$$MS_{Within} = \frac{SS_{Within}}{df_{Within}} \quad \text{(Equation 4.18)}$$

$$F_{Observed} = \frac{MS_{Between}}{MS_{Within}} \quad \text{(Equation 4.19)}$$

SS denotes the sum of squares, y is the concentration sorbed onto each polymer (see Tables 3.2 and 3.3), k is the number of treatments or polymers (8, in this case), n is the number of polymer samples per treatment (3, in this case), df denotes degrees of freedom, and MS is the mean square quantity.

Table 4.5: ANOVA for Formaldehyde at 5.05 ppm

Source	**SS**	**df**	**MS**	**$F_{Observed}$**
Between Polymers	37.13	7	5.3	380.55
Within Polymers	0.22	16	0.01	
Total	37.35	23		

Table 4.6: ANOVA for Ethanol at 5.00 ppm

Source	**SS**	**df**	**MS**	**$F_{Observed}$**
Between Polymers	21.51	7	3.07	216.3
Within Polymers	0.23	16	0.01	
Total	21.73	23		

Table 4.7: ANOVA for Acetaldehyde at 4.96 ppm

Source	**SS**	**df**	**MS**	**$F_{Observed}$**
Between Polymers	17.65	7	2.52	91.93
Within Polymers	0.44	16	0.03	
Total	18.09	23		

Table 4.8: ANOVA for Benzene at 5.10 ppm

Source	**SS**	**df**	**MS**	**$F_{Observed}$**
Between Polymers	19.29	7	2.76	129.7
Within Polymers	0.34	16	0.02	
Total	19.63	23		

Table 4.9: ANOVA for Formaldehyde at 0.73 ppm

Source	**SS**	**df**	**MS**	**$F_{Observed}$**
Between Polymers	0.48	7	0.07	5.39
Within Polymers	0.20	16	0.01	
Total	0.68	23		

Table 4.10: ANOVA for Formaldehyde at 0.09 ppm

Source	**SS**	**df**	**MS**	**$F_{Observed}$**
Between Polymers	0.0046	7	0.0007	3.97
Within Polymers	0.0027	16	0.0002	
Total	0.0073	23		

In the headings of Tables 4.5 to 4.10, each gas (analyte) was tested at a certain target concentration. This is the concentration of the specific gas (or analyte) in nitrogen, as used per treatment. For instance, considering Table 4.9, formaldehyde was present at a level of 0.73 ppm in nitrogen as the gas mixture flowed over the different polymers.

The $F_{Observed}$ value is compared to the $F_{Tabulated}$, which is equal to 2.66, to determine whether or not H_0 is true (see Equation 4.8). $F_{Tabulated}$ was determined in all cases from the tables of the F-distribution, with 7 degrees of freedom in the numerator, 16 degrees of freedom in the denominator, and the typical significance level α of 5% ($\alpha = 0.05$). For all of the different gases tested at approximately 5 ppm, as well as the lower concentrations of formaldehyde tested, $F_{Observed}$ was greater than $F_{Tabulated}$. Therefore, H_0 is rejected (see Equation 4.8) for Tables 4.5 through to 4.10. Hence, the τ_t's are not zero, and H_1 (the alternative research hypothesis or claim) seems to be supported by the collected data. This means then, that at least one of the treatment (or polymer) means is different from the overall mean. Thus, the difference between gas sorption values for polymers can be detected and is much larger than the difference within the same polymer, which is the random error due to chance fluctuations. Therefore, there is a difference between how the different polymers interacted with each gas. This is discussed in more detail and quantified in Sections 4.3.2 and 4.3.3.

4.3.2 Comparison Between Means Based on t-Test

The true averages (μ) of each polymer were compared by a hypothesis test (see Equations 4.20 and 4.21). For cases when a stronger statement is desired, such as that a certain population characteristic is below a certain value ($\mu_i < \mu_j$), a one sided test is used (see Equation 4.21). The variances (s^2) were assumed to be the same for each polymer and were pooled (s_p^2); see Equation 4.22. The degrees of freedom (df), see Equation 4.23, were used to find $t_{\alpha, df}$ at an alpha level (level of significance) equal to 0.05. A one-sided test was used on the calculated sample averages ($\overline{x}$) of the different polymers for each gas sorbed, where n_i and n_j were the sample sizes averaged (see Equation 4.24). In this t-test comparison, differences were tested between the two polymers of Tables 3.2 and 3.3, and $n_i = n_j = 3$.

H_0: $\mu_i = \mu_j$ (Equation 4.20)

H_1: $\mu_i < \mu_j$ (Equation 4.21)

$$s_p^2 = \frac{(n_i-1)s_i^2+(n_j-1)s_j^2}{(n_i+n_j-2)}$$ (Equation 4.22)

$$df = n_i + n_j - 2$$ (Equation 4.23)

$$(\bar{x}_j - \bar{x}_i) \pm t_{\alpha,df} s_p \sqrt{\frac{1}{n_i}+\frac{1}{n_j}}$$ (Equation 4.24)

The intervals that result from Equation 4.24 are listed in Tables 4.11 and 4.12 for all gases and concentrations for each polymer. If the interval contains zero, then H_0 is true and those two polymers for that gas and concentration are equal (in performance) and statistically there is no difference (in detection ability) between those two polymers. The intervals are highlighted, in Tables 4.11 and 4.12, if this is the case. On the other hand, if the interval does not contain zero, then H_1 is true and μ_j is greater than μ_i, where i is the polymer on the left and j is the polymer on the right in the first column of both Tables 4.11 and 4.12. Therefore, for a given gas, polymer j (the polymer that sorbed the most analyte) would be better for sensing since it sorbed more analyte. For example, in the first row in the second column, of both Tables 4.11 and 4.12, where the interval produced by the t-test did not contain zero, and thus H_0 was rejected, PANI sorbed more formaldehyde than PANI doped with 5% NiO.

Alternatively, PANI doped with 10% NiO and PANI with respect to ethanol had an interval that contained zero (see the second row and third column in Table 4.11). Consequently, these two polymers sorbed the same amount of ethanol and were statistically the same. Therefore, for ethanol, it would not make a difference which of these two polymers were used since they performed identically. This was also the case for formaldehyde at 0.09 ppm (see the second row and fourth column in Table 4.12) for PANI doped with 10% NiO and PANI. When comparing these two polymers for the other gases at higher concentrations, the polymers were statistically different, which means they sorbed different amounts of each gas. Since they were statistically different for the other gases, the polymer that performed better could be chosen with more confidence.

For the case of formaldehyde, it is ideal if the average sorbed concentration onto the polymer is as high as possible. Therefore, if H_0 is rejected, then that would mean that the sensitivity towards formaldehyde, for polymer j (the polymer listed on the right in the first column of Table 4.11), is greater than polymer i (the polymer listed on the left in the first column of Table 4.11); however, for the other three gases tested, which are interferents, it is ideal that the average sorbed concentration onto the polymer is as low as possible. Therefore, polymer i would be better. For good selectivity, the polymer should sorb much more formaldehyde and much less of the other three gases.

Table 4.11: Intervals for the Polymer Comparisons for Each Gas

Polymer Comparison	Formaldehyde		Ethanol		Acetaldehyde		Benzene	
PANI 5% NiO x PANI	0.622	0.638	0.628	0.638	0.243	0.323	1.264	1.303
PANI 10% NiO x PANI	0.435	0.518	-0.003	0.103	0.070	0.110	1.225	1.295
PANI 15% NiO x PANI	0.137	0.156	0.959	0.968	0.059	0.134	0.030	0.084
PANI 20% NiO x PANI	0.132	0.155	0.277	0.290	0.192	0.248	-0.003	0.117
PANI 5% NiO 15% Al_2O_3 x PANI	0.517	0.543	1.365	1.388	0.860	1.080	0.508	0.586
PANI 10% NiO 10% Al_2O_3 x PANI	0.150	0.170	0.185	0.195	0.047	0.086	0.347	0.413
PANI 15% NiO 5% Al_2O_3 x PANI	0.153	0.214	0.175	0.245	0.327	0.439	0.506	0.567
PANI 10% NiO x PANI 5% NiO	0.113	0.194	0.523	0.634	0.348	0.399	0.001	0.045
PANI 15% NiO x PANI 5% NiO	0.475	0.492	0.328	0.332	0.143	0.230	1.326	1.354
PANI 20% NiO x PANI 5% NiO	0.476	0.498	0.346	0.354	0.030	0.097	1.180	1.274
PANI 5% NiO 15% Al_2O_3 x PANI 5% NiO	0.088	0.112	0.734	0.752	0.571	0.803	0.711	0.763
PANI 10% NiO 10% Al_2O_3 x PANI 5% NiO	0.461	0.479	0.440	0.446	0.325	0.375	1.643	1.684
PANI 15% NiO 5% Al_2O_3 x PANI 5% NiO	0.417	0.476	0.390	0.456	0.605	0.728	1.802	1.838
PANI 15% NiO x PANI 10% NiO	0.288	0.372	0.864	0.963	0.163	0.210	1.287	1.347
PANI 20% NiO x PANI 10% NiO	0.289	0.378	0.181	0.286	0.297	0.323	1.140	1.266
PANI 5% NiO 15% Al_2O_3 x PANI 10% NiO	0.008	0.099	1.270	1.384	0.964	1.156	0.672	0.755
PANI 10% NiO 10% Al_2O_3 x PANI 10% NiO	0.275	0.359	0.089	0.191	0.018	0.028	1.604	1.676
PANI 15% NiO 5% Al_2O_3 x PANI 10% NiO	0.230	0.356	0.079	0.241	0.252	0.335	1.763	1.830
PANI 15% NiO x PANI 20% NiO	-0.009	0.016	0.677	0.683	0.092	0.155	0.058	0.168
PANI 5% NiO 15% Al_2O_3 x PANI 15% NiO	0.370	0.397	0.405	0.422	0.760	0.987	0.569	0.637
PANI 15% NiO x PANI 10% NiO 10% Al_2O_3	0.003	0.024	0.771	0.775	0.141	0.186	0.295	0.351
PANI 15% NiO x PANI 15% NiO 5% Al_2O_3	0.006	0.068	0.721	0.850	0.421	0.539	0.454	0.506
PANI 5% NiO 15% Al_2O_3 x PANI 20% NiO	0.371	0.402	1.083	1.104	0.646	0.854	0.423	0.557
PANI 10% NiO 10% Al_2O_3 x PANI 20% NiO	0.004	0.029	0.089	0.098	0.271	0.300	0.376	0.498
PANI 15% NiO 5% Al_2O_3 x PANI 20% NiO	0.007	0.073	0.039	0.108	0.554	0.653	0.535	0.652
PANI 5% NiO 15% Al_2O_3 x PANI 10% NiO 10% Al_2O_3	0.356	0.384	1.177	1.196	0.942	1.132	0.887	0.967
PANI 5% NiO 15% Al_2O_3 x PANI 15% NiO 5% Al_2O_3	0.312	0.381	1.127	1.206	1.222	1.485	1.046	1.121
PANI 15% NiO 5% Al_2O_3 x PANI 10% NiO 10% Al_2O_3	-0.008	0.055	-0.013	0.053	0.276	0.358	0.125	0.188

Table 4.12: Intervals for the Polymer Comparison for Formaldehyde at Different Concentrations

Polymer Comparison	5.05 ppm		0.73 ppm		0.09 ppm	
PANI 5% NiO x PANI	0.622	0.638	0.046	0.060	0.010	0.010
PANI 10% NiO x PANI	0.435	0.518	0.049	0.051	0.000	0.000
PANI 15% NiO x PANI	0.137	0.156	0.112	0.162	0.003	0.004
PANI 20% NiO x PANI	0.132	0.155	0.062	0.064	0.010	0.010
PANI 5% NiO 15% Al_2O_3 x PANI	0.517	0.543	0.145	0.168	0.040	0.040
PANI 10% NiO 10% Al_2O_3 x PANI	0.150	0.170	0.073	0.113	0.003	0.004
PANI 15% NiO 5% Al_2O_3 x PANI	0.153	0.214	0.124	0.156	0.006	0.007
PANI 10% NiO x PANI 5% NiO	0.113	0.194	-0.003	0.010	0.010	0.01
PANI 15% NiO x PANI 5% NiO	0.475	0.492	0.053	0.114	0.013	0.014
PANI 20% NiO x PANI 5% NiO	0.476	0.498	0.003	0.017	0.000	0.000
PANI 5% NiO 15% Al_2O_3 x PANI 5% NiO	0.088	0.112	0.086	0.121	0.030	0.030
PANI 10% NiO 10% Al_2O_3 x PANI 5% NiO	0.461	0.479	0.015	0.065	0.006	0.007
PANI 15% NiO 5% Al_2O_3 x PANI 5% NiO	0.417	0.476	0.066	0.108	0.003	0.004
PANI 15% NiO x PANI 10% NiO	0.288	0.372	0.063	0.111	0.003	0.003
PANI 20% NiO x PANI 10% NiO	0.289	0.378	0.013	0.014	0.010	0.010
PANI 5% NiO 15% Al_2O_3 x PANI 10% NiO	0.008	0.099	0.096	0.118	0.040	0.04
PANI 10% NiO 10% Al_2O_3 x PANI 10% NiO	0.275	0.359	0.024	0.062	0.000	0.004
PANI 15% NiO 5% Al_2O_3 x PANI 10% NiO	0.230	0.356	0.075	0.105	0.006	0.007
PANI 15% NiO x PANI 20% NiO	-0.009	0.016	0.049	0.098	0.013	0.014
PANI 5% NiO 15% Al_2O_3 x PANI 15% NiO	0.370	0.397	-0.015	0.055	0.043	0.043
PANI 15% NiO x PANI 10% NiO 10% Al_2O_3	0.003	0.024	0.000	0.086	0.007	0.007
PANI 15% NiO x PANI 15% NiO 5% Al_2O_3	0.006	0.068	-0.036	0.042	0.010	0.010
PANI 5% NiO 15% Al_2O_3 x PANI 20% NiO	0.371	0.402	0.082	0.105	0.030	0.030
PANI 10% NiO 10% Al_2O_3 x PANI 20% NiO	0.004	0.029	0.011	0.049	0.006	0.007
PANI 15% NiO 5% Al_2O_3 x PANI 20% NiO	0.007	0.073	0.062	0.092	0.003	0.004
PANI 5% NiO 15% Al_2O_3 x PANI 10% NiO 10% Al_2O_3	0.356	0.384	0.033	0.093	0.036	0.037
PANI 5% NiO 15% Al_2O_3 x PANI 15% NiO 5% Al_2O_3	0.312	0.381	-0.009	0.042	0.033	0.034
PANI 15% NiO 5% Al_2O_3 x PANI 10% NiO 10% Al_2O_3	-0.008	0.055	0.013	0.081	0.003	0.004

In general, based on the results of Tables 4.11 and 4.12, the polymers were statistically different with regards to the way they interacted with the different gases. The polymers that were more promising for the detection of formaldehyde were statistically different from all of the other polymers tested. Therefore, the polymers that were more promising with respect to formaldehyde detection could be chosen with confidence. This is discussed more in Section 4.4.

4.3.3 Least Significant Difference (LSD)

More rigorous testing of the difference between the polymers was conducted using a least significant difference (LSD) test. LSD (or Fisher's LSD) is a very useful tool for multiple comparisons. A more appropriate alpha (0.001), as per Equation 4.26, is calculated to reduce the effect of compounded error that results from multiple comparisons. This is equivalent to lowering the overall probability of making one incorrect rejection from 1 in 20 to 1 in 2000.

The least significant difference (LSD) is the value at which the difference between two means becomes significant. If the difference between two means, of two polymers, is equal or greater than the LSD, then there is a significant difference between the two polymers (see Equations 4.25 through 4.28).

$$c = \frac{k(k-1)}{2} \quad \text{(Equation 4.25)}$$

$$\alpha = \frac{0.05}{c} \quad \text{(Equation 4.26)}$$

$$s.e. = \sqrt{\frac{2s^2}{n}} \quad \text{(Equation 4.27)}$$

$$LSD = \left(t_{N-k,\frac{\alpha}{2}}\right) \cdot (s.e.) \quad \text{(Equation 4.28)}$$

In Equations 4.25 through to 4.28, c represents the total number of possible comparisons between two means, k is again the number of treatments (or polymers), which is 8 in this case, Equation 4.26 yields now a very reasonable (safe) level of significance for each individual test, s^2 is the MS_{Within} entry from the corresponding ANOVA Table (see Tables 4.5 through to 4.10), n is equal to 3, and N is equal to 24, for each case.

The differences between the polymer means (see Equation 4.29) are listed in Tables 4.13 and 4.14. The LSD is 0.28 for formaldehyde, 0.28 for ethanol, 0.39 for acetaldehyde, and 0.35 for benzene at a concentration of approximately 5 ppm (see Table 4.13). The LSD is 0.27 for formaldehyde at a concentration of 0.73 ppm and 0.03 for formaldehyde at a concentration of 0.09 ppm (see Table 4.14). The corresponding LSD also appears at the top of both Tables 4.13 and 4.14 for quick reference.

$$Difference = |\mu_i - \mu_j| \quad \text{(Equation 4.29)}$$

Table 4.13: Difference Between Sorption Means for Each Gas Tested at Approximately 5 ppm

Polymer Comparison	Formaldehyde	Ethanol	Acetaldehyde	Benzene
LSD	0.28	0.28	0.39	0.35
PANI x PANI 5% NiO	0.63	0.63	0.28	1.28
PANI x PANI 10% NiO	0.47	0.05	0.09	1.26
PANI x PANI 15% NiO	0.14	0.96	0.10	0.06
PANI x PANI 20% NiO	0.14	0.28	0.22	0.05
PANI x PANI 5% NiO 15% Al_2O_3	0.53	1.38	0.75	0.54
PANI x PANI 10% NiO 10% Al_2O_3	0.16	0.19	0.07	0.38
PANI x PANI 15% NiO 5% Al_2O_3	0.18	0.21	0.38	0.54
PANI 5% NiO x PANI 10% NiO	0.16	0.58	0.37	0.02
PANI 5% NiO x PANI 15% NiO	0.49	0.33	0.18	1.34
PANI 5% NiO x PANI 20% NiO	0.49	0.35	0.06	1.23
PANI 5% NiO x PANI 5% NiO 15% Al_2O_3	0.10	0.75	0.47	0.74
PANI 5% NiO x PANI 10% NiO 10% Al_2O_3	0.47	0.44	0.35	1.66
PANI 5% NiO x PANI 15% NiO 5% Al_2O_3	0.45	0.42	0.66	1.82
PANI 10% NiO x PANI 15% NiO	0.33	0.91	0.19	1.32
PANI 10% NiO x PANI 20% NiO	0.33	0.23	0.31	1.21
PANI 10% NiO x PANI 5% NiO 15% Al_2O_3	0.06	1.33	0.84	0.72
PANI 10% NiO x PANI 10% NiO 10% Al_2O_3	0.31	0.14	0.02	1.64
PANI 10% NiO x PANI 15% NiO 5% Al_2O_3	0.29	0.16	0.29	1.80
PANI 15% NiO x PANI 20% NiO	0.00	0.68	0.12	0.11
PANI 15% NiO x PANI 5% NiO 15% Al_2O_3	0.39	0.42	0.65	0.60
PANI 15% NiO x PANI 10% NiO 10% Al_2O_3	0.02	0.77	0.17	0.32
PANI 15% NiO x PANI 15% NiO 5% Al_2O_3	0.04	0.75	0.48	0.48
PANI 20% NiO x PANI 5% NiO 15% Al_2O_3	0.39	1.10	0.53	0.49
PANI 20% NiO x PANI 10% NiO 10% Al_2O_3	0.02	0.09	0.29	0.43
PANI 20% NiO x PANI 15% NiO 5% Al_2O_3	0.04	0.07	0.60	0.59
PANI 5% NiO 15% Al_2O_3 x PANI 10% NiO 10% Al_2O_3	0.37	1.19	0.82	0.92
PANI 5% NiO 15% Al_2O_3 x PANI 15% NiO 5% Al_2O_3	0.35	1.17	1.13	1.08
PANI 10% NiO 10% Al_2O_3 x PANI 15% NiO 5% Al_2O_3	0.02	0.02	0.31	0.16

Table 4.14: Difference Between Sorption Means for Formaldehyde at All Concentrations Tested

Polymer Comparison	5.05 ppm	0.73 ppm	0.09 ppm
LSD	0.28	0.27	0.03
PANI x PANI 5% NiO	0.63	0.05	0.01
PANI x PANI 10% NiO	0.47	0.05	0.00
PANI x PANI 15% NiO	0.14	0.13	0.01
PANI x PANI 20% NiO	0.14	0.06	0.01
PANI x PANI 5% NiO 15% Al_2O_3	0.53	0.15	0.04
PANI x PANI 10% NiO 10% Al_2O_3	0.16	0.09	0.00
PANI x PANI 15% NiO 5% Al_2O_3	0.18	0.14	0.00
PANI 5% NiO x PANI 10% NiO	0.16	0.00	0.01
PANI 5% NiO x PANI 15% NiO	0.49	0.08	0.02
PANI 5% NiO x PANI 20% NiO	0.49	0.01	0.00
PANI 5% NiO x PANI 5% NiO 15% Al_2O_3	0.10	0.10	0.03
PANI 5% NiO x PANI 10% NiO 10% Al_2O_3	0.47	0.04	0.01
PANI 5% NiO x PANI 15% NiO 5% Al_2O_3	0.45	0.09	0.01
PANI 10% NiO x PANI 15% NiO	0.33	0.08	0.01
PANI 10% NiO x PANI 20% NiO	0.33	0.01	0.01
PANI 10% NiO x PANI 5% NiO 15% Al_2O_3	0.06	0.10	0.04
PANI 10% NiO x PANI 10% NiO 10% Al_2O_3	0.31	0.04	0.00
PANI 10% NiO x PANI 15% NiO 5% Al_2O_3	0.29	0.09	0.00
PANI 15% NiO x PANI 20% NiO	0.00	0.07	0.02
PANI 15% NiO x PANI 5% NiO 15% Al_2O_3	0.39	0.02	0.05
PANI 15% NiO x PANI 10% NiO 10% Al_2O_3	0.02	0.04	0.01
PANI 15% NiO x PANI 15% NiO 5% Al_2O_3	0.04	0.01	0.01
PANI 20% NiO x PANI 5% NiO 15% Al_2O_3	0.39	0.09	0.03
PANI 20% NiO x PANI 10% NiO 10% Al_2O_3	0.02	0.03	0.01
PANI 20% NiO x PANI 15% NiO 5% Al_2O_3	0.04	0.08	0.01
PANI 5% NiO 15% Al_2O_3 x PANI 10% NiO 10% Al_2O_3	0.37	0.06	0.04
PANI 5% NiO 15% Al_2O_3 x PANI 15% NiO 5% Al_2O_3	0.35	0.01	0.04
PANI 10% NiO 10% Al_2O_3 x PANI 15% NiO 5% Al_2O_3	0.02	0.05	0.00

If the value is less than the corresponding LSD, it is highlighted. For example, in Table 4.13, PANI and PANI doped with 5% NiO are significantly different for formaldehyde, ethanol, and benzene, but not for acetaldehyde. This means that for the average sorbed amount of acetaldehyde onto PANI and PANI doped with 5% NiO there is no significant difference detected between these two polymers for acetaldehyde.

If Tables 4.13 and 4.14 are scrutinized further, it can be seen that many of the polymers that were previously determined to be different (see Section 4.3.2), were actually statistically the same and therefore interact similarly with a gas at a specific concentration. For instance, PANI and PANI doped with 5% NiO were statistically different for all concentrations of formaldehyde tested (see Table 4.12) based on the t-test performed in Section 4.3.2. However, when the more rigorous LSD test was used, there was no significant difference at the lower concentrations of formaldehyde between PANI and PANI doped with 5% NiO (see Table 4.14).

In general, more polymers were significantly different at the higher concentrations of formaldehyde than at the lower concentrations tested (see Table 4.14). However, the error for formaldehyde tested at a concentration of 0.73 ppm, was of the same order of magnitude as the difference within the polymers. The variation within the polymer, which can be seen in Figure 4.5, was due to small variances between the replicates as well as random (chance) concentration fluctuations within the gas that flowed over the polymers.

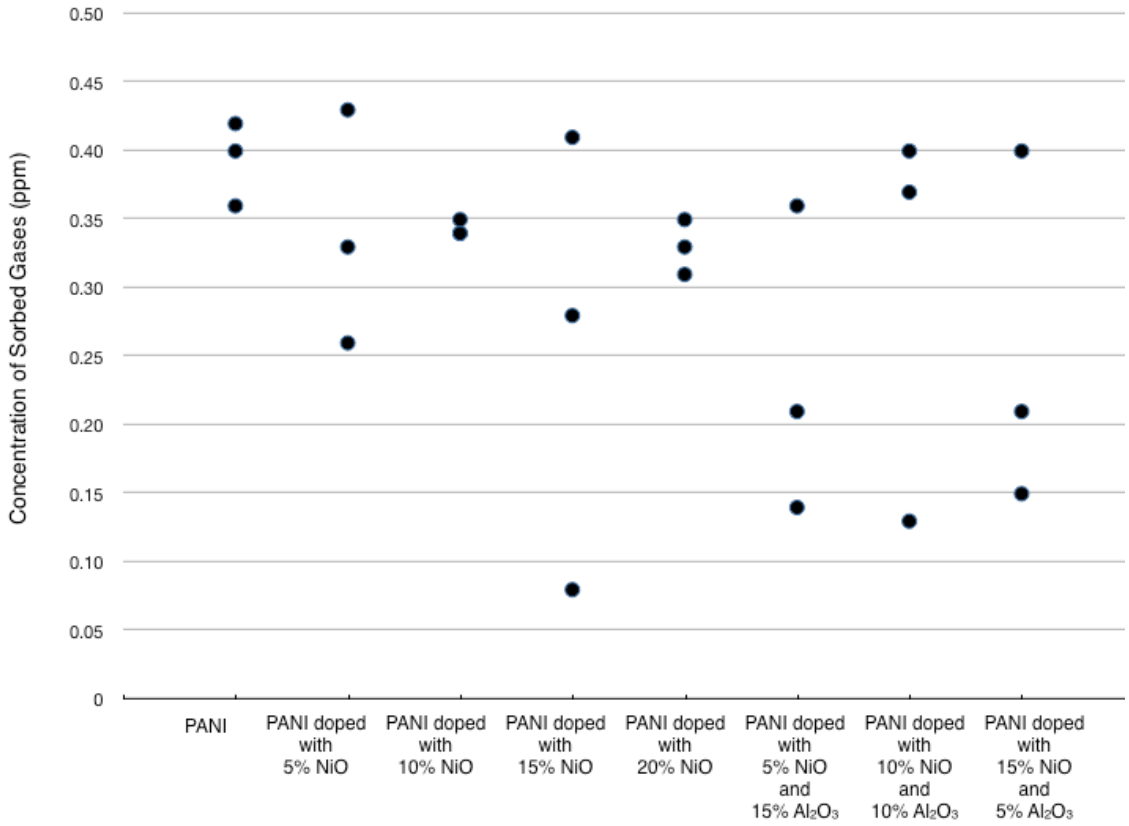

Figure 4.5: Sorbed formaldehyde for each polymer sample at a concentration of 0.73 ppm.

At this point of the analysis, it should be noted that, overall, the polymers that were more promising for the detection of formaldehyde, especially PANI doped with 5% NiO and 15% Al_2O_3, were significantly different from the other polymers. This is discussed in further detail in Section 4.4.

4.4 Comparison of Polymers for the Sensing of Formaldehyde

4.4.1 Polymer Comparison for Formaldehyde Sensing

Four gases (formaldehyde, ethanol, acetaldehyde, and benzene) were tested individually to determine their sorption to the different polymers. The average sorption values of each of the four gases, at approximately 5 ppm, were plotted for each polymer (see Figure 4.6). A polymer that sorbed a lot of formaldehyde and much less of the other three gases is ideal for formaldehyde sensing, since it is selective towards formaldehyde with respect to the other gases. This was the case for PANI doped with 5% NiO and 15% Al_2O_3 (see Figure 4.6).

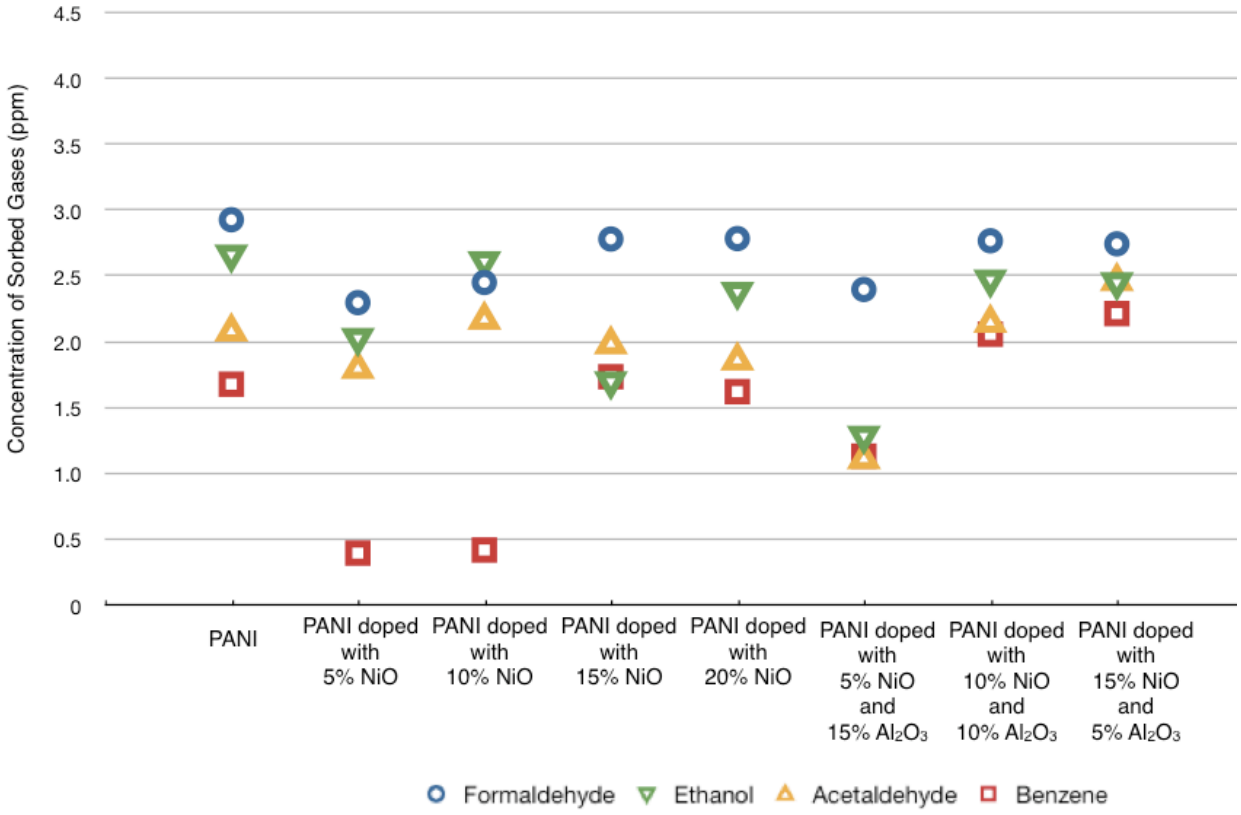

Figure 4.6: Concentration of sorbed gases for each polymer tested.

There were a few trends that can be seen in Figure 4.6. As the amount of NiO increased, so did the sensitivity towards formaldehyde and benzene; however, the sensitivity of the NiO-doped PANI never reached the sensitivity of PANI alone. In addition, the increase in NiO did not

affect the sensitivity towards ethanol or acetaldehyde (see Figure 4.7). At the same time, the change in NiO concentration did not affect the selectivity of the polymers.

A decrease in the concentration of Al_2O_3, combined with an increase in the concentration of NiO, resulted in an increase in sensitivity towards all four of the gases tested (see Figure 4.8). On the other hand, selectivity was improved with an increase in Al_2O_3 and a decrease in NiO concentration. This is in agreement with Campanella et al. (2006). Trend lines are added in Figures 4.7 and 4.8 to aid in the visualization of the trends observed.

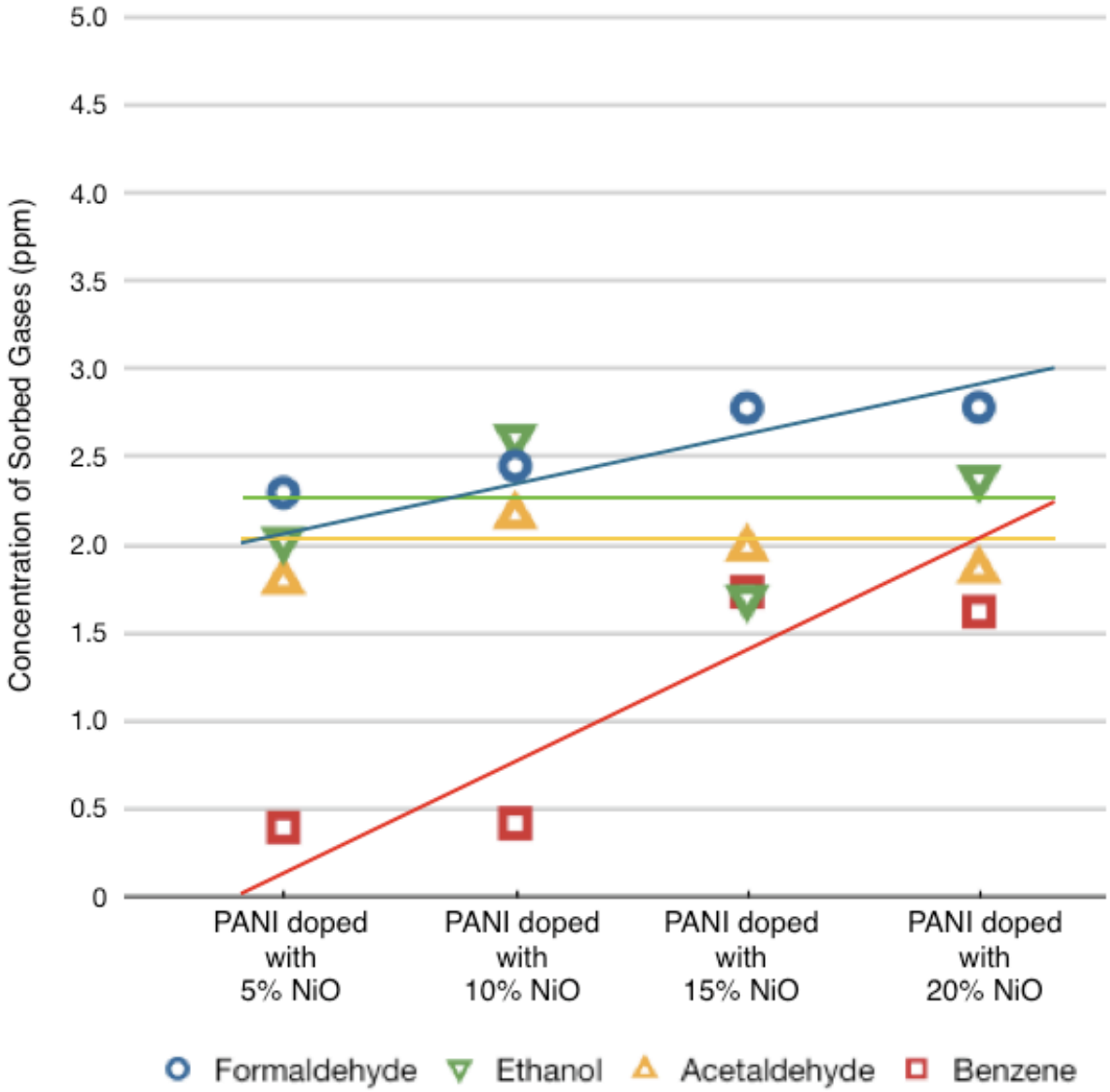

Figure 4.7: PANI doped with NiO trends.

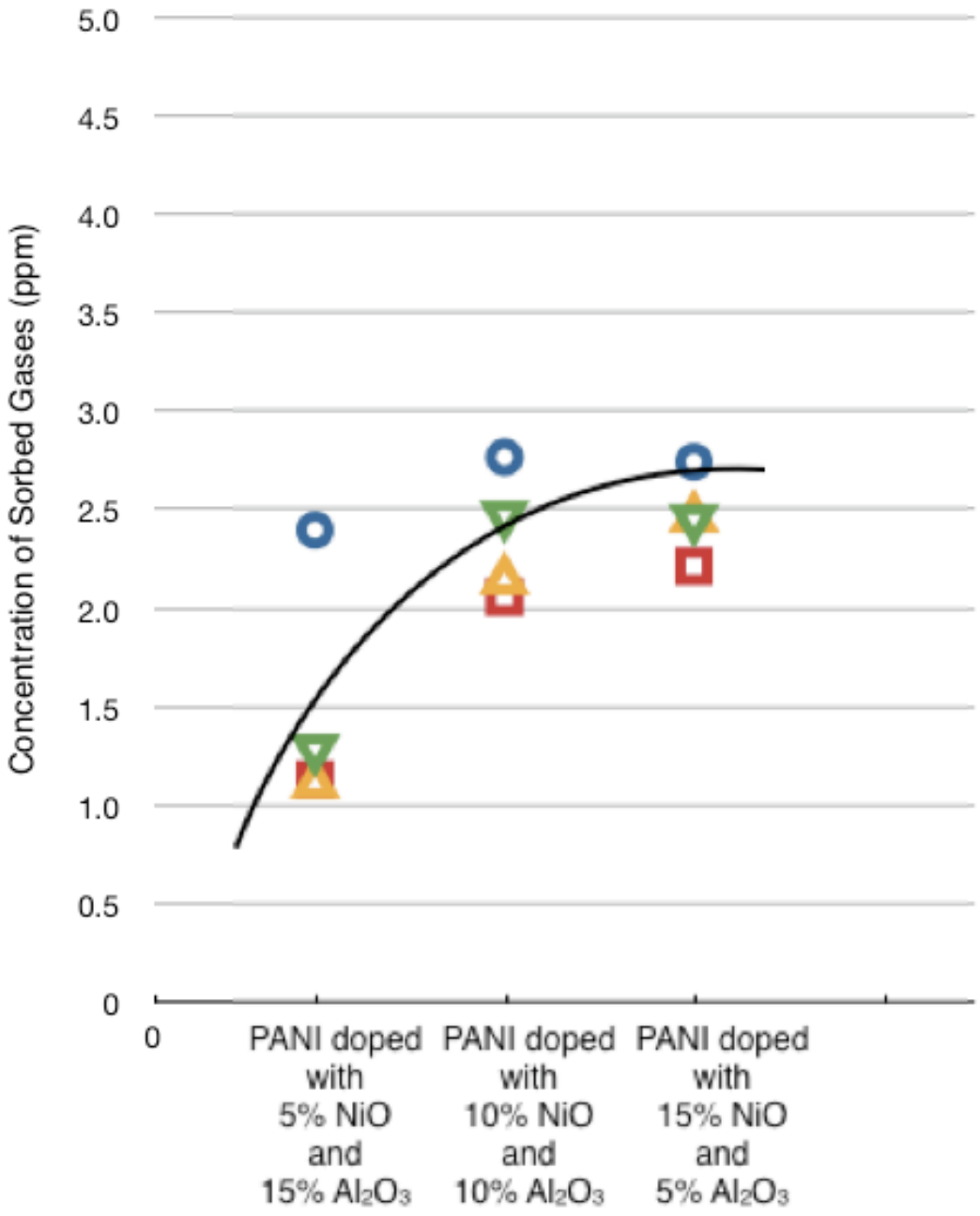

Figure 4.8: PANI doped with NiO and Al_2O_3 trends.

Overall, PANI had the highest sensitivity towards each gas tested since it sorbed the most; however, PANI did not have very good selectivity (see Table 4.15). Although many other polymers have a higher sorption of formaldehyde, it is the selectivity towards formaldehyde that separates PANI doped with 5% NiO and 15% Al_2O_3 from the rest of the polymers as the optimal sensing material for formaldehyde.

Table 4.15: Selectivity of Each Polymer Towards Formaldehyde

Polymer	Ethanol	Acetaldehyde	Benzene
PANI	1.10	1.40	1.74
PANI 5% NiO	1.13	1.27	5.76
PANI 10% NiO	0.94	1.13	5.80
PANI 15% NiO	1.63	1.40	1.60
PANI 20% NiO	1.17	1.49	1.72
PANI 5% NiO 15% Al_2O_3	1.86	1.79	2.11
PANI 10% NiO 10% Al_2O_3	1.12	1.29	1.34
PANI 15% NiO 5% Al_2O_3	1.12	1.11	1.24

Good selectivity is a value greater than 1.75.

4.4.2 Selectivity of PANI doped with 5% NiO and 15% Al_2O_3

The selectivity of PANI doped with 5% NiO and 15% Al_2O_3 for single gases is shown in Figure 4.9. The selectivity of PANI doped with 5% NiO and 15% Al_2O_3 for formaldehyde was 1.86 with respect to ethanol, 1.79 with respect to acetaldehyde, and 2.11 with respect to benzene. It should be noted that good selectivity is a value greater than 1.75. Therefore, PANI doped with 5% NiO and 15% Al_2O_3 had good selectivity towards formaldehyde with respect to the other three gases tested.

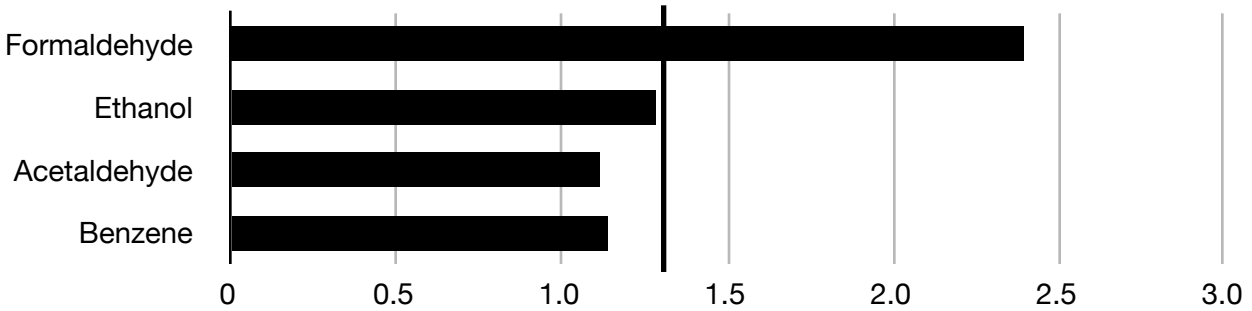

Figure 4.9: Selectivity of PANI doped with 5% NiO and 15% Al_2O_3 when each gas is individually tested.

The line is drawn at the concentration where selectivity would be equal to 1.75. Ideally, formaldehyde should be much higher than this line on the bar graph, and the other three gases should be much lower. If this is the case, like it is in Figure 4.9, then the polymer is selective towards formaldehyde with respect to the other three gases.

Gas mixtures were also tested to show the selectivity of PANI doped with 5% NiO and 15% Al_2O_3 in a more realistic setting. A quaternary mixture that combined all of the gases at approximately 1 ppm (per analyte) was tested as well as binary gas mixtures of formaldehyde with each of the other gases at a concentration of approximately 2 ppm (for each analyte).

The selectivity of PANI doped with 5% NiO and 15% Al_2O_3 towards formaldehyde in the quaternary gas mixture was 1.28 with respect to ethanol, 2.79 with respect to acetaldehyde, and 14.56 with respect to benzene. Therefore, PANI doped with 5% NiO and 15% Al_2O_3 was selective towards formaldehyde with respect to acetaldehyde and benzene, but not with respect to ethanol when all four gases were present in the test mixture (see Figure 4.10). The line again represents the concentration at which selectivity is 1.75.

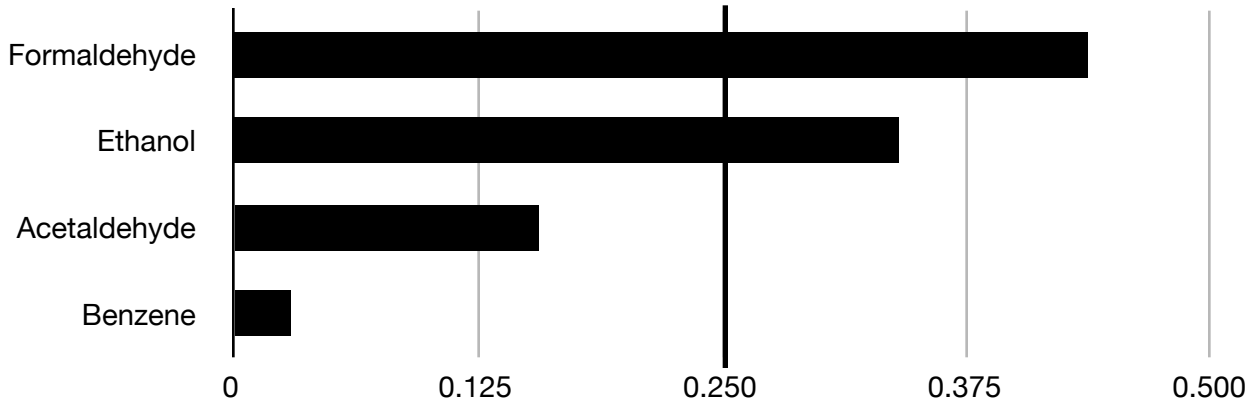

Figure 4.10: Selectivity of PANI doped with 5% NiO and 15% Al_2O_3 when all four gases are present.

The quaternary gas mixture showed less selectivity towards formaldehyde with respect to ethanol for PANI doped with 5% NiO and 15% Al_2O_3 than the individual gases tested. This may have been due to ethanol hydrogen bonding to formaldehyde that had already bound to the polymer's active sites, as well as binding to the polymer itself. On the other hand, the selectivity of PANI doped with 5% NiO and 15% Al_2O_3 towards formaldehyde was better with respect to acetaldehyde and benzene. This may have been due to the preferential binding of formaldehyde due to both the affinity between the polymer and formaldehyde as well as formaldehyde's smaller size, which would have allowed it to absorb into smaller active sites within the polymer. Since neither acetaldehyde nor benzene have a hydrogen that is able to generate a hydrogen bond, neither can bind to formaldehyde once an active site has been occupied.

PANI doped with 5% NiO and 15% Al_2O_3 was also tested in binary gas mixtures of formaldehyde with each other gas (ethanol, acetaldehyde, and benzene) to determine its selectivity (see Figure 4.11). The selectivity of the binary mixtures for formaldehyde was 1.55 with respect to ethanol, 2.03 with respect to acetaldehyde, and 2.70 with respect to benzene. The concentration at which selectivity is 1.75 is represented by the vertical line in the graphs.

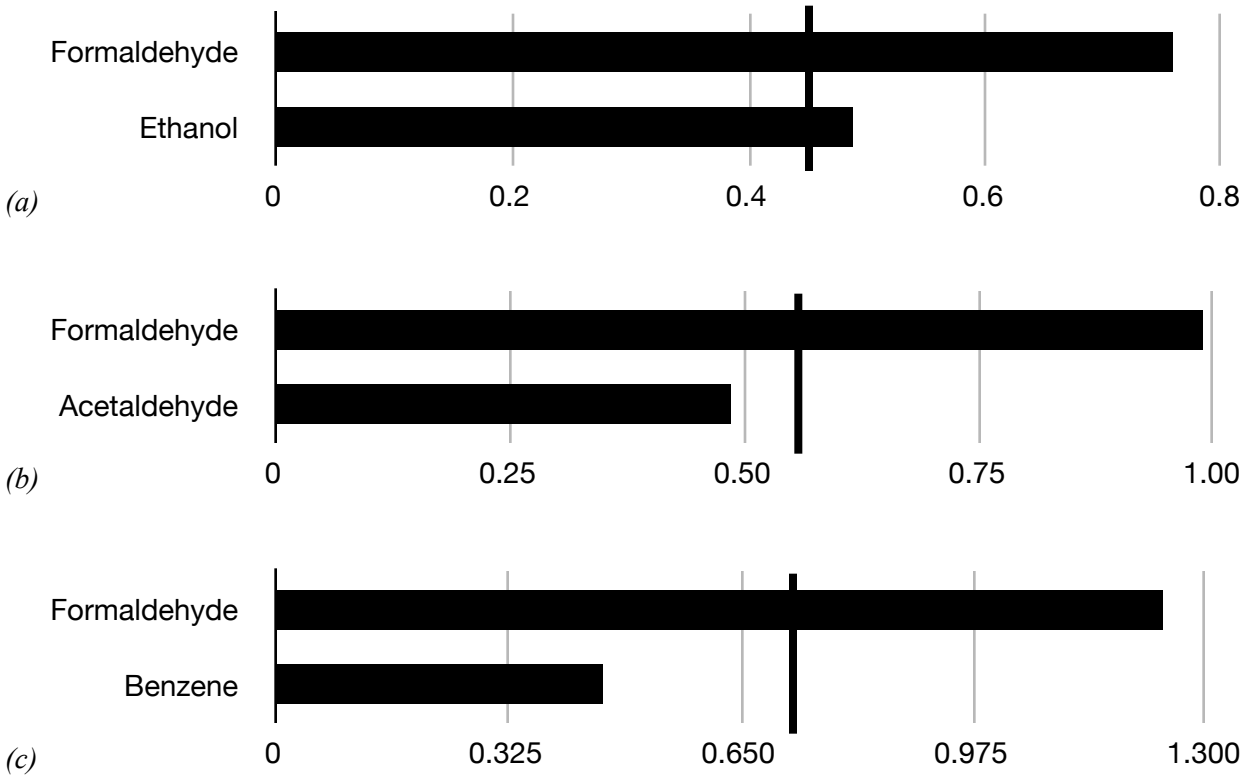

Figure 4.11: Selectivity of PANI doped with 5% NiO and 15% Al_2O_3 for binary gas mixtures of formaldehyde with (a) ethanol, (b) acetaldehyde, and (c) benzene.

The selectivity of each gas tested decreased in the binary mixtures from the single gases, but was still better than in the quaternary gas mixture. The gases, even at low concentrations, interact with one another, which can make it more difficult to determine the effects of interferents.

Overall, at higher concentrations, PANI doped with 5% NiO and 15% Al_2O_3 was very good for sensing formaldehyde. PANI doped with 5% NiO and 15% Al_2O_3 had both enough sensitivity to detect formaldehyde down to 1 ppm, but also had relatively good selectivity towards the other three gases tested, especially acetaldehyde and benzene.

4.4.3 Sensitivity at Low Concentrations of Formaldehyde

Although PANI doped with 5% NiO and 15% Al_2O_3 had good selectivity towards formaldehyde at higher concentrations (above 1 ppm), at very low concentrations, below 0.09 ppm, formaldehyde did not sorb onto it (see Figure 4.12). This is a problem since the sensitivity is not there for the desired application.

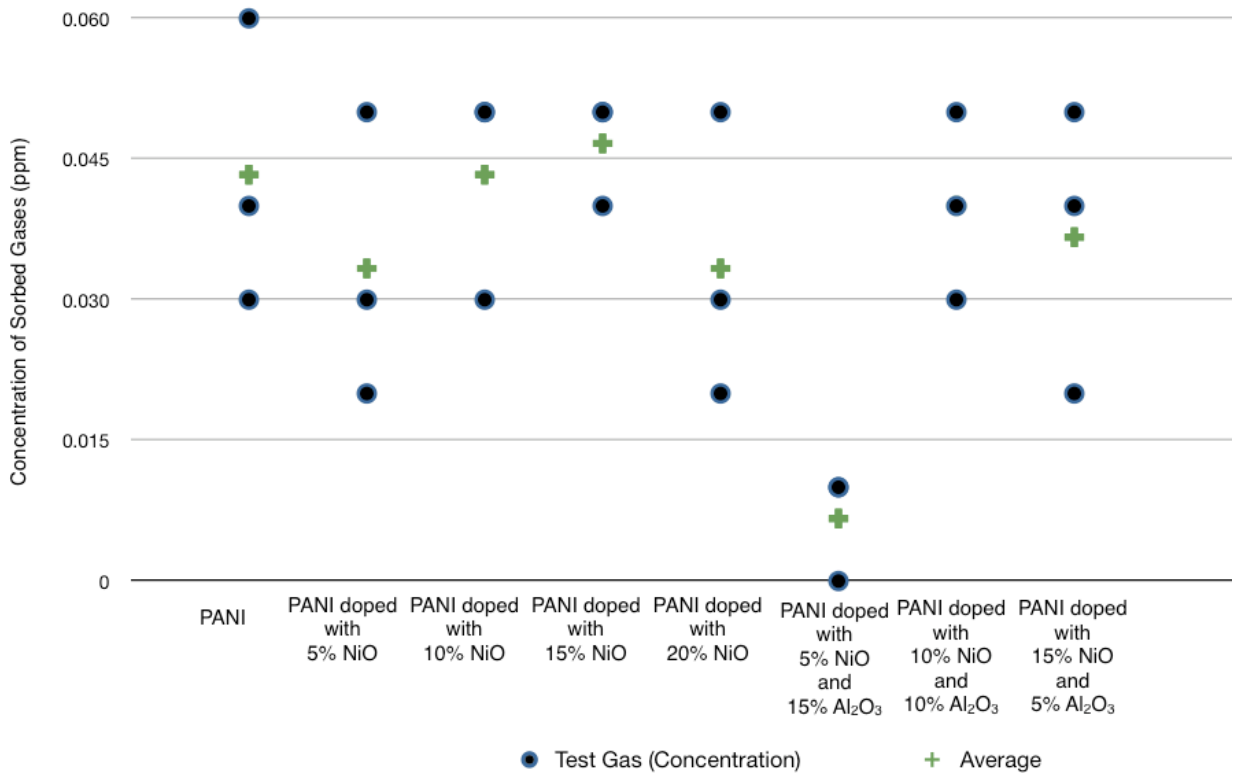

Figure 4.12: Formaldehyde sorption of all polymers at the 0.09 ppm target concentration.

Since PANI doped with 5% NiO and 15% Al_2O_3 was not able to detect formaldehyde at very low concentrations, another polymer needed to be used. PANI doped with 15% NiO appeared to be the second most promising in terms of selectivity (1.63 with respect to ethanol, 1.40 with respect to acetaldehyde, and 1.60 with respect to benzene); see Figure 4.13. It also had the highest sorption of formaldehyde at the lowest concentration tested (see Figure 4.12). Therefore, PANI doped with 15% NiO was tested next for selectivity at lower target concentrations.

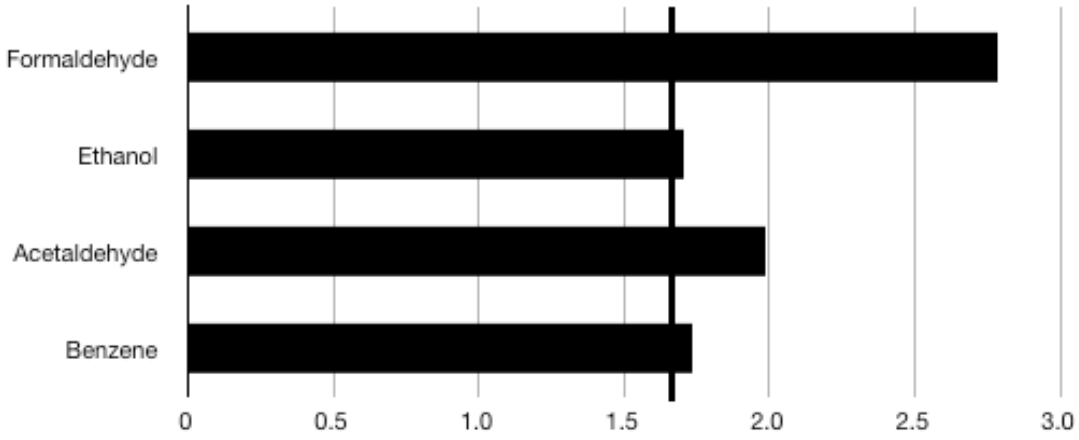

Figure 4.13: Selectivity of PANI doped with 15% NiO for single gases at approximately 5 ppm.

A quaternary gas mixture, of formaldehyde, ethanol, acetaldehyde, and benzene with concentrations of 0.35 ppm, 0.31 ppm, 0.32 ppm, and 0.24 ppm, respectively, was used to determine the selectivity of PANI doped with 15% NiO at low concentrations (see Figure 4.14). The selectivity towards formaldehyde with respect to ethanol was 1.09, with respect to acetaldehyde was 1.55, and with respect to benzene was 5.10. The vertical line represents the concentration at which selectivity is equal to 1.75.

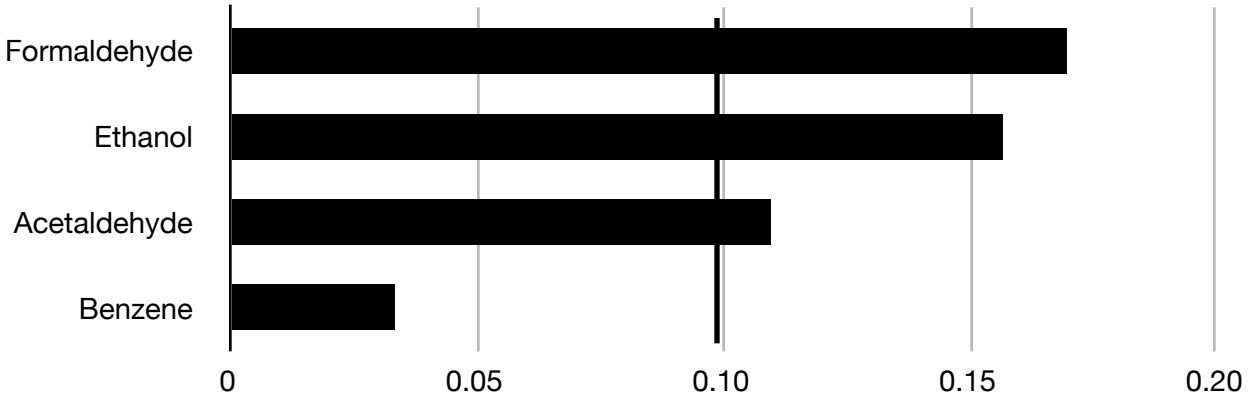

Figure 4.14: Selectivity of PANI doped with 15% NiO when all four gases are present.

The selectivity of PANI doped with 15% NiO towards formaldehyde with respect to ethanol decreased from the single gases tested at higher concentrations, but increased with respect to acetaldehyde and benzene. At very low concentrations, ethanol and to a lesser extent acetaldehyde, would interfere with the sensor and produce a false positive, but benzene would not.

At very low concentrations, PANI doped with 15% NiO had the highest sensitivity towards formaldehyde; however, the selectivity was poor with respect to ethanol. To improve the selectivity of a sensor, two sensing materials could be used and the signal from both could be optimized to determine the concentration of formaldehyde. To determine the concentration of formaldehyde, both PANI doped with 15% NiO and PANI doped with 5% NiO and 15% Al_2O_3 could be used. Since PANI doped with 5% NiO and 15% Al_2O_3 did not sorb any formaldehyde at 0.09 ppm, it could be used to determine the concentration of the interferents. The concentration of the interferents, determined by PANI doped with 15% NiO, could be subtracted from the concentration of all the gases, determined by PANI doped with 5% NiO and 15% Al_2O_3. Therefore, by combining two sensing materials, the concentration of formaldehyde could be determined at very low concentrations.

4.5 Approach to Designing a Sensor for a General Analyte

Sensing materials are chosen based on the analyte as well as the type of sensor that will be used. The type of analyte and sensor chosen narrow down the options for sensing materials.

From these options, the best sensing material for the desired application can be chosen. Figure 4.15 offers some general tips that can be applied to the detection of a general analyte.

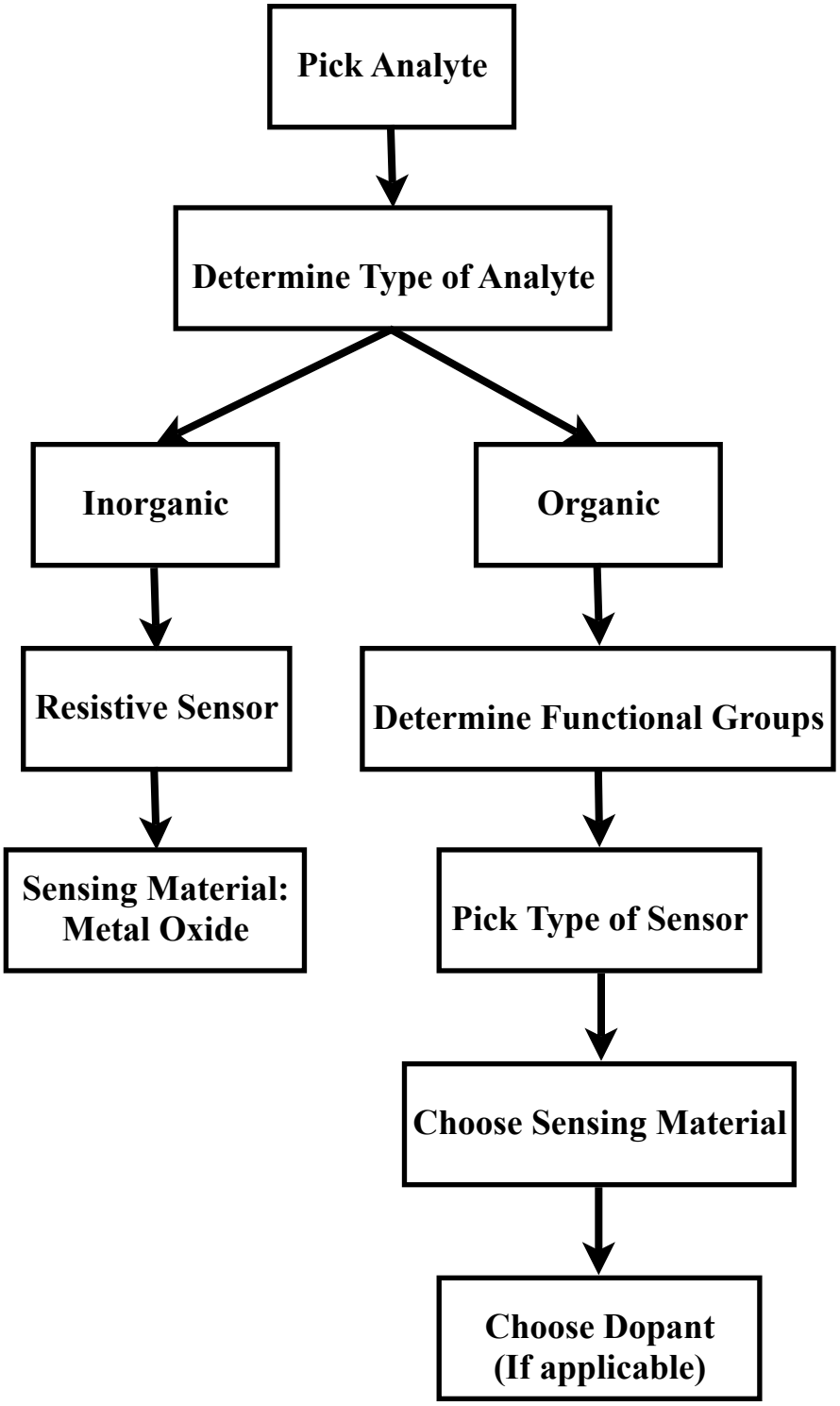

Figure 4.15: General schematic for choosing sensing materials.

The type of analyte will determine the materials that will be more attractive. The analyte can be classified based on its chemical make up. The analyte is classified as either organic or inorganic. If the analyte is inorganic, then some type of metal oxide is the best option for the sensing material. If the analyte is organic, then the analyte can be further classified by functional group.

Organic analytes are classified by functional groups such as amines, aromatics, alcohols, and aldehydes. Some analytes may have multiple functional groups, which allows for more options in sensing materials. For instance, an alcohol will hydrogen bond to a sensing material, whereas aromatics may just be absorbed by the sensing material. Some type of dopant (such as a metal or metal oxide) may also be considered to improve the sensing abilities of the sensing material.

In the next step, the type of sensor must be chosen. This will determine the sensor constraints and further narrow down the options for the sensing materials. For instance, a sensor that functions based on a change in resistance would require a sensing material that is conductive, whereas a sensor that measures a change in mass would require a sensing material with minimal weight.

Other factors such as limit of detection, temperature of detection, and regeneration of sensing material should also be taken into consideration. The sensing material must be able to detect the target analyte down to a specified concentration and be able to do so at an appropriate working temperature. In most cases, it is ideal to have a sensor that is reusable; thus, the sensing material should be able to be regenerated.

Once all the factors have been considered, a small list of sensing materials should be obtained. From here, the list may further be reduced based on processability and cost of materials. It may not be possible to narrow the sensing material down to one, so a few sensing materials may have to be tested (in an experimental set-up as the one proposed and discussed in Chapters 3 and 4 of this thesis) to determine which performs the best.

The general schematic, shown in Figure 4.15, is used to determine a sensing material for formaldehyde. By following the steps, it was deduced that polyaniline doped with nickel oxide (NiO) and/or alumina (Al_2O_3) would be optimal candidates (see Figure 4.16). Once these sensing materials had been chosen, testing was required to determine which material performed best for the desired application.

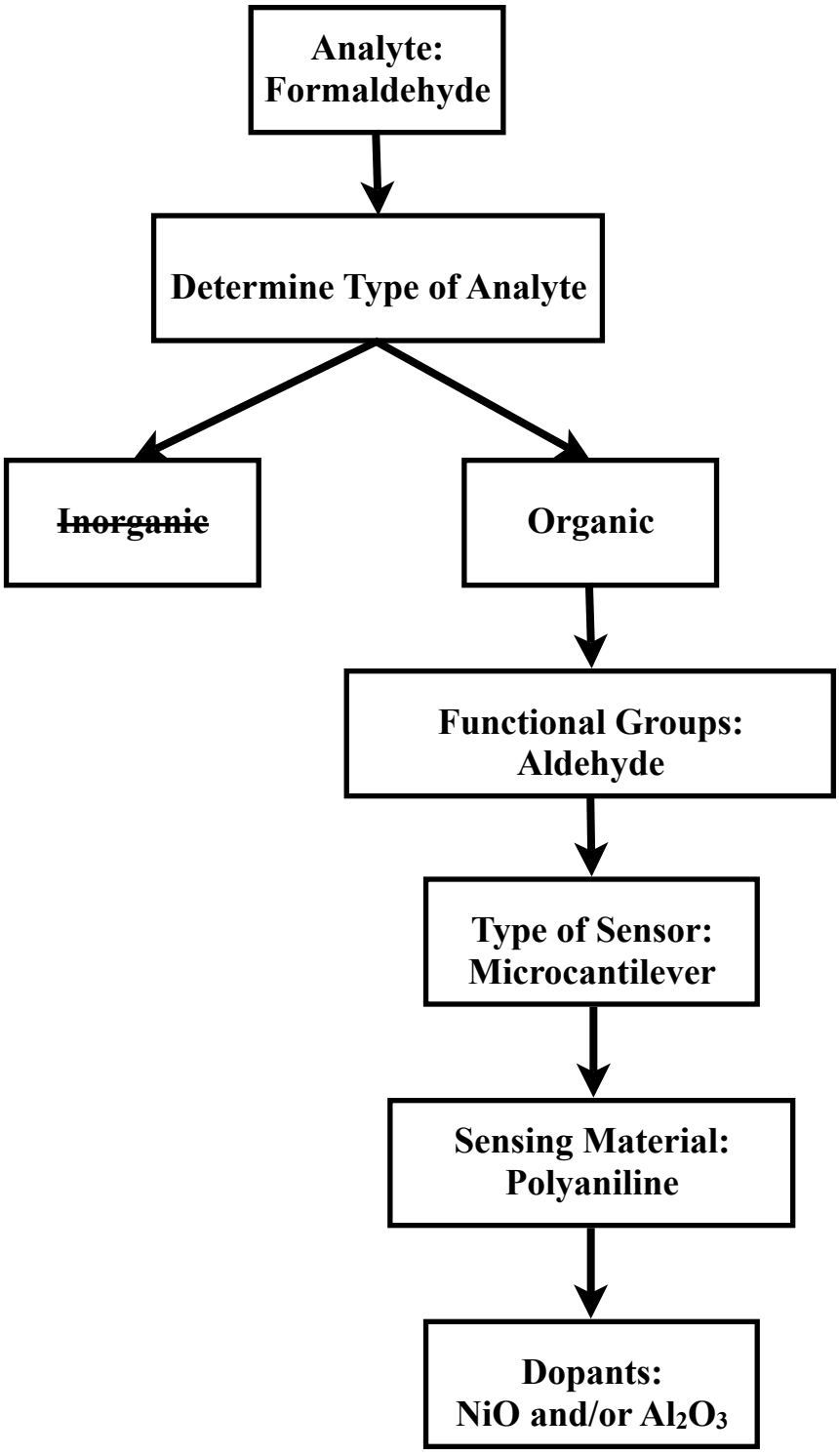

Figure 4.16: Schematic for choosing the sensing material for formaldehyde.

Chapter 5: Concluding Remarks and Future Recommendations

5.1 Concluding Remarks

5.1.1 Detection at High Concentration (Above 1 ppm)

The two most important characteristics of a sensing material are sensitivity and selectivity; however, they tend to oppose one another. Therefore, a sensing material that balances both is ideal. For the detection of formaldehyde at higher concentrations, PANI doped with 5% NiO and 15% Al_2O_3 manages this balance. Although PANI doped with 5% NiO and 15% Al_2O_3 was not the most sensitive towards formaldehyde, it had the desired selectivity.

The selectivity towards formaldehyde, with respect to acetaldehyde and benzene was good, even in binary and quaternary gas mixtures. The selectivity towards formaldehyde with respect to ethanol however, was poor in the quaternary and binary gas mixtures, despite being good for single gases tested. Therefore, the main interferent to formaldehyde was ethanol possibly due to its ability to hydrogen bond.

Despite the poorer selectivity with respect to ethanol, PANI doped with 5% NiO and 15% Al_2O_3 was still the best choice for a sensing material for formaldehyde at higher concentrations. It may be possible to improve the selectivity by changing the dopant concentration by increasing the Al_2O_3 by a couple of percent and by decreasing the NiO by a couple of percent.

5.1.2 Detection at Low Concentration (Below 1 ppm)

Although PANI doped with 5% NiO and 15% Al_2O_3 had sensitivity towards formaldehyde at a concentration of 0.73 ppm, at very low concentrations (0.09 ppm), PANI doped with 5% NiO and 15% Al_2O_3 did not sorb any formaldehyde. Therefore, for the application of indoor air quality testing, where the concentration of formaldehyde must be detected below 0.08 ppm, PANI doped with 5% NiO and 15% Al_2O_3 would be a poor choice as a sensing material.

Since PANI doped with 15% NiO had the highest sensitivity towards formaldehyde at 0.09 ppm, it was tested for selectivity. At a concentration of approximately 0.30 ppm, a quaternary gas mixture was used to test the selectivity of PANI doped with 15% NiO at low concentrations. Although PANI doped with 15% NiO had good selectivity with respect to benzene, it had poor selectivity with respect to acetaldehyde and very poor selectivity with respect to ethanol. Therefore, at low concentrations, PANI doped with 15% NiO had good sensitivity, but not very good selectivity.

By designing a dual sensor that used both PANI doped with 5% NiO and 15% Al_2O_3 and PANI doped with 15% NiO, a sensitive and selective sensor could be built. PANI doped with 15% NiO could be used to determine the concentration of formaldehyde and the interferents and PANI doped with 5% NiO and 15% Al_2O_3 could be used to determine the concentration of the interferents, since formaldehyde does not sorb onto it at very low concentrations. Therefore, the interferents could be subtracted from the total sorbed and the concentration of formaldehyde could be determined.

5.2 Recommendations for Future Work

5.2.1 Short Term Goals

5.2.1.1 PANI doped with 5% NiO and 15% Al_2O_3

A confirmation of the lack of formaldehyde sorption of PANI doped with 5% NiO and 15% Al_2O_3 should be done since it was the only polymer that did not sorb any formaldehyde when a concentration of 0.09 ppm was tested, as seen in Figure 4.12.

5.2.1.2 Other Dopants

To compare the effects of Al_2O_3 as a dopant for PANI to detect formaldehyde, PANI/ Al_2O_3 samples could be made and tested. This would help to determine the optimum dopant type and concentration for PANI for the detection of formaldehyde. Also, Al_2O_3 and NiO powders could be tested individually to determine the effects of each of these dopants on the detection of formaldehyde.

5.2.1.3 Surface Imaging

The screening studies in Chapter 4 did not look into the detailed structure of the PANI and the PANI mixtures. The microstructures must have an important role in setting sensitivity and selectivity of the materials for sorption of analytes, so studies should be carried out to characterize the materials in more detail. To determine the number of active sites (active surface area) and to see how the dopants affect the structure of PANI, the polymer samples should be imaged via the Brunauer, Emmett and Teller method (BET method), via scanning electron microscopy (SEM), and/or transmission electron microscopy (TEM).

5.2.1.4 Type of Sensor

The overall objective for this study is that the sensing materials studied will be part of a microcantilever sensor. The sensor to be used ultimately is comprised of a silicon base that is etched to create a microcantilever beam terminated by a sensing plate. The sensing material would be attached to the top of the sensing plate. The sensing plate also has an integrated heater

made of gold that is laid in a pattern between the sensing plate and the sensing material (Khater et al., 2009); see Figure 5.1.

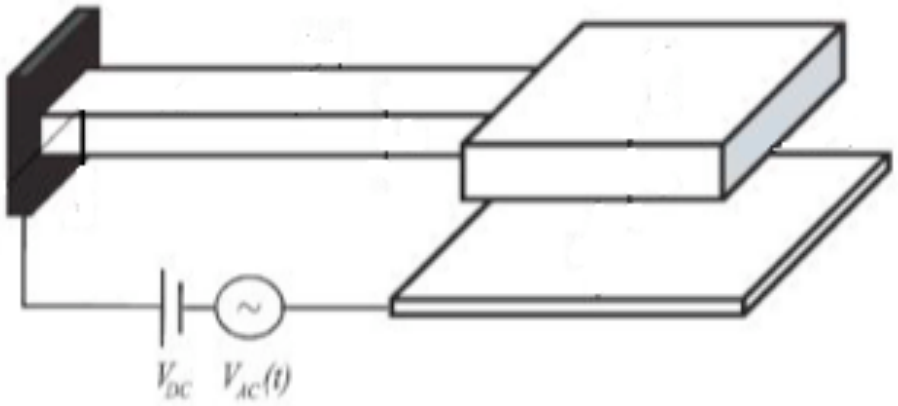

Figure 5.1: Schematic of the sensor (Khater et al., 2009).

The sensor works based on changes in weight. As the target analyte interacts with the sensing material, the weight of the sensing plate increases and causes the beam to bend by a certain amount, which is subsequently converted to an electrical signal. The electrical signal is proportional to the mass of the analyte that interacts with the sensing material and thus the concentration of the sensing material can be deduced. This sensor could also be set up as an on/ off type sensor such that if a threshold concentration were reached, a signal would be set off (Khater et al., 2009).

5.2.1.5 Deposition of Sensing Material onto Sensor

In order to prepare the sensor with the selected sensing material, it will be necessary to attach the film to the sensor. 16-mercaptohexadecanoic acid (MHDA) could be used to attach the PANI thin film to the gold layer on the sensor. The sulfur groups would bind to the gold, which would leave carboxylic acid groups to bind to PANI. MHDA forms self-assembled monolayers (SAMs) (Jung and Lee, 2008) and has a high thermal stability relative to PANI (Chandekar et al., 2010).

Both PANI and MHDA could be dissolved into ethylene glycol and deposited onto the sensor plate using dip-pen nanolithography (DPN). The MHDA would be deposited first and the ethylene glycol then allowed to slowly evaporate off, resulting in a SAM. PANI would be deposited in the same way and again ethylene glycol would be allowed to evaporate off.

DPN would be used because of the precision with which the sensing film could be deposited. DPN deposits an "ink" onto the substrate ("paper") through direct contact between the pen, coated in "ink", and the "paper" (Kramer et al., 2010). In this case, the "ink" is the sensing film and the "paper" is the sensor. The affinity of the "ink" towards the "paper" is the

driving force for the deposition. This affinity, for example, could be the result of a chemical interaction and/or an electrostatic interaction (Li et al., 2010).

5.2.1.6 Modified Experimental Setup

Four gases (formaldehyde, acetylaldehyde, ethanol, and benzene) were used to determine both the sensitivity and selectivity of the sensor. These gases were 5 ppm in nitrogen and could be diluted further to the desired concentrations. These gases were mixed in a mixing chamber and further diluted with nitrogen, which was also the carrier gas. Various concentrations and gas mixtures were tested.

In a modified experimental set-up, the gases would exit the mixing chamber and be split into two lines. The first line would run into the test chamber that holds the sensor and the second line would run into the GC (see Figure 5.2). The GC response would be used as a standard or reference to determine the concentrations of the gases. The GC setup in this experiment can detect into the ppb range and is able to differentiate between formaldehyde and acetaldehyde. An MKS pressure controller, followed by an MKS flow meter was used to equally split the gas flowing through the line exiting the mixing chamber.

In the future, a sensor could be tested at different relative humidities. A bubbler could be used, which would pass nitrogen through ultra pure (milli-Q) water (see Figure 5.2). By changing the flow rate of the nitrogen, different humidities could be achieved. The water vapour would flow directly into the test chamber. A humidity sensor and thermometer would be placed inside the test chamber to determine both the relative humidity and the temperature.

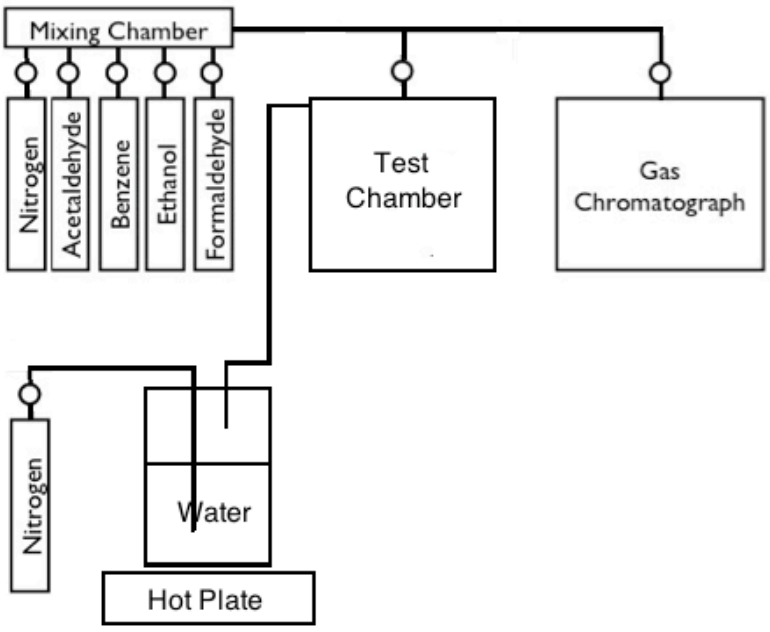

Figure 5.2: Schematic of experimental setup. The circles denote mass flow controllers.

5.2.1.7 Effect of Humidity

Humidity in the air is measured as a percent and given as the relative humidity (RH). It causes problems because water binds to the hydrophilic PANI and its derivatives, and induces a signal response. To avoid water molecules binding to PANI, a hydrophobic coating can be applied. Kim et al. (2005) achieved this by creating a copolymer of PANI and poly(vinylidene fluoride) (PVF_2). This copolymer will be referred to as coPANI. The hydrophobic PVF_2 blocked water from bonding to the amine group of PANI.

PANI was affected by relative humidity 50% more than coPANI; however, the sensitivity of coPANI was much less than PANI, since many of the VOC sensing sites were blocked by PVF_2. This significantly reduced the binding of water to the sensor but also sensitivity (Kim et al., 2005).

Han et al. (2009) used two sensors with different responses to the target analyte, but the same response to the interferent, which was water vapour. This allowed both the concentration of the analyte and the interferent to be separated and determined. It was found that Gallium-doped zinc oxide particles of different sizes had the same response to water vapour, but different responses to formaldehyde. However, this takes the case into a totally different sensor class, namely, a metal oxide.

Since humidity can affect the sensor, it should be tested. By varying the relative humidity in the test chamber of the modified experimental setup, the affect of humidity on the sensor can be determined.

5.2.1.8 Optimum Temperature of Operation

Other gases may induce a signal, resulting in lower selectivity. To improve selectivity, an optimum operating temperature must be found. This temperature may not provide the largest signal for formaldehyde, but provides a large enough signal for formaldehyde that can be detected, while other gases give low or negligible responses (Lee et al., 2007). The microcantilever sensor is equipped with a heating element that can be used to control the temperature of the sensor.

Humidity poses a problem, since PANI is hydrophilic. Therefore, the adsorption and absorption (or sorption) of water causes false positives. By elevating the operation temperature of the sensor, the hydrogen bonds that weakly bind the water molecules to the PANI sensing layer are broken. Kukla et al. (1996) showed that by elevating the temperature by even 10 - 12°C above room temperature, the humidity effect would be negligible (see Figure 5.3). They used a sensor that measured a change in resistance, where R is the resistance after sorption of the analyte and R_0 is the resistance in air.

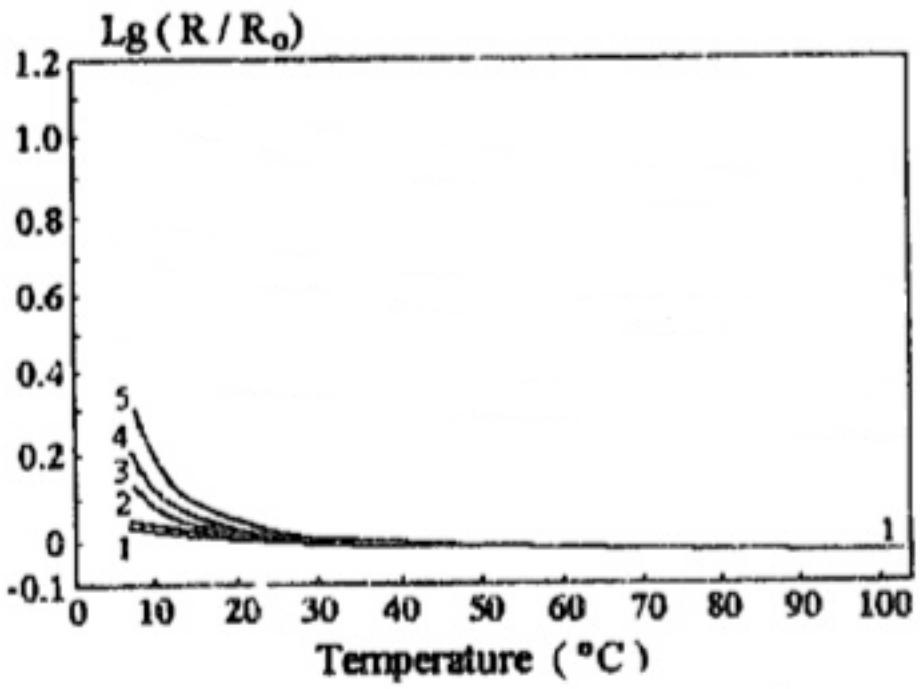

Figure 5.3: The relationship of signal (log (R/R_0)) versus temperature. (1) Argon gas. (2) Dry air (3) 60% RH. (4) 75% RH. (5) 90% RH. Note that above ~30°C, the lines are almost the same, with or without humidity (Kukla et al., 1996).

5.2.1.9 Temperature of Regeneration

The recovery time of a sensor of the type we are using is related to the polar affinity between formaldehyde and PANI (Choudhury, 2009). An increase in temperature provides more energy to the formaldehyde molecules, which weakens the affinity and would quicken regeneration of a sensing film. The heating element on the microcantilever sensor will be used to vary the temperature of the sensor.

A higher temperature may be beneficial; however, PANI begins to decompose between 104°C and 107°C (Kulka et al., 1996). By adding a small amount of NiO, the thermal stability of PANI can be increased since the interaction between PANI and NiO resists thermal motion. Although a small amount of NiO increases the thermal stability, too much NiO will actually weaken the interaction between the PANI chains and thus decrease the degradation temperature. Therefore, an optimum amount of NiO must be determined to improve both sensitivity and selectivity, as well as thermal stability (Song et al., 2007).

5.2.1.10 Multi-sensor Arrays

By combining two or more sensing materials on separate sensors, it may be possible to reduce the impact of interferents. This could be done by combining one sensing material, which

detects both the target analyte as well as an interferent, with a second sensing material that only detects the interferent. Therefore, by subtracting the interferent signal, the concentration of the target analyte could be determined. This could also be expanded to several different sensing materials to detect many different target analytes.

For the detection of formaldehyde at low concentrations, a combination of PANI doped with 15% NiO and PANI doped with 5% NiO and 15% Al_2O_3 maybe a good starting combination. This is because PANI doped with 5% NiO and 15% Al_2O_3 did not detect formaldehyde at low concentrations. Therefore, if PANI doped with 5% NiO and 15% Al_2O_3 did detect interferents at low concentrations, then it would be an ideal candidate as a second sensing material in combination with PANI doped with 15% NiO for the detection of formaldehyde at low concentrations.

5.2.2 Long Term Goals

5.2.2.1 Testing Other Sensing Materials

The testing system is set up such that more gases may be added to the mixing chamber (up to 13). Therefore, the test system could be used to test many different sensing materials. By testing sensing materials first, it would save time when testing fully built sensors.

By testing many different sensing materials for various analytes, a general overview or set of prescriptions may be determined as a starting point for optimal sensing materials. This is because similar analytes interact with sensing materials in a similar fashion. Therefore, it may be possible to rule out certain groups of sensing materials based on the sensor requirements for a specific analyte (see Section 4.5).

5.2.2.2 Testing Other Sensors

The test system is set up such that it can easily be expanded, many different sensors could be tested using the seystem. Therefore, many other sensors for various VOCs could be tested with this experimental set-up. Depending on what gases are tested, the column in the GC may have to be replaced to ensure separation of the gases along the column. For instance, the current column being used is unable does not distinguish between acetaldehyde and methanol, and acetone and ethanol.

References

Adhikari, B. And S. Majumdar. “Polymers in Sensor Applications” Progress in Polymer Science **29** (2004) 699-766.

Agbor, N. E., M. C. Petty, and A. P. Monkman. “Polyaniline Thin Films for Gas Sensing” Sensors and Actuators B **28** (1995) 173-179.

Agilent Technologies. Pulsed Discharge Helium Ionization Detector (PDHID): User Information (2006) United States of America pg. 8-10.

Ai, L., J.-C. Mau, W.-F. Liu, M.-Y. Fu, and T.-C. Chen. “Ammonia Gas Fiber Sensor Based on Polyaniline Sensing Film Coated on Superstructure Fiber Bragg Gratings” Microwave and Optical Technology Letters **49** (2007) 3036-3066.

Aruna, I., F. E. Kruis, S. Kundu, M. Muhler, R. Theissmann, and M. Spasova. “CO ppb Sensors Based on Monodispersed SnO_x:Pd Mixed Nanoparticle Layers: Insight into Dual Conductance Response” J. Appl. Phys. **105** (2009) 064312.

Ataka, Y., S. Kato, S. Murakami, Q. Zhu, K. Ito, and T. Yokota. “Study of Effect of Adsorptive Building Material on Formaldehyde Concentrations: Development of Measuring Methods and Modeling of Adsorption Phenomena” Indoor Air **14** (2004) 51-64.

Athwale, A. A., and M. V. Kulkarni. “Polyaniline and its Substituted Derivatives as a Sensor for Aliphatic Alcohols” Sensors and Actuators B **67** (2000) 173-177.

Ayad, M. M., A. H. Gemaey, N. Salahuddin, and M. A. Shenashin. “The Kinetics and Spectral Studies of the In Situ Polyaniline Film Formation” Journal of Colloid and Interface Science **263** (2003) 196-201.

Brown, S. K. “Volatile Organic Pollutants in New and Established Buildings in Melbourne, Australia” Indoor Air **12** (2002) 55-63.

Campanella, L., M. Battilotti, R. Dragone, and I. Mevola. “Suitable Solid State Chemical Sensor for HCHO Determination” International Journal of Environment and Pollution **27**, 4 (2006) 313-323.

Chandekar, A., S. K. Senggupta, and J. E. Whitten. “Thermal Stability of Thiol and Silane Monolayers: A Comparative Study” Applied Surface Science **256** (2010) 2742-2749.

Chen, T., Q. L. Liu, Z. L. Zhou, and Y. D. Wang. "The fabrication and Gas-sensing Characteristics of the Formaldehyde Gas Sensors with High Sensitivity" Sensors and Actuators B **131** (2008) 301-305.

Chen, X., J. Sun, and J. Shen. "Patterning of Layer-by-Layer Assembled Organic-Inorganic Hybrid Films: Imprinting Versus Lift-off" Langmuir **25** (2009a) 3316-3350.

Chen, X. X., L. Rieth, M. S. Miller, and F. Solzbacher. "High Temperature Humidity Sensor Based on Sputtered Y-doped $BaZrO_3$ Thin Films" Sensors and Actuators B **137** (2009b) 578-585.

Chen, Z.-K., S.-C. Ng, S. F. Y. Li, L. Zhong, L. Xu and H. S. O. Chan. "The Fabrication and Evaluation of a Vapour Sensor Based on Quartz Crystal Microbalance Coated with Poly(*o*-anisidine) Langmuir-Blodgett Layers" Synthetic Metals **87** (1997) 201-204.

Choudhury, A. "Polyaniline/Silver Nanocomposite: Dielectric Properties and Ethanol Vapour Sensitivity" Sensors and Actuators B **138** (2009) 318-325.

Dahnke, H., G. Von Basum, K. Kleinermanns, P. Hering, and M. Mürtz. "Rapid Formaldehyde Monitoring in Ambient Air by Means of Mid-infrared Cavity Leak-out Spectroscopy" Applied Physics B: Lasers and Optics **75** (2002) 311-316.

De Wit, M., E. Vanneste, H. J. Geise, and L. J. Nagels. "Chemiresistive Sensors of Electrically Conducting Poly(2,5-thienylene vinylene) and Copolymers: Their Response to Nine Organic Vapours" Sensors and Actuators B **50** (1998) 164-172.

Degerlier, M., and N. Celebi "Indoor Radon Concentrations in Adana, Turkey" Radiation Protection Dosimetry **131**, 2 (2008) 259–264.

Dirksen, J. A., K. Duval, and T. A. Ring. "NiO Thin Film Formaldehyde Gas Sensor" Sensors and Actuators B **80** (2001) 106-115.

Dündar, D. And F. Köleli. "Synthesis, Characterization and SEESR Spectroscopic Investigations of Indole/Aniline Copolymers" Journal of Applied Polymer Science **109**, 5 (2008) 3044-3049.

Endo, T., Y. Yenagida, and T. Hatsuzawa. "Colourimetric Detection of Volatile Organic Compounds using Colloidal Crystal-based Chemical Sensor for Environmental Applications" Sensors and Actuators B **125** (2007) 589-595.

Feast, W.J., J. Tsibouklis, K. L. Pouwer, L. Groenendaal, and E. W. Meijer. "Synthesis, Processing and Material Properties of Conjugated Polymers" Polymer **37** 22 (1996) 5017-5047.

Fergus, J. W. "A review of Electrolyte and Electrode Materials for High Temperature Electrochemical CO_2 and SO_2 Gas Sensors" Sensors and Actuators B **134** (2008) 1034-1041.

Figueroa, O. L., C. Lee, S. A. Akbar, N. F. Szabo, J. A. Trimboli, P. K. Dutta, N. Sawaki, A. A. Soliman, and H. Verweij. "Temperature-comtrolled CO, CO_2, and NO_x Sensing in a Diesel Engine Exhaust Stream" Sensors and Actuators B **107** (2005) 839-848.

Galdikas A., A. Mironas, D. Senulien, A. Setkus. "CO-gas-induced Resistance Switching in SnO_2/ultrathin Pt Sandwich Structure" Sensors and Actuators B **32** (1996) 87-92.

Geniès, E. M., A. Boyle, M. Lapkowski, and C. Tsintavis. "Polyaniline: A Historical Survey" Synthetic Metals **36** (1990) 139-182.

Gillett, R. W., H. Kreibich, and G. P. Ayers. "Measurement of Indoor Formaldehyde Concentrations with a Passive Sampler" Environmental Science and Technology **34** (2000) 2051-2056.

Grob, R. L. and E. F. Barry. Modern Practice of Gas Chromatography: Fourth Edition John Wiley and Sons Inc. (2004) United States of America, pg. 25-59.

Han, J., G. Song, R. Guo. "Synthesis of Rectangular Tubes of Polyaniline/NiO Composites" Journal of Polymer Science Part A: Polymer Chemistry **44** (2006) 4229-4234.

Han, N., Y. Tian, X. Wu, and Y. Chen. "Improving Humidity Selectivity in Formaldehyde Gas Sensing by a Two-sensor Array made of Ga-doped ZnO" Sensors and Actuators B **138** (2009) 228-235.

Ho, C. K. and S. W. Webb. Gas Transport in Porous Media Springer (2006) The Netherlands, pg. 314.

Horstjann, M., Y. A. Bakhirkin, A. A. Kosterev, R. F. Curl, F. K. Tittel, C. M. Wong, C. J. Hill, and R. Q. Yang. "Formaldehyde Sensor Using Interband Cascade Laser Based Quartz-enhanced Photoacoustic Spectroscopy" Applied Physics B: Lasers and Optics **79** (2004) 799-803.

Hosono, K., I. Matsubara, N. Murayama, S. Woosuck, and N. Izu. "Synthesis of Polypyrrole/ MoO_3 Hybrid Thin Films and Their Volatile Organic Compound Gas-sensing Properties" Chemical Materials **17** (2005) 349-354.

Hosseini, S. H., S. H. A. Oskooei, and A. A. Entezani. "Toxic Gas and Vapour Detection by Polyaniline Gas Sensor" Iranian Polymer Journal **14**, 4 (2005) 333-344.

Itoh, T., I. Matsubara, W. Shin, and N. Izu. “Layered Hybrid Thin Film of Molybdenum Trioxide with Poly(2,5-dimethylaniline) for Gas Sensor Sensitive to VOC Gases in ppm Level” Chemistry Letters **36**, 1 (2007a) 100-101.

Itoh, T., I. Matsubara, W. Shin, N. Izu, and M. Nishibori. “Highly Aldehyde Gas-Sensing Responsiveness and Selectivity of Layered Organic-Guest/MoO_3-Host Hybrid Sensor” Journal of the Ceramic Society of Japan **115**, 11 (2007b) 742-744.

Itoh, T., I. Matsubara, W. Shin, and N. Izu. “Synthesis and Characterization of Layered Organic/ Inorganic Hybrid Thin Films Based on Molybdenum Trioxide with Poly(*N*-methylaniline) for VOC Sensor” Materials Letters **61** (2007c) 4031-4034.

Itoh, T., I. Matsubara, W. Shin, N. Izu, and M. Nishibori. “Preparation of Layered Organic-Inorganic Nanohybrid Thin Films of Molybdenum Trioxide with Polyaniline Derivatives for Aldehyde Gases of Several Tens ppb Level” Sensors and Actuators B **128** (2008) 512-520.

Jung, M.-H., and H. Lee. “Patterning of Conducting Polymers Using Charged Self-assembled Monolayers” Langmuir **24** (2008) 9825-9831.

Kawamura, K., K. Kerman, M. Fujihara, N. Nagatani, T. Hashiba, and E. Tamiya. “Development of a Novel Hand-held Formaldehyde Gas Sensor for the Rapid Detection of Sick Building Syndrome” Sensors and Actuators B **105** (2005) 495-501.

Khater, M. E., E. M. Abdel-Rahman, and A. H. Nayfeh. “A Mass Sensing Technique for Electrostatically Activated MEMS” Proceeding of the ASME International Design Engineering Technical Conferences & Computers and Information in Engineering Conference, August 30 - September 2, 2009. San Diego, California, USA.

Kida, T., T. Minomi, S. Kishi, M. Yuasa, K. Shimanoe, and N. Yamazoe. “Planar-type $BiCuVO_x$ Solid Electrolyte Sensor for the Detection of Volatile Organic Compounds” Sensors and Actuators B **137** (2009) 147-153.

Kim, J.-S., S.-O. Sohn, and J.-S. Huh. “Fabrication and Sensing Behaviour of PVF2 Coated Polyaniline Sensor for Volatile Organic Compounds” Sensors and Actuators B **108** (2005) 409-413.

Knake, R., P. Jacquinot, A. W. E. Hodgson, and P. C. Hauser. “Amperometric Sensing in the Gas-phase” Analytica Chimica Acta **549** (2005) 1-9.

Knake, R., P. Jacquinot, and P. C. Hauser. “Amperometric Detection of Gaseous Formaldehyde in the ppb Range” Electroanalysis **13**, 8 (2001) 631-634.

Koleli, F. and D. Dundar. “Synthesis, Characterization and SEESR Spectroscopic Investigations of Indole/Aniline copolymers” Journal of Applied Polymer Science **109** (2008) 3044-3049.

Kramer, M. A., H. Jaganathan, and A. Ivanisevic. “Serial and Parallel Dip-pen Nanolithography Using a Colloidal Probe Tip” Journal of the American Chemical Society **132** (2010) 4532-4533.

Kukla, A. L., Y. M. Shirshov, and S. A. Piletsky. “Ammonia Sensors Based on Sensitive Polyaniline Films” Sensors and Actuators B **37** (1996) 135-140.

Lee, C.-Y., C.-M. Chiang, Y.-H. Wang, and R.-H. Ma. “A Self-heating Gas Sensor with Integrated NiO Thin-film for Formaldehyde Detection” Sensors and Actuators B **122** (2007) 503-510.

Lee, C.-Y., P.-R. Hsieh, C.-H. Lin, P.-C. Chou, L.-M. Fu, and C.-M. Chiang. “MEMS-based Formaldehyde Gas Sensor Integrated with a Micro-hotplate” Microsystem Technologies **12** (2006) 893-898.

Lee, Y.-I., K.-J. Lee, D.-H. Lee, Y.-K. Jeong, H. S. Lee, and Y.-H. Choa. “Preparation and Gas Sensitivity of SnO_2 Nanopowder Homogeneously Doped with Pt Nanoparticles” Current Applied Physics **9** (2009) 579-581.

Li, H., D. K. Ashcroft, B. D. Freeman, M. E. Stewart, M. K. Jank, and T. R. Clark. “Non-invasive Headspace Measurements for Characterizing Oxygen Scavenging in Polymers” Polymer (2008) 4541-4545.

Li, Y., H. Sun, and H. Chu. “Controlled Preparation of Inorganic Nanostructures on Substrates by Dip-pen Nanolithography” Chemical Asian Journal **5** (2010) 980-990.

Liu, C.-D., S.-Y. Wu, J.-L. Han, and K.-H Hsieh. “Patterned Conductive Polyaniline Films Fabricated Using Lithography and *In Situ* Polymerization” Journal of Applied Polymer Science **115** (2010) 2271-2276.

Lv, P., Z. Tang, G. Wei, J. Yu, and Z. Huang. “Recognizing Indoor Formaldehyde Binary Gas Mixtures with a Micro Gas Sensor Array and a Neutral Network” Measurement Science and Technology **18** (2007) 2997-3004.

Mabrook, M. And P. Hawkins. “A Rapidly-responding Sensor for Benzene, Methanol, and Ethanol Vapours Based on Films of Titanium Dioxide Dispersed in a Polymer Operating at Room Temperature” Sensors and Actuators B **75** (2001) 197-202.

Mädler, L., T. Sahm, A. Gurlo, J.-D. Grunwaldt, N. Barsan, U. Weimar, and S. E. Pratsinis. “Sensing Low Concentrations of CO Using Flame-spray-made Pt/SnO_2 Nanoparticles” Journal of Nanoparticle Research **8** (2006) 783-796.

Mascaro, L. H., D. Gonçalves, and L. O. S. Bulhões. "Electrocatalytic Properties and Electrochemical Stability of Polyaniline and Polyaniline Modified with Platinum Nanoparticles in Formaldehyde Medium" Thin Solid Films **461** (2004) 243-249.

Miles, J., F. Ibrahimi, and K. Birch "Moisture-resistant Passive Radon Detectors" Journal of Radiological Protection **29** (2009) 269–271.

Misra, S. C. K., P. Mathur, M. Yadav, M. K. Tiwari, S. C. Garg, and P. Tripathi. "Preparation and Characterization of Vacuum Deposited Semiconducting Nanocrystalline Polymeric Thin Film Sensor for Detection of HCl" Polymer **45** (2004a) 8623-8628.

Misra, S. C. K., P. Mathur, and B. K. Srivastava. "Vacuum-deposited Nanocrystalline Polyaniline Thin Film Sensors for Detection of Carbon Monoxide" Sensors and Actuators A **114** (2004b) 30-35.

Mitsubayashi, K., H. Amagai, H. Watanabe, and Y. Nakayama. "Bioelectronic Sniffer with a Diaphragm Flow-cell for Acetylaldehyde Vapour" Sensors and Actuators B **95** (2003) 303-308.

Mitsubayashi, K., K. Yokoyama, T. Takeuchi, and I. Karube. "Gas-Phase Biosensor for Ethanol" Analytical Chemistry **66** (1994) 3297-3302.

Mitsubayashi, K. and Y. Hashimoto. "Bioelectronic Sniffer Device for Trimethylamine Vapour using Flavin Containing Monooxygenase" IEEE Sensors Journal **2** 3 (2002a) 133-139.

Mitsubayashi, K. and Y. Hamshimoto. "Bioelectronic Nose for Methyl Mercaptan Vapour using Xenobiotic Metabolizing Enzyme: Flavin-containing Monooxygenase" Sensors and Actuators B **83** (2002b) 35-40.

Nicolas-Debarnot, D. and F. Poncin-Epaillard. "Polyaniline as a New Sensitive Layer for Gas Sensors" Analytica Chimica Acta **475** (2003) 1-15.

Plashnitsa, V. V., V. Gupta, and N. Miura. "Mechanochemical Approach for Fabrication of a Nano-structured NiO-sensing Electrode used in a Zirconia-based NO_2 Sensor" Electrochimica Acta **55** (2010) 6941-6945.

Qin, Z., P.-N. Wang, and Y. Wang. "Enhanced Sensing Performance of the Amperometric Gas sensor by Laser-patterning of the Polymer Membrane Electrode" Sensors and Actuators B **107** (2005) 805-811.

Ruangchuay, L., A. Sirivat, and J. Schwank. "Polypyrrole/Poly (methylmethacrylate) Blend as Selective Sensor for Acetone in Lacquer" Talanta **60** (2003) 25-30.

Safavi, A., N. Maleki, F. Farjami, and E. Farjami. “Electrocatalytic Oxidation of Formaldehyde on Palladium Nanoparticles Electrodeposited on Carbon Ionic Liquid Composite Electrode” Journal of Electroanalytical Chemistry **626** (2009) 75-79.

Sekhar, P. K., E. L. Brosha, R. Mukundan, W. Li, M. A. Nelson, P. Palanisamy, and F. H. Garzon. “Application of Commercial Automotive Sensor Manufacturing Methods for the NO_x/ NH_3 Mixed Potential Sensors for On-board Emissions Control” Sensors and Actuators B **144** (2010) 112-119.

Shimizu, Y., M. Okimoto, and N. Souda. “Solid-state SO_2 Sensor using a Sodium-ionic Conductor and a Metal-sulfide Electrode” International Journal of Applied Ceramic Technology **3**, 3 (2006) 193-199.

Song, G., J. Han, and R. Guo. “Synthesis of Polyaniline/NiO Nanobelts by a Self-Assembly Process” Synthetic Metals **157** (2007) 170-175.

Steiskal, J. and R. G. Gilbert. “Polyaniline. Preparation of a Conducting Polymer” (IUPAC Technical Report) Pure and Applied Chemistry **74**, 5 (2002) 857-867.

Tang, Q., X. Su, Q. Li, J. Wu, J. Lin, and M. Huang. “Synthesis of Oriented Polyaniline Flake Arrays” Material Letters **63** (2009) 540-542.

Ulmann, M., R. Kostecki, J. Augustynski, D. J. Strike, and M. Koudelka-Hep. “Modification des Polymères Conducteurs avec de Petites Particules Métalliques; Propriétés des Films de Polypyrrole et de Polyaniline Platinés” Chimia **46** (1992) 138-140.

Vianello, F., A. Stefani, M. L. Di Paolo, A. Rigo, A. Lui, B. Margesin, M. Zen, M. Scarpa, and G. Soèncini. “Potentiometric Detection of Formaldehyde in Air by an Aldehyde Dehydrogenase FET” Sensors and Actuators B **37** (1996) 49-54.

Wang, J., B. Zou, S. Ruan, J. Zhao, and F. Wu. “Synthesis, Characterization, and Gas-sensing Property for HCHO of Ag-doped In_2O_3 Nanocrystalline Powders” Materials Chemistry and Physics **117** (2009a) 489-493.

Wang, J., L. Liu, S.-Y. Cong, J.-Q. Qi, and B.K. Xu. “An Enrichment Method to Detect Low Concentration Formaldehyde” Sensors and Actuators B **134** (2008a) 1010-1015.

Wang, J., M. Ichiro, N. Murayama, S. Woosuck, and N. Izu. “The Preparation of Polyaniline Intercalated MoO_3 Thin Films and its Sensitivity to Volatile Organic Compounds” Thin Film Solids **514** (2006) 329-333.

Wang, J., P. Zeng, J.-Q. Qi, and P.-J. Yao. "Silicon-based Micro-gas Sensors for Detecting Formaldehyde" Sensors and Actuators B **136** (2009b) 399-404.

Wang, X., M. Zhang, J. Liu, T. Luo, and Y. Qian. "Shape- and Phase-controlled Synthesis of In_2O_3 with Various Morphologies and their Gas-sensing Properties" Sensors and Actuators B **137** (2009c) 103-110.

Wang, Y.-H., C.-Y. Lee, C.-H. Lin, and L.-M. Fu. "Enhanced Sensing Characteristics in MEMS-based Formaldehyde Gas Sensors" Microsystems Technology **14** (2008b) 995-1000.

Wieckowski, A., E. R. Savinova, and C. G. Vayenas. Catalysis and Electrocatalysis at Nanoparticle Surfaces Marcel Dekker Inc. (2003) USA, pg. 916-917.

Wiedijk, P. "Flat-based Water Vapour Sensor of the Phosphorous Pentoxide Type" Journal of Physics E: Scientific Instruments **13** (1980) 993-994.

WHO Regional Office for Europe "Air Quality Guidelines: Second Edition" Copenhagen, Denmark, 2001.

WHO Regional Office for Europe "Local Housing and Health Action Plans: A Project Manual" Copenhagen, Denmark, 2004.

Wu, Y. M., W. S. Li, J. Lu, J. H. Du, D. S. Lu, and J. M. Fu. "Electrocatalytic Oxidation of Small Organic Molecules on Polyaniline-Pt-H_xMoO_3" Journal of Power Sources **145** (2005) 286-291.

Yang, J.-C., J. V. Spirig, D. Karweik, J. L. Routbort, D. Singh, and P. K. Dutta. "Compact Electrochemical Bifunctional NO_x/O_2 Sensor with Metal/Metal Oxide Internal Reference Electrode for High Temperature Applications" Sensors and Actuators B **131** (2008) 448-454.

Yang, L., A. Cai, C. Luo, Z. Liu, W. Shangguan, and T. Xi. "Performance Analysis of a Novel TiO_2-coated Foam-nickel PCO Air Purifier in HVAC Systems" Separation and Purification Technology **68** (2009) 232-237.

Yi, A. Y., W. Lu., D. F. Farson, and L. J. Lee. "Overview of Polymer Micro/Nanomanufacturing for Biomedical Applications" Advances in Polymer Technology" **27**, 4 (2008) 188-198.

Zhang, L., J. Hu, P. Song, H. Qin, X. Liu, and M. Jiang. "Formaldehyde-sensing Characteristics of Perovskite $La_{0.68}Pb_{0.32}FeO_3$ Nano-materials" Physica B **370** (2005) 259-263.

Zhang, T., S. Mubeen, E. Bekyarova, B. Y. Yoo, R. C. Haddon, N. V. Myung, and M. A. Deshusses. "Poly(m-aminobenzene sulfonic acid) Functionalized Single-wall Carbon Nanotubes Based Gas Sensor" Nanotechnology **18** (2007) 165504-165509.

Zhou, J., P. Li, S. Zhang, F. Zhou, Y. Huang, P. Yang, and M. Bao. “A Novel MEMS Gas Sensor with Effective Combination of High Sensitivity and High Selectivity” IEEE (2002) 471-474.

Zhou, M. And A. Ahmad. “Sol-gel Processing of In-doped $CaZrO_3$ Solid Electrolyte and the Impedimetric Sensing Characteristics of Humidity and Hydrogen” Sensors and Actuators B **129** (2008) 285-291.

Zhou, Z.-L., T.-F. Kang, Y. Zhang, and S.-Y. Cheng. “Electrochemical Sensor for Formaldehyde Based on Pt-Pd Nanoparticles and a Nafion-modified Glassy Carbon Electrode” Microchimica Acta **164** (2009) 133-138.

Zhuiykov, S. and V. Dowling. “The Nanostructured Au-doped Cobalt Oxyhydroxide Based Carbon Monoxide Sensor for Fire Detection at its Earlier Stages” Measurement Sciences and Technology **19** (2008) 024001.

Appendix A

Raw Data: Gas Chromatograms

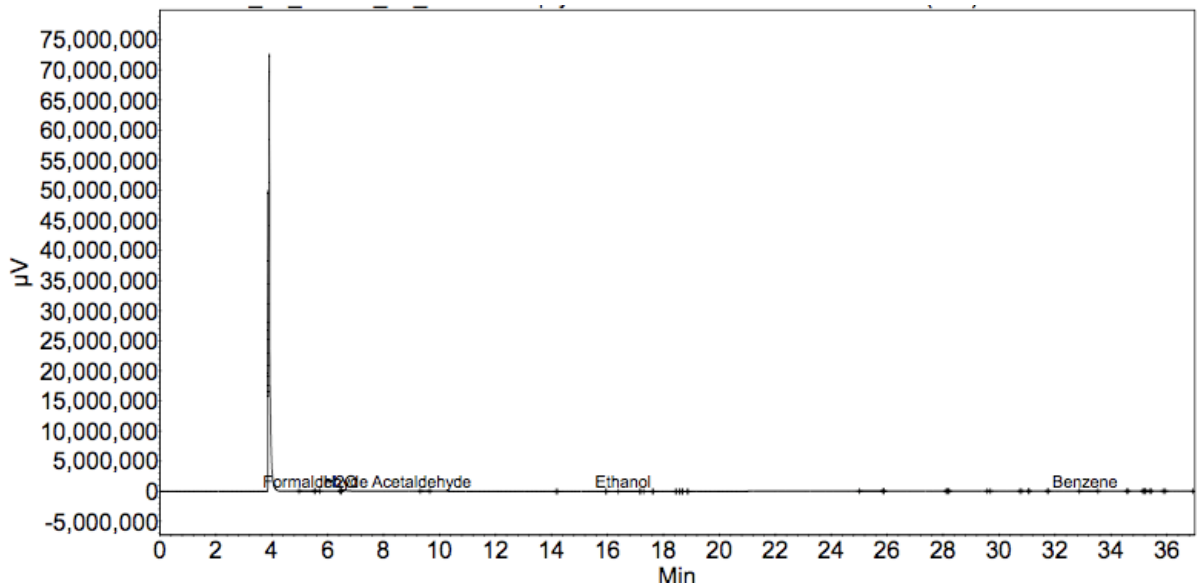

Figure A.1: Chromatogram of all four gases at approximately 1 ppm each.

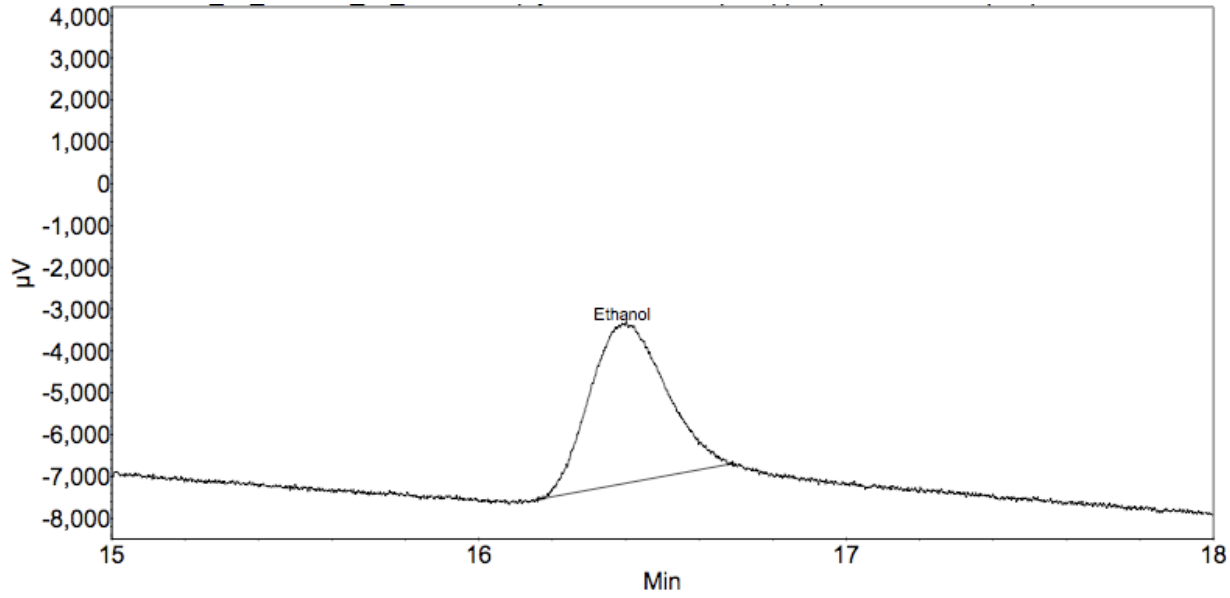

Figure A.2: Chromatogram of ethanol at a concentrations of 5.00 ppm.

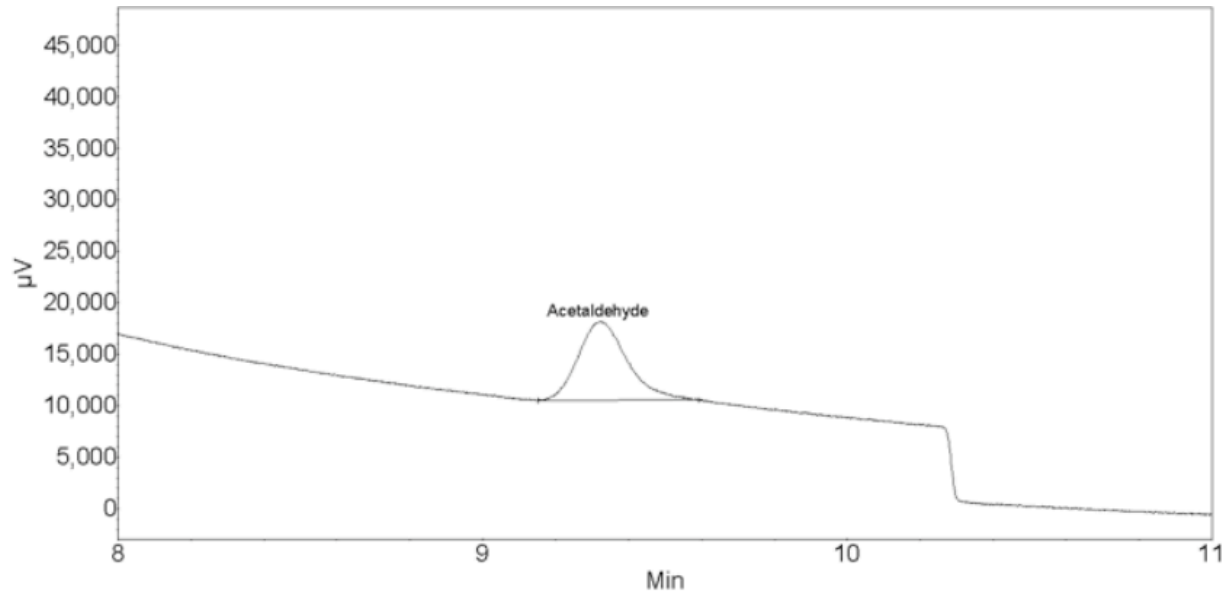

Figure A.3: Chromatogram of acetaldehyde at a concentration of 4.96 ppm.

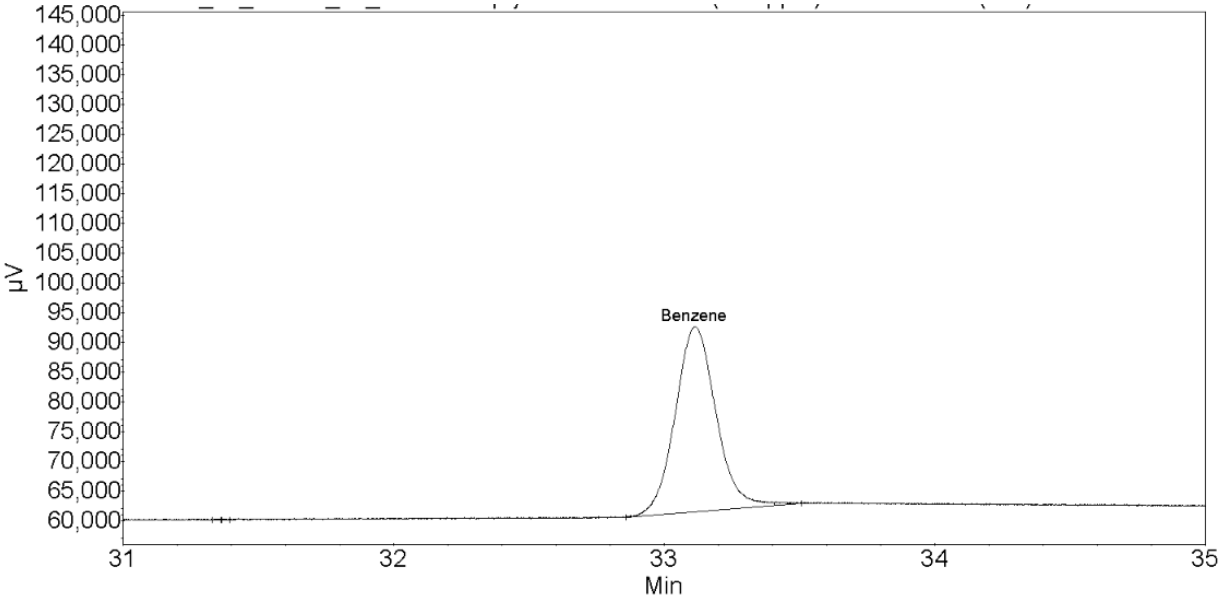

Figure A.4: Chromatogram of benzene at a concentration of 5.10 ppm.

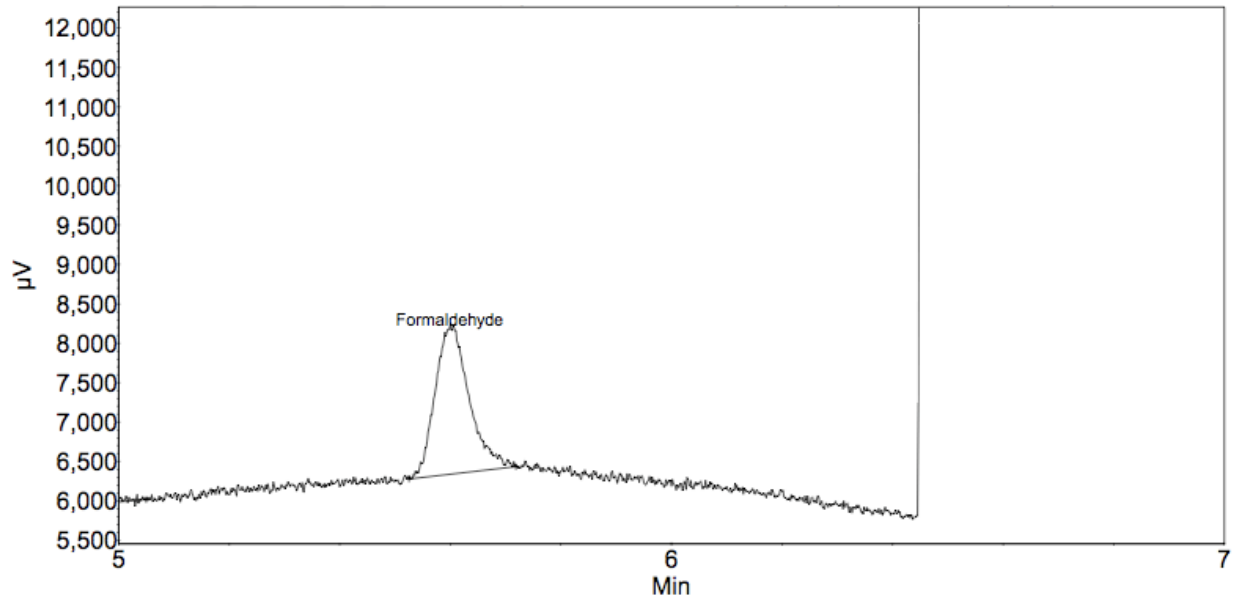

Figure A.5: Chromatogram of formaldehyde at a concentration of 0.73 ppm.

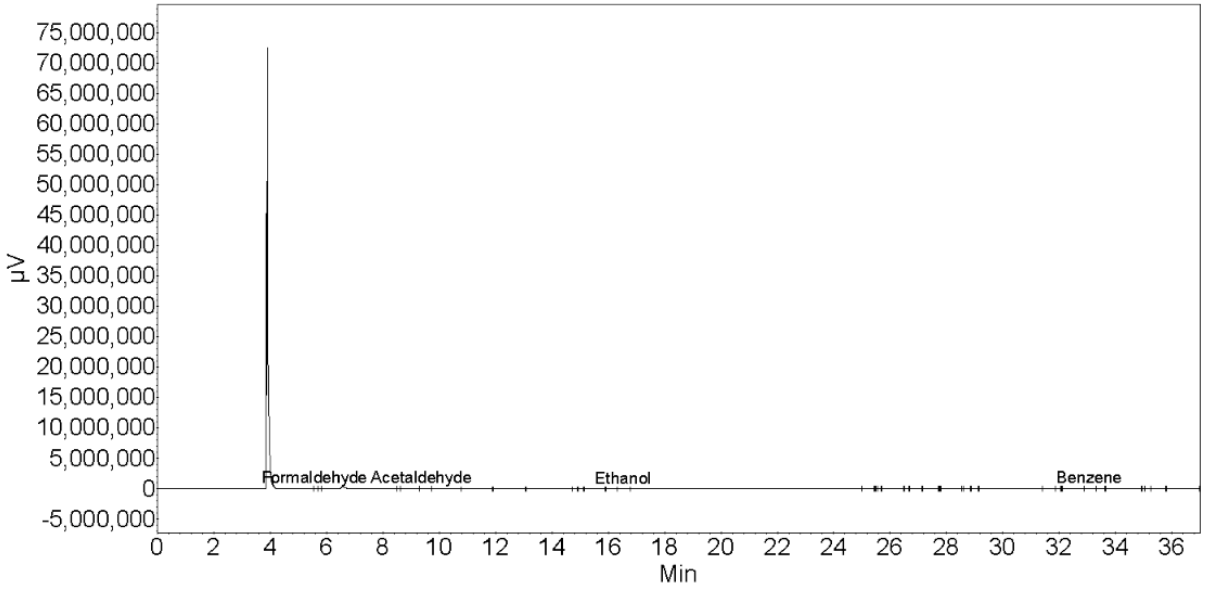

Figure A.6: Chromatogram of all four gases for PANI doped with 5% NiO and 15% Al_2O_3 at a concentration of approximately 1 ppm each.